DoE
EPA

United States
Department of Energy

Division of Solid Fuel
Mining and Preparation
Pittsburgh PA 15213

FE-9001-1

U.S. Environmental Protection Agency
Office of Research and Development

Industrial Environmental Research
Laboratory
Research Triangle Park NC 27711

EPA-600/7-79-008
January 1979

Surface Phenomena in the Dewatering of Coal

Interagency Energy/Environment R&D Program Report

RESEARCH REPORTING SERIES

Research reports of the Office of Research and Development, U.S. Environmental Protection Agency, have been grouped into nine series. These nine broad categories were established to facilitate further development and application of environmental technology. Elimination of traditional grouping was consciously planned to foster technology transfer and a maximum interface in related fields. The nine series are:

1. Environmental Health Effects Research
2. Environmental Protection Technology
3. Ecological Research
4. Environmental Monitoring
5. Socioeconomic Environmental Studies
6. Scientific and Technical Assessment Reports (STAR)
7. Interagency Energy-Environment Research and Development
8. "Special" Reports
9. Miscellaneous Reports

This report has been assigned to the INTERAGENCY ENERGY-ENVIRONMENT RESEARCH AND DEVELOPMENT series. Reports in this series result from the effort funded under the 17-agency Federal Energy/Environment Research and Development Program. These studies relate to EPA's mission to protect the public health and welfare from adverse effects of pollutants associated with energy systems. The goal of the Program is to assure the rapid development of domestic energy supplies in an environmentally-compatible manner by providing the necessary environmental data and control technology. Investigations include analyses of the transport of energy-related pollutants and their health and ecological effects; assessments of, and development of, control technologies for energy systems; and integrated assessments of a wide range of energy-related environmental issues.

EPA REVIEW NOTICE

This report has been reviewed by the participating Federal Agencies, and approved for publication. Approval does not signify that the contents necessarily reflect the views and policies of the Government, nor does mention of trade names or commercial products constitute endorsement or recommendation for use.

This document is available to the public through the National Technical Information Service, Springfield, Virginia 22161.

Price: Paper Copy $9.00
Microfiche $3.00

FE-9001-1
(EPA-600/7-79-008)
January 1979
Distribution Category UC-90b

Surface Phenomena in the Dewatering of Coal

by

D.V. Keller, Jr., G.J. Stelma, and Y.M. Chi

Syracuse University
Department of Chemical Engineering and Materials Science
Syracuse, New York 13210

EPA/DoE Interagency Agreement No. DXE685AK
Program Element No. EHE623A

EPA Project Officer: David A. Kirchgessner

Industrial Environmental Research Laboratory
Research Triangle Park, NC 27711

DoE Project Officer: Albert F. Baker

Division of Solid Fuel Mining and Preparation
Pittsburgh, PA 15213

Prepared for

U.S. ENVIRONMENTAL PROTECTION AGENCY
Office of Research and Development
Washington, DC 20460

and

U.S. DEPARTMENT OF ENERGY
Division of Solid Fuel Mining and Preparation
Pittsburgh, PA 15213

FINAL REPORT
October 1, 1978

SURFACE PHENOMENA IN THE DEWATERING OF COAL

by

Professor D. V. Keller, Jr., Director

G. J. Stelma, Graduate Research Assistant

and

Y. M. Chi, Graduate Research Assistant

for

DEPARTMENT OF ENERGY

CONTRACT NO. ET-75-G-01-9001

Contract Officer: Mr. Albert Deurbrouck
Pittsburgh Energy Research Center
Pittsburgh, Pennsylvania 15213

Department of Chemical Engineering and Materials Science
Syracuse University
Syracuse, New York 13210
MTS-6707-DK-FR-1078

ABSTRACT

The influence of certain surfactants on the dewatering of fine coal has been investigated. The surfactants investigated were found to have a two-fold effect. They were found to effect the pressure differentials required for dewatering in addition to the residual water contents of the coal beds attainable by this dewatering. Both effects were attributed to surfactant adsorption.

Adsorption at the liquid-air interface resulted in a decrease in the interfacial tension beween the two phases. The effect this decrease had on the pressure differentials required for dewatering was found to be in agreement with that predicted by the capillary theory applied to the system.

Adsorption at the solid-liquid interface was correlated with the complex behavior of the residual water contents as a function of surfactant addition. A comprehensive model for the adsorption of the surfactants onto the coal was presented, based on the Stern-Grahame theory of adsorption at an electrical double layer. The model allowed for the mode of physisorption to change as the amount of surfactant adsorbed increased, and also for a phenomenon known as hemi-micellation. Using the model, consistent and reasonable results were found for the specific surface area of the coal and for the standard free energies of adsorption. The model was also found to be appropriate when the heterogeneous nature of the coal was considered. Furthermore, the hydrophobicity of the molecular groups of the molecules, expected from the model to be controlling the hydrophobicity of the interface, was also found to be in agreement with that predicted by other means.

TABLE OF CONTENTS

		PAGE
LIST OF TABLES		iv
LIST OF FIGURES		v
I.	INTRODUCTION	1
	Overview	1
	Background	6
II.	CAPILLARY THEORY OF DEWATERING	11
III.	COAL	16
IV.	SURFACTANTS	21
V.	ADSORPTION	27
	Stern-Grahame Theory of Adsorption	27
	Adsorption from Solution	32
	Measurement of Concentration Change	36
VI.	MATERIALS	38
	Coal	38
	Surfactants	39
	1. Aerosol A-196 (anionic)	39
	2. Triton X-114 (non-ionic)	39
	3. Dodecyl Pyridinium Chloride (cationic)	42
	4. Sodium Dodecyl Sulfate (anionic)	42
	5. Aerosol-OT (anionic)	46

VII. EXPERIMENTAL 49

Introduction 49

Pressure Dewatering (equilibrium) 51

Vacuum Dewatering (non-equilibrium) 56

Liquid-Air Interfacial Tension Measurements (γ_{LA}) 60

Liquid-Air Interfacial Tensions of Aqueous Surfactant Solutions 63

Surfactant Adsorption Experiments 65

VIII. RESULTS 67

Pressure Dewatering (equilibrium) 67

Vacuum Dewatering (non-equilibrium) 87

Liquid-Air Interfacial Tension (γ_{LA})-Concentration Curves . . 92

Influence of Coal on the Interfacial Tension of Distilled Water 97

Adsorption Isotherms 99

Standard Free Energy of Adsorption 108

IX. DISCUSSION 112

Interfacial Tension-Concentration Curves 112

Pressure Dewatering 114

The Coal-Surfactant Interaction 122

X. CONCLUSION 157

APPENDIX A 159

APPENDIX B 160

REFERENCES 166

LIST OF TABLES

TABLE NO.		PAGE
I.	GROUP HLB VALUES	26
II.	DATA FOR PRESSURE DEWATERING EXPERIMENTS	69
III.	WEIGHT OF COAL SAMPLES USED IN VACUUM DEWATERING EXPERIMENTS	88
IV.	CRITICAL MICELLE CONCENTRATION AND MAXIMUM SLOPE DETERMINED FROM THE γ_{LA}-LN C CURVES OF EACH SURFACTANT	96
V.	INFLUENCE OF COAL ON THE INTERFACIAL TENSION OF DISTILLED WATER	98
VI.	CRITICAL MICELLE CONCENTRATIONS OF AQUEOUS SURFACTANT SOLUTIONS	113
VII.	RATIO OF THE AVERAGE COAL PARTICLE RADIUS TO THE AVERAGE PORE RADIUS OF THE COAL BEDS	118
VIII.	DATA FOR CALCULATION OF THE SPECIFIC SURFACE AREA OF THE COAL BASED ON THE CAPILLARY MODEL	121
IX.	ADSORBED AREA OF SURFACTANT MOLECULES	127
X.	SPECIFIC SURFACE AREA OF THE COAL DETERMINED ON THE BASIS OF THE SURFACTANT ADSORPTION MODEL	144
XI.	SURFACTANT EFFECTIVENESS	154
B1.	DATA FOR THE ADSORPTION ISOTHERM OF AEROSOL A-196	161
B2.	DATA FOR THE ADSORPTION ISOTHERM OF TRITON X-114	162
B3.	DATA FOR THE ADSORPTION ISOTHERM OF DODECYL PYRIDINIUM CHLORIDE	163
B4.	DATA FOR THE ADSORPTION ISOTHERM OF SODIUM DODECYL SULFATE	164
B5.	DATA FOR THE ADSORPTION ISOTHERM OF AEROSOL-OT	165

LIST OF FIGURES

FIGURE NO. PAGE

1. INTERFACIAL TENSIONS AT THE POINT OF THREE PHASE CONTACT IN A CAPILLARY. 12
2. DEWATERING CURVE FOR A BED OF PARTICLES WITH A BROAD SIZE DISTRIBUTION 14
3. DEWATERING CURVE FOR A BED OF PARTICLES WITH A NARROW SIZE DISTRIBUTION 14
4. POSSIBLE ORGANIC STRUCTURE OF BITUMINOUS COAL 17
5. TYPICAL BEHAVIOR OF THE SOLUTION-AIR INTERFACIAL TENSION OF AQUEOUS SURFACTANT SOLUTIONS AS A FUNCTION OF SURFACTANT CONCENTRATION 22
6. EXAMPLE OF A SURFACTANT MOLECULE: SODIUM DODECYL SULFATE. . 22
7. POSSIBLE CROSS-SECTION OF A SPHERICAL MICELLE 24
8. POSSIBLE CROSS-SECTIONS OF BILAYER MICELLES 24
9. ILLUSTRATION OF THE ELECTRICAL DOUBLE LAYER 28
10. THE ELECTRICAL DOUBLE LAYER: VARIATION OF THE POTENTIAL WITH DISTANCE, SHOWING THE INNER AND OUTER HELMHOLTZ PLANES. 29
11. STRUCTURAL FORMULA OF AEROSOL A-196 (SODIUM DICYCLOHEXYL SULFOSUCCINATE) 40
12. MOLECULAR MODEL OF A DICYCLOHEXYL SULFOSUCCINATE ION, (SIDE AND TOP VIEW) 41
13. STRUCTURAL FORMULA OF TRITON X-114 (OCTYLPHENOXY POLYETHOXY ETHANOL). 43

FIGURE NO. PAGE

14. MOLECULAR MODEL OF TRITON X-114. 43

15. STRUCTURAL FORMULA OF DODECYL PYRIDINIUM CHLORIDE. 44

16. MOLECULAR MODEL OF A DODECYL PYRIDINIUM ION. 44

17. STRUCTURAL FORMULA OF SODIUM DODECYL SULFATE 45

18. MOLECULAR MODEL OF A DODECYL SULFATE ION 45

19. STRUCTURAL FORMULA OF AEROSOL-OT (SODIUM DI (2-ETHYLHEXYL) SULFOSUCCINATE). 47

20. MOLECULAR MODEL OF A DI (2-ETHYLHEXYL) SULFOSUCCINATE ION, (SIDE AND TOP VIEW). 48

21. TEFLON DEWATERING CELL 52

22. PRESSURE DEWATERING APPARATUS. 53

23. VACUUM DEWATERING APPARATUS. 57

24. PRESSURE DEWATERING CURVE OBTAINED FOR A 35 X 60 MESH COAL BED CONTAINING DISTILLED WATER 70

25. PRESSURE DEWATERING CURVE OBTAINED FOR A 35 X 60 MESH COAL BED CONTAINING AN AQUEOUS SOLUTION OF AEROSOL A-196; $C = 1.32 \times 10^{-6}$ MOLE FRACTION. 71

26. PRESSURE DEWATERING CURVE OBTAINED FOR A 35 X 60 MESH COAL BED CONTAINING AN AQUEOUS SOLUTION OF AEROSOL A-196; $C = 2.02 \times 10^{-6}$ MOLE FRACTION. 72

27. PRESSURE DEWATERING CURVE OBTAINED FOR A 35 X 60 MESH COAL BED CONTAINING AN AQUEOUS SOLUTION OF AEROSOL A-196; $C = 1.42 \times 10^{-4}$ MOLE FRACTION. 73

28. PRESSURE DEWATERING CURVE OBTAINED FOR A 35 X 60 MESH COAL BED CONTAINING AN AQUEOUS SOLUTION OF TRITON X-114; $C = 3.20 \times 10^{-7}$ MOLE FRACTION. 74

FIGURE NO. PAGE

29. PRESSURE DEWATERING CURVE OBTAINED FOR A 35 X 60 MESH COAL BED CONTAINING AN AQUEOUS SOLUTION OF TRITON X-114; C = 1.45 X 10^{-6} MOLE FRACTION. 75

30. PRESSURE DEWATERING CURVE OBTAINED FOR A 35 X 60 MESH COAL BED CONTAINING AN AQUEOUS SOLUTION OF DODECYL PYRIDINIUM CHLORIDE; C = 4.75 X 10^{-5} MOLE FRACTION 76

31. PRESSURE DEWATERING CURVE OBTAINED FOR A 35 X 60 MESH COAL BED CONTAINING AN AQUEOUS SOLUTION OF SODIUM DODECYL SULFATE; C = 7.20 X 10^{-6} MOLE FRACTION. 77

32. PRESSURE DEWATERING CURVE OBTAINED FOR A 35 X 60 MESH COAL BED CONTAINING AN AQUEOUS SOLUTION OF SODIUM DODECYL SULFATE; C = 2.10 X 10^{-5} MOLE FRACTION 78

33. PRESSURE DEWATERING CURVE OBTAINED FOR A 35 X 60 MESH COAL BED CONTAINING AN AQUEOUS SOLUTION OF AEROSOL-OT; C = 3.00 X 10^{-6} MOLE FRACTION. 79

34. PRESSURE DEWATERING CURVE OBTAINED FOR A 35 X 60 MESH COAL BED CONTAINING AN AQUEOUS SOLUTION OF AEROSOL-OT; C = 1.20 X 10^{-5} MOLE FRACTION. 80

35. PRESSURE DEWATERING CURVE OBTAINED FOR A 35 X 60 MESH COAL BED CONTAINING AN AQUEOUS SOLUTION OF AEROSOL-OT; C = 1.85 X 10^{-5} MOLE FRACTION. 81

36. PRESSURE DEWATERING CURVE OBTAINED FOR A 35 X 60 MESH COAL BED CONTAINING AN AQUEOUS SOLUTION OF AEROSOL-OT; C = 2.00 X 10^{-5} MOLE FRACTION. 82

FIGURE NO. PAGE

37. EFFECT OF AEROSOL A-196 ON THE AMOUNT OF AQUEOUS SOLUTION RETAINED BY THE PRESSURE DEWATERED COAL BED (ISOBARIC DATA; COAL SIZE: 35 X 60 MESH). 83

38. EFFECT OF TRITON X-114 ON THE AMOUNT OF AQUEOUS SOLUTION RETAINED BY THE PRESSURE DEWATERED COAL BED. (ISOBARIC DATA; COAL SIZE: 35 X 60 MESH). 84

39. EFFECT OF DODECYL PYRIDINIUM CHLORIDE ON THE AMOUNT OF AQUEOUS SOLUTION RETAINED BY THE PRESSURE DEWATERED COAL BED. (ISOBARIC DATA; COAL SIZE: 35 X 60 MESH) 85

40. EFFECT OF SODIUM DODECYL SULFATE ON THE AMOUNT OF AQUEOUS SOLUTION RETAINED BY THE PRESSURE DEWATERED COAL BED. (ISOBARIC DATA; COAL SIZE: 35 X 60 MESH). 85

41. EFFECT OF AEROSOL-OT ON THE AMOUNT OF AQUEOUS SOLUTION RETAINED BY THE PRESSURE DEWATERED COAL BED. (ISOBARIC DATA; COAL SIZE: 35 X 60 MESH). 86

42. EFFECT OF AEROSOL A-196 ON THE RESIDUAL AQUEOUS SOLUTION CONTENT OF THE VACUUM DEWATERED COAL BED. (ISOCHRONAL DATA AT $\Delta P = 1$ ATM; COAL SIZE: 35 X 60 MESH). 89

43. EFFECT OF TRITON X-114 ON THE RESIDUAL AQUEOUS SOLUTION CONTENT OF THE VACUUM DEWATERED COAL BED. (ISOCHRONAL DATA AT $\Delta P = 1$ ATM; COAL SIZE: 35 X 60 MESH) 89

44. EFFECT OF DODECYL PYRIDINIUM CHLORIDE ON THE RESIDUAL AQUEOUS SOLUTION CONTENT OF THE VACUUM DEWATERED COAL BED. (ISOCHRONAL DATA AT $\Delta P = 1$ ATM; COAL SIZE: 35 X 60 MESH. 90

FIGURE NO. PAGE

45. EFFECT OF SODIUM DODECYL SULFATE ON THE RESIDUAL AQUEOUS SOLUTION CONTENT OF THE VACUUM DEWATERED COAL BED. (ISOCHRONAL DATA AT ΔP = 1 ATM; COAL SIZE: 35 X 60 MESH). . . 90

46. EFFECT OF AEROSOL-OT ON THE RESIDUAL AQUEOUS SOLUTION CONTENT OF THE VACUUM DEWATERED COAL BED. (ISOCHRONAL DATA AT ΔP = 1 ATM; COAL SIZE: 35 X 60 MESH). 91

47. LIQUID-AIR INTERFACIAL TENSION OF AQUEOUS SOLUTIONS OF AEROSOL A-196 AT 25°C. [36]. 93

48. LIQUID-AIR INTERFACIAL TENSION OF AQUEOUS SOLUTIONS OF TRITON X-114 AT 25°C 93

49. LIQUID-AIR INTERFACIAL TENSION OF AQUEOUS SOLUTIONS OF DODECYL PYRIDINIUM CHLORIDE AT 25°C. 94

50. LIQUID-AIR INTERFACIAL TENSION OF AQUEOUS SOLUTIONS OF TRITON X-114 AT 25°C 94

51. LIQUID-AIR INTERFACIAL TENSION OF AQUEOUS SOLUTIONS OF AEROSOL-OT AT 25°C 95

52. LIQUID-AIR INTERFACIAL TENSION OF FIXED AMOUNTS OF AQUEOUS SOLUTIONS OF AEROSOL A-196 IN CONTACT WITH AN ADSORBENT COAL SAMPLE, TOGETHER WITH THE DATA TAKEN WITHOUT THE COAL PRESENT, FOR DETERMINATION OF THE CHANGE IN SOLUTION CONCENTRATION ON ADSORPTION. 100

53. LIQUID-AIR INTERFACIAL TENSION OF FIXED AMOUNTS OF AQUEOUS SOLUTIONS OF TRITON X-114 IN CONTACT WITH AN ADSORBENT COAL SAMPLE, TOGETHER WITH THE DATA TAKEN WITHOUT THE COAL PRESENT, FOR DETERMINATION OF THE CHANGE IN SOLUTION CONCENTRATION ON ADSORPTION. 100

FIGURE NO. PAGE

54. LIQUID-AIR INTERFACIAL TENSION OF FIXED AMOUNTS OF AQUEOUS SOLUTIONS OF DODECYL PYRIDINIUM CHLORIDE IN CONTACT WITH AN ADSORBENT COAL SAMPLE, TOGETHER WITH THE DATA TAKEN WITHOUT THE COAL PRESENT, FOR DETERMINATION OF THE CHANGE IN SOLUTION CONCENTRATION ON ADSORPTION. 101

55. LIQUID-AIR INTERFACIAL TENSION OF FIXED AMOUNTS OF AQUEOUS SOLUTIONS OF SODIUM DODECYL SULFATE IN CONTACT WITH AN ADSORBENT COAL SAMPLE, TOGETHER WITH THE DATA TAKEN WITHOUT THE COAL PRESENT, FOR DETERMINATION OF THE CHANGE IN SOLUTION CONCENTRATION ON ADSORPTION. 101

56. LIQUID-AIR INTERFACIAL TENSION OF FIXED AMOUNTS OF AQUEOUS SOLUTIONS OF AEROSOL-OT IN CONTACT WITH AN ADSORBENT COAL SAMPLE, TOGETHER WITH THE DATA TAKEN WITHOUT THE COAL PRESENT, FOR DETERMINATION OF THE CHANGE IN SOLUTION CONCENTRATION ON ADSORPTION. 102

57. ADSORPTION ISOTHERM FOR AEROSOL A-196 ON 35 X 60 MESH COAL FROM AQUEOUS SOLUTION AT 25°C. 103

58. ADSORPTION ISOTHERM FOR TRITON X-114 ON 35 X 60 MESH COAL FROM AQUEOUS SOLUTION AT 25°C. 104

59. ADSORPTION ISOTHERM FOR DODECYL PYRIDINIUM CHLORIDE ON 35 X 60 MESH COAL FROM AQUEOUS SOLUTION AT 25°C. . . . 105

60. ADSORPTION ISOTHERM FOR SODIUM DODECYL SULFATE ON 35 X 60 MESH COAL FROM AQUEOUS SOLUTION AT 25°C 106

FIGURE NO. PAGE

61. ADSORPTION ISOTHERM FOR AEROSOL-OT ON 35 X 60 MESH COAL FROM AQUEOUS SOLUTION AT 25°C. 107

62. STANDARD FREE ENERGY OF ADSORPTION FOR AEROSOL A-196 ON 35 X 60 MESH COAL AT 25°C. 109

63. STANDARD FREE ENERGY OF ADSORPTION FOR TRITON X-114 ON 35 X 60 MESH COAL AT 25°C. 109

64. STANDARD FREE ENERGY OF ADSORPTION FOR DODECYL PYRIDINIUM CHLORIDE ON 35 X 60 MESH COAL AT 25°C 110

65. STANDARD FREE ENERGY OF ADSORPTION FOR SODIUM DODECYL SULFATE ON 35 X 60 MESH COAL AT 25°C. 110

66. STANDARD FREE ENERGY OF ADSORPTION FOR AEROSOL-OT ON 35 X 60 MESH COAL AT 25°C 111

67. RELATIONSHIP BETWEEN THE LIQUID-AIR INTERFACIAL TENSION, γ_{LA}, OF THE AQUEOUS SOLUTION PRESENT IN THE COAL BED AND THE PRESSURE DIFFERENTIAL, ΔP, AT WHICH THE RESPECTIVE DEWATERING CURVE HAD ITS MAXIMUM SLOPE. 115

68. GENERAL BEHAVIOR OF THE STANDARD FREE ENERGY OF ADSORPTION FOR SURFACTANT ADSORPTION ON COAL. 130

69. POSSIBLE ADSORBED BILAYER OF SURFACTANT MOLECULES WITH TWO HYDROCARBON CHAINS PER MOLECULE 134

70. ADSORBED LAYER OF DODECYL PYRIDINIUM IONS SHOWING AN ALTERNATE ORIENTATION FOR THE MOLECULES 138

71. CLOSELY PACKED ADSORBED LAYER OF DODECYL PYRIDINIUM IONS. 138

72. POSSIBLE "L" CONFIGURATION OF THE ADSORBED TRITON X-114 MOLECULE AT THE POINT OF CROWDING 142

FIGURE NO. PAGE

73. CHANGE IN THE ADSORBED AREA PER TRITON X-114 MOLECULE TO ACCOMODATE MORE ADSORBED MOLECULES. 142

74. PORTION OF A HYPOTHETICAL REAL COAL SURFACE WITH TEN POSSIBLE ADSORPTION SITES. 150

75. PORTION OF A HYPOTHETICAL REAL COAL SURFACE WITH ADSORBED WATER MOLECULES 150

76. PORTION OF A HYPOTHETICAL REAL COAL SURFACE WITH AN ADSORBED LAYER OF ANIONIC SURFACTANT MOLECULES 152

77. PORTION OF A HYPOTHETICAL REAL COAL SURFACE WITH THE ADSORBED ANIONIC SURFACTANT MOLECULES IN THE HEMI-MICELLE STATE. 152

I. INTRODUCTION

Overview

The presence of water in coal prior to its utilization as a source of energy can, for the most part, be considered as an undesirable impurity. The reasons are almost too numerous to list; however, one needs only to consider that the purpose of the coal is energy conversion, and water present during this conversion consumes energy for evaporation. Furthermore, coal is normally transported many millions of ton-miles per yearly production at a considerable cost. If ten percent of this coal transport cost were due to water, virtually millions of dollars are wasted moving unnecessary water back and forth across the country just to have that water, in the end, reduce the utilization efficiency of the coal. Certainly the total elimination of the water problem under the present conditions appears to be beyond our grasp since water not only forms a structural part of natural coal, but water also inundates most of the coal mines, it is the basis of our beneficiation schemes and furthermore the weather continually drenches the stockpiles and open transport facilities. A more detailed inspection of the problem, on the other hand, does point to certain areas where an understanding of the physio-chemical phenomena of water adhesion to coal could in some degree improve the situation, particularly in the beneficiation of fine coal. Water in coal may exist in three forms [1]:

a. Surface water - that water which lies on the surface of the coal and has a vapor pressure with its surroundings which is very nearly equivalent to the equilibrium vapor pressure of water.

b. Capillary water - sometimes called "inherent water" or structural water" is that water which is absorbed into the capillary structure of the coal itself. The capillary diameters of coal (average 40 Å) vary in size according to the age of the coal, i.e., the average pore diameter in anthracite is exceedingly small and that for western coal (Wyoming) is relatively quite large. The water contents in this class vary from much less than one percent to in excess of thirty percent, respectively. The vapor pressure of water in the capillary system is less than that of the surface system of (a) by virtue of the Kelvin equation [2].

c. Chemical water - those water molecules held in chemical structure such as Heulandite($(Ca,Na)_2Al_2Si_7O_{18}\cdot 6H_2O$). This water is usually involved with certain minerals in coal and is rarely measured since total dehydration will only occur at temperatures well above the decomposition point of coal.

An investigation of the dewatering of coal, in order to retain a practical stance, must be concerned only with the first class of water cited above, surface water, since only the severest of thermal drying treatments will achieve a substantial degree of capillary dewatering.

The surface moisture on coal can vary from zero to greater than thirty percent depending on the following variables [3]:

a. Rank of coal

b. Ambient relative humidity

c. Mineral composition and concentration in the sample

d. Particle size distribution

e. Temperature

f. Mechanical treatments

g. Water impurities

h. Prior treatments, e.g., oxidation, chemical additives, etc.

all of which tend to reflect the surface states of the system and the adhesion of water to coal.

For example, freshly mined anthracite coal which has a hydrophobic, oil-like,surface [4] and a particle size distribution between 1.3 and 0.8 cm will retain less than two percent water by simple mechanical agitation of the mass on a vibrating screen since the void spaces between the particles are too large to retain a significant amount of water by capillarity and the coal surface tends to reject the water. On the other hand, well aged Iowa coal with a particle size distribution of 0.25 mm x 0 would be most difficult to dewater below twenty-five percent water even in a centrifuge, since in this case we have a coal surface readily wetted by water (hydrophilic) and a fine particle system which establishes a small interparticle capillary system which will also aid in the retention of the water. The effects of the interparticle capillary system on moisture retention in a body have been under investigation by ceramists and soil engineers for years [4]. Coal preparation engineers have also been faced with similar problems in that shaker screens and vibrating screens will usually dewater coal particles greater than or equal to one centimeter in diameter to about five percent water, but for coal with size distributions below

0.6 mm x 0,* and dependent on the amount of 0.07 mm x 0 material, the dewatering process rarely achieves water contents below twelve percent. Filtration and centrifugation which are usually used when large concentrations of 0.1 mm x 0 coal are present, incur similar problems even though the forces on the liquid are higher. Discharge from these devices rarely is below fifteen percent moisture under ambient conditions.

Deurbrouck [5] demonstrated that, in general, as the coal size was reduced the pyritic sulfur (as the mineral FeS_2) release for eventual separation from the relatively clean coal, was increased. Single stage water froth flotation which has been commonly used in very fine coal cleaning (0.6 mm x 0) has been recently expanded to a more efficient system called "double froth flotation" [6]. In both cases the product coal is less than 0.6 mm x 0 with a large concentration of very fine material, the mass of which must be dewatered preferably to below ten percent moisture to meet today's specifications. The tendency in the industry today is to clean large quantities of 0.6 mm x 0 coal and bear the expense of thermal drying.

The present investigation viewed the water problem from the standpoint of the surface phenomena involved. The problem lies with the adhesion of the water to the solid surface and the molecular interactions that occur along the coal-water interface. Furthermore,examination of the list of variables "a" through "h" which influence surface moisture revealed that the last one, i.e., prior treatments, and in particular "chemical additives" seemed to be where the most control over this system could be exercised. That is, if the simple addition of a chemical could to a

---

*This refers to the size distribution of particles which have passed through a sieve whose hole size was 0.6 x 0.6 mm. The maximum size is 0.6 mm and the minimum size is zero, i.e., sub-micron dust particles.

large degree alter the affinity of water for the coal surface, then the water retention might be readily decreased. Furthermore, if this could be accomplished at a very low concentration of that chemical, then the economics would be favorable for utilization. The above direction was also influenced by the knowledge that certain classes of chemical compounds are known to effect remarkable changes in interfacial properties. Also, some attempts, reported in the literature, have been made to use them for the improvement of coal dewatering as shall be discussed in detail below. These compounds are known as surfactants. The present investigation is concerned with their effect on coal dewatering and the reasons for which their influence is felt.

Surfactants were chosen specifically for two reasons. First, they are known to decrease the interfacial tension of the air-water interface drastically at extremely low concentrations. In terms of overcoming the capillary forces of a bed of small granulated particles this interfacial tension is proportional to the work required to displace the liquid. Any improvement is worthwhile.

Secondly, similar molecules have been used by the mineral industry in the area of ore flotation [7]. In this case the molecules are absorbed at the surface of a mineral and render it hydrophobic such that through the attachment of air bubbles the particles are caused to float to the surface of the liquid where they are recovered. Such molecules change a hydrophilic surface to hydrophobic.

Background

Dewatering is a process whereby liquid held by capillary forces within the interparticle voids of a bed of fine particles is displaced by the application of desaturating forces. These forces can be applied, for example, by centrifugation in which case they act on the body of the liquid to pull the liquid out, or through the presence of a gas pressure differential across the bed, which if an over-pressure pushes the liquid out or if a vacuum, the liquid is drawn out. In each case there is always a certain amount of liquid retained in the bed. Investigations of dewatering may address either the process of achieving final water content or studying the final value irrespective of the process, or both.

In general, factors which can influence the dewatering are particle size, particle shape, mode of particle packing, dimensions of the bed, density and viscosity of the fluids (i.e., displacing gas and displaced liquid), temperature, pressure gradient, rate of displacement, and the interfacial tensions at the liquid-air and solid-liquid interfaces [8]. Considerable effort has been involved in the investigation of the above variables for a variety of bed materials, but surprisingly little work has been applied specifically to coal.

Dewatering, in general, can be considered from the viewpoint of the theory of flow through saturated porous media, specifically packed beds of particles. Briefly, the theory utilizes the modified Darcy equation:

$$Q = \frac{KA\Delta P}{\eta L} \qquad (1)$$

where

Q = fluid flow

A = cross-sectional area of the bed

ΔP = pressure differential across the bed

η = viscosity of the fluid

L = bed thickness

K = bed permeability

$$= 1/a = m^2 \varepsilon k \tag{2}$$

a = specific bed resistance

m = mean hydraulic radius

ε = porosity

k = empirical constant

Equation (2) was developed by Kozeny [9] and confirmed by Carman [10] for beds of many solids. The theory becomes applicable to dewatering when two-phase flow is considered, where one is liquid (water) and the other is air. This approach to dewatering has been considered by Brownell and Katz [11] and Dombrowski and Brownell [12] for a variety of materials and by Silverblatt and Dahlstrom [13] for beds of fine coal in particular.

However, as pointed out by Gray [3] this semi-empirical approach to dewatering is not satisfactory for a complete description of the situation. A major objection was that the flow theory need not consider the actual distribution of pore sizes of the packed bed, to be applied. It just resolves the entire distribution into a single "mean hydraulic radius", m, and characterizes the bed by an overall permeability K. The flow theory, therefore, describes flow "through" a bed not "from" a bed. Actually, as dewatering proceeds, the system through which the liquid flows changes according to the distribution of the pores of the bed yet to be emptied. Initially dewatering is governed by the larger pores and the retention of

the liquid by the smallest pores in addition to other modifying factors.

One of these other factors which is not adequately considered by the flow theory is the nature of the interfaces that are involved in the system, i.e., the liquid-gas, liquid-solid, and solid-gas interfaces. This is especially critical in dewatering, as there is contact of all three phases at the point where the liquid is retracting from the solid. Furthermore, interfacial tensions are thermodynamic quantities and as such are defined under equilibrium conditions which may not be reflected by consideration of a dynamic flow situation.

For such reasons and especially because specific surface phenomena are not appreciated by the flow treatment of dewatering it was decided, like Gray, to approach dewatering from the viewpoint of capillary theory which does allow the treatment of interfacial effects. This approach will be treated in detail below.

Only a few attempts have even considered the role of specific interfacial phenomena involved in coal dewatering. Those investigations [3,13-15] which did involve interfacial parameters most usually were limited to the liquid-air interface and the effect of decreasing its tension. Some research employed the use of a class of substances known as surfactants in this endeavor; however, little attention was given to their effect at the solid (coal)-liquid (water) interface. Some speculations were made [3,13-15].

Silverblatt and Dahlstrom [13] in 1954 investigated the effect of liquid viscosity and the liquid-air interfacial tension on the moisture content of a dewatered fine-coal filter bed. Their investigation involved the addition of the surfactants Tergitol-CW and Aerosol-OT in solution to the feed coal. They found that the addition of those surfactants re-

sulted in a lower residual moisture content of the dewatered coal product, and speculated that the effect was probably not due to the change in the liquid-air interfacial tension, which they found to have a less pronounced effect than viscosity on the dynamics of dewatering, but rather from some kind of solid surface reaction between the surfactants and the coal.

Gray [3] in 1958 investigated the dewatering of fine coal from the point of view of capillary theory and measured the equilibrium water contents of saturated coal beds after incrementally applying a pressure differential across the bed. The dewatering rate, the dewatering behavior of various narrow size distributions, and the addition of several flocculants, oils, and wetting agents (surfactants) were investigated. Gray found that dewatering was improved by each of the above additions; and he alludes to the fact that the efficacy of several highly impure oils in dewatering may be due to their content of surface active materials. Furthermore, the wetting agents, which were assumed only to lower the liquid-air interfacial tension of the liquid, also improved the final moisture content of the beds. Gray also noted that the liquid-air interfacial tensions of the expelled solutions were higher than that originally introduced to the bed and concluded that the wetting agents were removed from the solution by strong adsorption to the coal surface.

Dolina and Kaminskii [14] in 1971 reported the effect of the addition of a number of surfactants each on the residual moisture content of vacuum filtered coal beds. They found that the residual water contents were as likely to increase as well as decrease depending upon which surfactant was used. Again the authors only speculate that the effect might have something to do with adsorption of the surfactants by the coal, and not

be wholly dependent on the decrease in the liquid-air interfacial tension.

Finally, Nicol [15] recently (1976) has observed improvement in dewatering of coal with the addition of surfactants and also speculates on a solid surface interaction.

However, no controlled experiments have been found in the literature concerning the adsorption of surfactants by coal or an attempt at a correlation with gross dewatering phenomena.

II. CAPILLARY THEORY OF DEWATERING

If we consider a bed of fine particles, such as coal, less than a millimeter in diameter, when partially immersed in water, the bed will act as a bundle of capillary tubes and cause the water to be drawn up into that system of pores. The removal of this water involves the application of a force to initiate flow out of the system.

If we consider the general case for one capillary, the force per unit area necessary to counteract the capillary pressure within a capillary of radius r is given by the capillary equation

$$\Delta P = \frac{2\gamma_{LG} \cos \theta}{r} \qquad (3)$$

where ΔP is the pressure differential across the capillary, γ_{LG} is the interfacial tension of the liquid at the gas (air) interface and Θ is the receding contact angle between the capillary wall and the liquid [16]. The contact angle, Θ, is defined by Young's equation

$$\gamma_{SG} = \gamma_{LG} \cos \Theta + \gamma_{LS} \qquad (4)$$

at the point of three phase contact, as shown in Figure 1 where γ_{SG} is the interfacial tension of the solid-gas interface and γ_{LS} is that of the liquid-solid interface. There is considerable evidence in the literature [17] to permit the assumption that the receding contact angle of water on coal is zero, and the capillary equation may, therefore, be written as

$$\Delta P = \frac{2\gamma_{LG}}{r} \qquad (5)$$

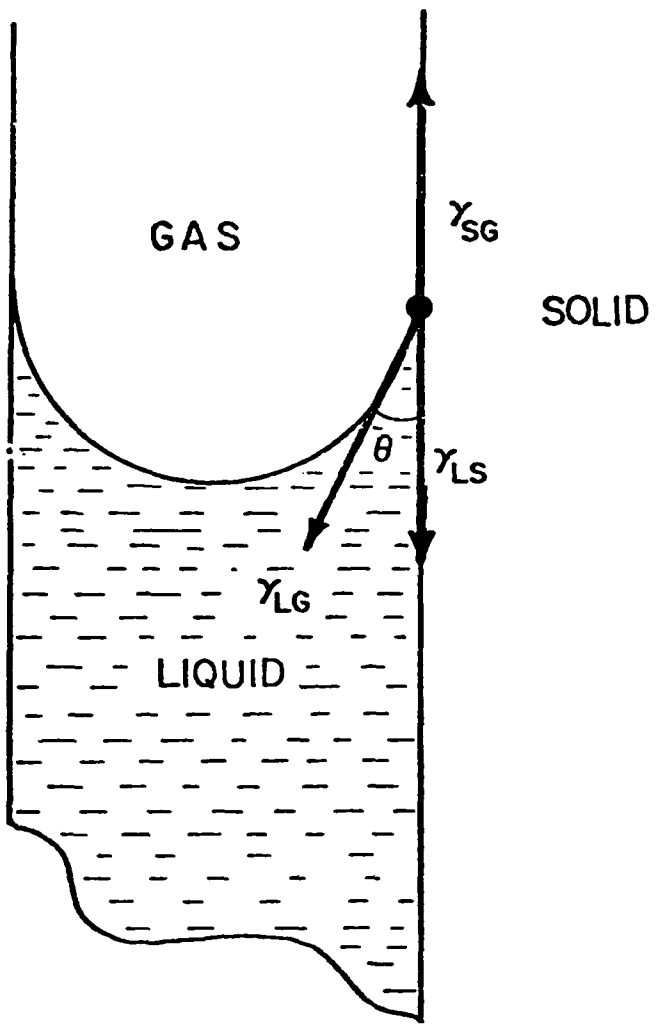

FIGURE 1. INTERFACIAL TENSIONS AT THE POINT OF THREE PHASE CONTACT IN A CAPILLARY.

We are now going to assume that a bed of coal particles acts as a bundle of straight capillaries so that the above equation may be applied. Later we will examine the validity of this assumption. One recognizes that capillaries of radius r, within the coal bed, will drain with the application of an applied pressure differential, ΔP, just greater than $2\gamma/r$ while no drainage will occur when $\Delta P = 2\gamma/r$ since the capillary and applied forces are equal.

If there is a wide distribution of particle sizes in the bed there will also be a wide variation of pore radii within the bed; and consequently, a wide range of pressures will be necessary to dewater the entire system. A plot of the amount of retained water in the coal bed as a function of applied pressure differential, i.e., a dewatering curve, will reflect the real pore radii distribution. If we assume, for instance, that the particles are uniform spheres and are arranged in a close packed structure, then the radius, r_A, of the enclosed spherical void surrounded by the tetrahedral arrangement of particles is 0.225 r_B, where r_B is the solid particle radius, so that the ratio of particle radius to pore radius is 4.44. If there is a range of r_B, there will also be a range of r_A; consequently, for a broad particle size distribution, a dewatering curve would resemble Figure 2. However, if the particle size distribution is narrowed, as was established for the experiments reported herein, then r_A will be relatively constant, and therefore a great amount of dewatering will occur in an extremely narrow pressure range as shown in Figure 3, which would be a step function in an ideal case, where r was single valued.

Due to the inverse proportionality between r and ΔP in Equation (5), a coal bed with uniform large pores, i.e., large particles, will de-

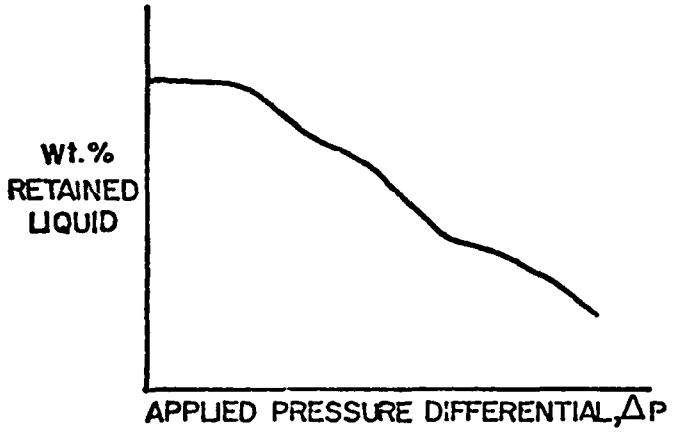

FIGURE 2. DEWATERING CURVE FOR A BED OF PARTICLES WITH A BROAD SIZE DISTRIBUTION.

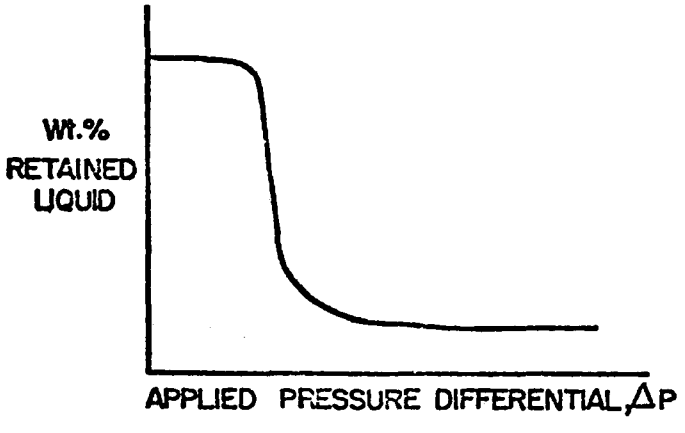

FIGURE 3. DEWATERING CURVE FOR A BED OF PARTICLES WITH A NARROW SIZE DISTRIBUTION.

water at lower values of applied pressure differential and a bed with small pores at higher values of applied pressure differential. Equilibrium dewatering curves like that of Figure 3, were, in fact, observed in the experiments performed.

III. COAL

Coal can be considered to be composed of two classes of constituents. The first, the carbonaceous material, is a highly complex matrix of organic molecules with an empirical formula which may be roughly given as $C_{135}H_{97}O_9NS$ for a typical low volatile bituminous coal [18]. The second constituent comprises the inorganic mineral matter, for example, iron pyrite, illite, silica, montmorillonite, and various other slates, clays, and rock matter.

Coal is the result of the natural application of heat and pressure, without air, on the vegetation found in tropical prehistoric forests. Coalification, i.e., the degree of transformation, appears to follow the sequence beginning with peat, through sub-bituminous, bituminous, and semi-anthracite to anthracite and eventually to graphite. The subcategories are called the rank of coal. The main change through the series is in the relative amount of carbon present, which increases in the order presented.

Based on evidence from standard analytical techniques a hypothetical organic structure of low volatile bituminous coal can be imagined. An element distribution and sketch of such a structural unit is shown in Figure 4, as conceived by Bailey [18]. The structure consists of clusters of condensed aromatic rings linked by cycloaliphatic rings, with peripheral etherial oxygen and hydroxyl groups. The organic part of the coal surface alone therefore can present three distinct regions.

On a macroscale, the organic matter in coal is also considered as composed of a multiphase system called macerals [19] which are further

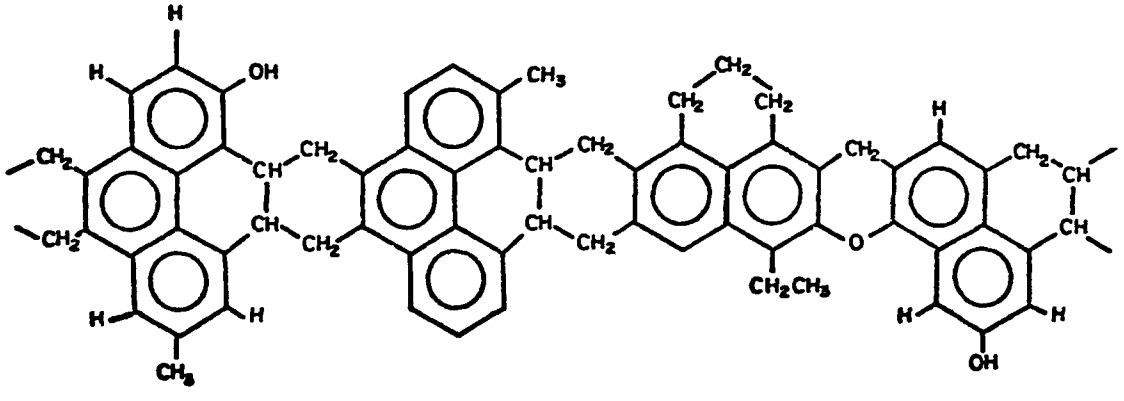

FIGURE 4. POSSIBLE ORGANIC STRUCTURE OF BITUMINOUS COAL

classified as fusain, clarain, durain, and vitrain. Although these classes are based on morphological appearances they certainly reflect gross modifications in their respective chemical systems relative to hydrocarbon distributions as well as mineral matter contents.

The inorganic mineral matter content of coal also consists of numerous unique phases, part distinct from the hydrocarbon system and part directly associated with the complex molecular arrangements.

A common example of the mineral matter present in coal is contained in a group called illite. Illite is considered a variation of muscovite, which is a hydrated silicate of aluminum, with replacement atoms of potassium or magnesium. The clay minerals possess complex crystal structures and atomic arrangements. For example, montmorillonite, also a relative of illite, is a clay which is made of layers of silicon oxide (SiO_4) tetrahedrally arranged such as to share corners with octahedrally arranged aluminum ions (Al^{+3}) which in turn have coordinated oxygen and hydroxyl groups. Molecules of water lie in between the layers of silicate sheets.

A prevalent non-oxide mineral found in coal is iron pyrite, FeS_2, an ionic solid, and a crystal modification of FeS_2 called marcasite.

All the crystalline solids found in coal can present their various crystal planes, structures and compositions to their free surfaces.

A sample of coal then may be regarded as being an exceedingly hetrogeneous material with surface characteristics which must be at least as complex as the bulk chemistry.

Due to the fact that there is an abrupt discontinuity at a surface, the balanced chemical bond configurations which exist in the bulk solid

do not necessarily exist at the free surface. Charge neutrality is altered, and bonds may be left "dangling" at the surface [20]. The surface attempts to satisfy this imbalance and lower the overall free energy; however, certain surface potentials remain. These potentials are reflected in the behavior of liquids in contact with the free surfaces and are measured as a zeta potential [21], i.e., the potential difference between a point well removed from the surface, in field free space, and a point in the liquid shear plane adjacent to that surface. Note should be taken that the zeta potential only refers to the liquid adjacent to the surface and not the potential determining ions or atoms in the solid surface itself. Cambell and Sun [22] have determined the zeta potential of whole coal and its lithotypes and found that it varies for each type from -30 millivolts to 0 millivolts in a neutral aqueous solution. Silica [23] is reported to have a negative and alumina a positive potential [23]. Pyrite has a negative zeta potential in neutral aqueous solution and its change with pH has been found similar to that of coal [24]. The components of the coal exhibit different signs and magnitudes of surface potential; and therefore, the surface system of coal may be regarded as electrostatically heterogeneous.

Coal should be considered as a solid gel consisting of a framework enveloping many pores throughout the system. These pores or capillaries vary in diameter from approximately 2 to 1000 angstroms in diameter with an average of about 40 Å depending on the rank of the coal. The system generates between 100 - 200 m^2/g of surface area again depending on the rank (age) of the coal. The possible interaction of the coal with any other molecules, for example during an adsorption process, could well be influenced by the pore distribution, that is, molecules larger than the

pore diameter cannot penetrate the outer surface while smaller molecules may envelope the whole system. The problem is carefully examined in a recent paper [25] where the discrepancy of coal specific surface areas determined by gas adsorption (BET) for different gases was considered. The problem primarily lies in the fact that there is a distribution of pore sizes which apriori is unknown.

In conclusion, therefore, the coal surface can be considered as being chemically, electrostatically and topographically heterogeneous.

IV. SURFACTANTS

Surfactants are ionic or polar derivatives of high molecular weight hydrocarbons. They are rather unique in that they are amphiphilic substances, that is one part of the molecule has an affinity for water, which is termed hydrophilic, and another has an oil affinity, which is termed hydrophobic. The hydrophilic portion is often referred to as the "head" and the hydrophobic hydrocarbon chain as the "tail" of the molecule. The name surfactant is just a convenient contraction of "surface active agent".

The amazing property of surfactants is that as solutes in aqueous solution, even at extremely small concentrations, they produce a dramatic decrease in the liquid-air interfacial tension of the solution, e.g. 72 dyn/cm for pure water to 30 dyn/cm for concentrations in water as small as 10^{-4} mole fraction. An example of a surface active agent is common toilet soap or household detergents. A solution-air interfacial tension curve as a function of concentration for typical aqueous surfactant solutions is illustrated in Figure 5.

Surfactant molecules are usually anisotropic in shape. Many are usually considerable in length but limited in width. An example is sodium dodecyl sulfate shown in Figure 6.

There are two main classes of surfactants: ionic and non-ionic. The ionic class is composed of two sub-classes, anionic and cationic. After ionization of a surfactant molecule in water the charge on the hydrocarbon portion of the molecule establishes the nomenclature of the parent molecule. For example, an anionic surfactant is sodium

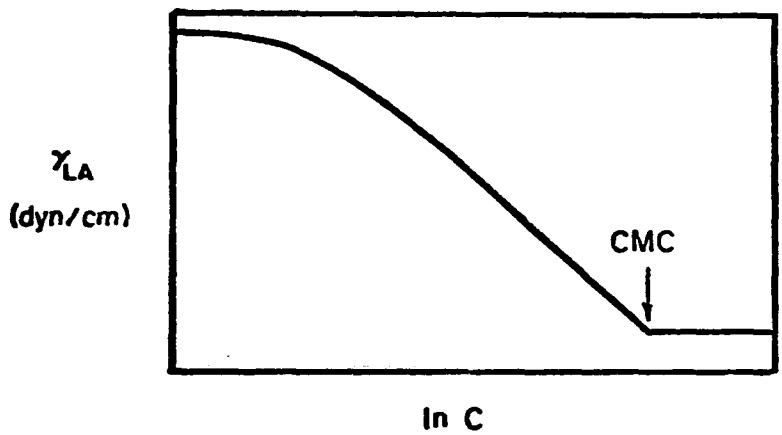

FIGURE 5. TYPICAL BEHAVIOR OF THE SOLUTION-AIR INTERFACIAL TENSION OF AQUEOUS SURFACTANT SOLUTIONS AS A FUNCTION OF SURFACTANT CONCENTRATION.

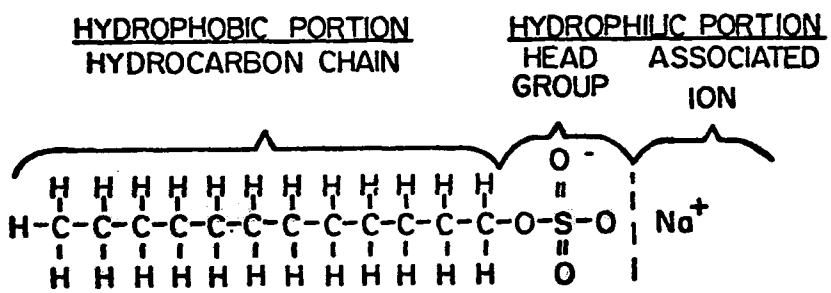

FIGURE 6. EXAMPLE OF A SURFACTANT MOLECULE: SODIUM DODECYL SULFATE.

dodecyl sulfate, where

$$CH_3(CH_2)_{11}SO_4^-$$

is the anionic portion. An example of a cationic surfactant is dodecyl pyridinium chloride where

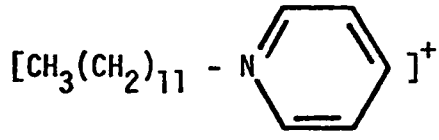

is the cationic portion.

Non-ionic surfactants usually have hydroxyl groups and/or polyoxyethylene chains as the hydrophilic portion of the molecule. Polyoxyethylene p - tertoctylphenyl ether is an example:

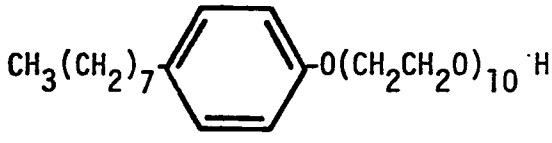

where the $(CH_2CH_2O)_{10}$ group is the polyoxyethylene chain.

Another unique property of surfactants is that as their number in aqueous solution is increased a point is reached when it is energetically favorable to form an aggregate, or precipitate , of the monomers. This aggregate or colloidal particle is called a micelle. The concentration at which this occurs is termed the "critical micelle concentration" and is frequently abbreviated CMC. One example of the structure of a micelle is shown in Figure 7. The hydrophobic hydrocarbon chains are directed toward the inside of the micelle remote from the water-based phase, and the polar head groups are on the outside of the particle as illustrated.

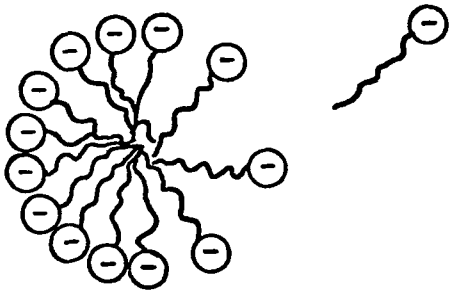

FIGURE 7. POSSIBLE CROSS-SECTION OF A SPHERICAL MICELLE.

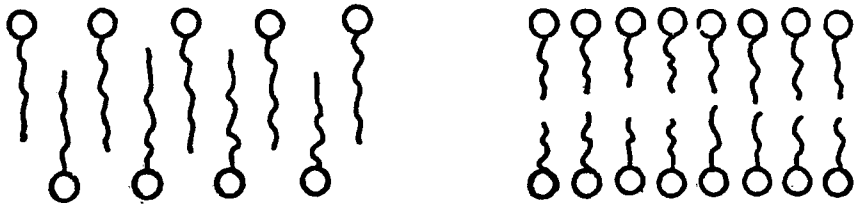

FIGURE 8. POSSIBLE CROSS-SECTIONS OF BILAYER MICELLES.

Micellation is actually a phase separation process and the product is not necessarily spherical. Included among the configurations possible [26] is also a bilayer arrangement as shown in Figure 8. Micelle formation is a direct result of the dual nature of the molecules with their antipathetic affinity for water. Another consequence of the dual nature leads to adsorption of the molecules at the solution-air interface. The hydrocarbon portions of the molecule oppose the solubility of the whole molecule and try to alleviate the high hydrocarbon-water interfacial energy by moving to the free surface where the hydrocarbon portion of the molecule extends as far out of the water as is physically possible. This is also the case at any other interface in contact with the solution, e.g. any solid-liquid interface. When adsorption at interfaces can no longer reduce the free energy of the system as the solute concentration increases the hydrocarbon chains associate in the bulk solution proceeding to "micellation".

Griffin [27] and Davies [28] suggested a utilitarian way of classifying surfactants based on the relative sizes and strengths of the hydrophilic and lipophilic (oil preference) groups of the molecules which is called the Hydrophile-Lipophile Balance, abbreviated HLB. The HLB is a number calculated for each surfactant as

$$HLB=\Sigma(\text{values for hydrophilic groups})-\Sigma(\text{values for hydrophobic groups}) + 7$$

Some group values are given in Table I. The HLB system was devised to organize much of the disjointed information about surfactants in order to formulate a rational method of using them for controlling oil-water

emulsions. Although detailed use of this concept was not applied in this study, the HLB index does provide a way of comparing the relative hydrophobicity of surfactants; and consequently, a partial measure of their willingness to adsorb at interfaces and once adsorbed a measure of the water affinity of its adsorbed film.

TABLE I

GROUP HLB VALUES [29]

HYDROPHILIC GROUPS	HLB	LIPOPHILIC GROUPS	HLB
$-SO_4$ Na	38.7	-CH-	
-COO K	21.1	$-CH_2-$	0.475
-COO Na	19.1	$-CH_3-$	
Sulfonate	11.0	-CH=	
-N (tertiary amine)	9.4		
-COOH	2.1		
-OH (free)	1.9		
-O-	1.3		
-OH (sorbitan ring)	0.5		

V. ADSORPTION

Stern-Grahame Theory of Adsorption

The surfactant molecules in a water-solid system are greatly influenced by the charge state of the solid surface, i.e., the electrical double layer which is formed in the solution.

According to the Stern treatment [30], the electrical double layer region that lies at the solid-liquid interface can be envisioned as a compact and a diffuse type of ion arrangement. If the solid surface has a net electric charge then that field in an ionic solution will attract a balancing charge from ions in that solution. The ions form two regions adjacent to the surface. The first consists of adsorbed ions which is called the "Stern layer". The second is a more diffuse layer which is known as the "Gouy layer". The sum of the charges in all of the layers counter balances that charge in the solid surface. A sketch of the arrangement is shown in Figure 9, where the solid is shown with a positive charge due to those ions of the solid at its surface. Adsorbed at the surface sites are the negative ions from the solution, i.e., the Stern layer. The charge density in the solution is presumed to decrease exponentially from the solid surface. Also shown is the probable layer of shear in which a measureable potential is obtained which is called the zeta potential.

Grahame [31] modified the Stern theory by subdividing the Stern layer into two planes depending on the state of hydration of the adsorbed ions. These are known as the inner and outer Helmholtz planes, and are shown in Figure 10.

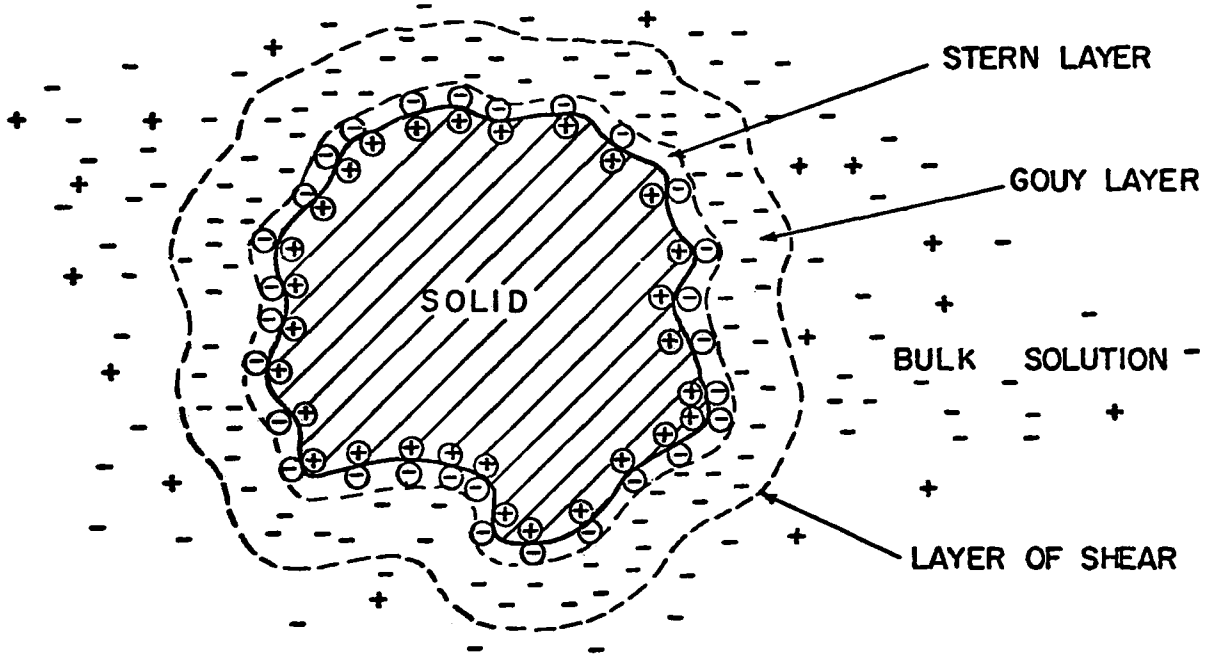

FIGURE 9. ILLUSTRATION OF THE ELECTRICAL DOUBLE LAYER

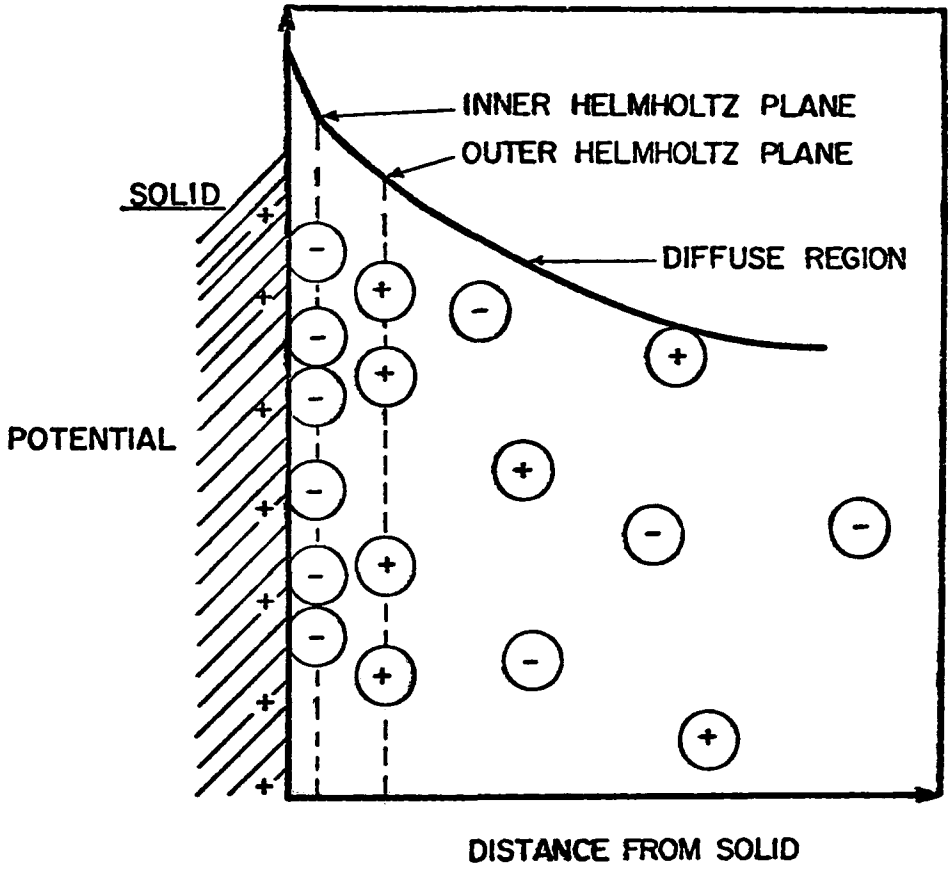

FIGURE 10. THE ELECTRICAL DOUBLE LAYER: VARIATION OF THE POTENTIAL WITH DISTANCE, SHOWING THE INNER AND OUTER HELMHOLTZ PLANES.

The more specific treatment established by Grahame was used in the analysis of the adsorption of the surfactant molecules at the coal-water interface. According to this treatment adsorption of ions at an electrical double layer can be described according to the following relationship, for each type of ion adsorbed:

$$\Gamma = 2r\ C\ \exp(-\Delta G^{o}_{ADS}/RT) \qquad (6)$$

where Γ is the number of moles of the ion adsorbed per square centimeter of surface, r is the radius of the non-solvated ion, C is the concentration of the ion in solution, ΔG^{o}_{ADS} is the standard free energy of adsorption, R is the gas constant, and T is the absolute temperature.

The standard free energy of adsorption, ΔG^{o}_{ADS}, is defined as

$$\Delta G^{o}_{ADS} = (\mu^{o}_{i})^{s} - \mu^{o}_{i} \qquad (7)$$

where $(\mu^{o}_{i})^{s}$ is the chemical potential of the ith species in standard state at the surface and μ^{o}_{i} is that chemical potential in the bulk solution at standard state.

The standard free energy of adsorption can be considered [23] as the summation of all the interaction energies involved in the adsorption; for example,

$$\Delta G^o_{ADS} = \Delta G^o_C + \Delta G^o_{chem} + \Delta G^o_{HC} + \Delta G^o_{solv} + \Delta G^o_{polar} \cdots \qquad (8)$$

where ΔG^o_C is the electrostatic (coulombic) contribution, ΔG^o_{HC} represents the association of hydrocarbon chains of adsorbed molecules (surfactants) at the interface, ΔG^o_{chem} represents the formation of any covalent bonds with the surface, ΔG^o_{solv} the contribution of solvation effects on the water soluble portion of the molecule, and ΔG^o_{polar} represents the contribution of any polar interaction with the surface for polar molecules. Of these only the electrostatic, hydrocarbon association, and chemical interactions in the adsorption have been investigated.

For the electrostatic interactions

$$\Delta G^o_C = vF\psi \qquad (9)$$

where v is the valence of the adsorbate including sign, F is the Faraday constant, and ψ is the potential in the Stern plane.

The hydrocarbon chain interaction is

$$\Delta G^o_{HC} = n\phi \qquad (10)$$

where ϕ has been evaluated [32] to be about 0.6 kcal/mole for each $-CH_2-$ component of the hydrocarbon chain and n is the number of components in that chain.

Adsorption From Solution

The experimental measurement in adsorption from solution is the change in concentration of the solution from which molecules are adsorbed. Since concentration changes are involved, one must be aware of the fact that more than one component is present and able to adsorb. There exists, therefore, a competition between components for adsorption sites on the solid.

Let us define adsorption from a two component solution on a more rigorous basis. Consider a solution of n_1 moles of solute and n_2 moles of solvent where

$$n_1 + n_2 = n \tag{11}$$

and the mole fractions are given by

$$X_1 = \frac{n_1}{n} \qquad X_2 = \frac{n_2}{n} \tag{12}$$

and $X_1 + X_2 = 1$. If to this solution we add w grams of a second phase, e.g., a solid, some fraction of each component of the solution will adsorb to the solid surface, i.e., n_1^s moles of component 1 per gram of solid and n_2^s moles of component 2 per gram of solid. The adsorbed molecules will deplete the solution phase of their respective components to new values n_1' and n_2' such that

$$n_1 = n_1' + n_1^s w$$

$$n_2 = n_2' + n_2^s w \tag{13}$$

Let us define

$$n_1' + n_2' = n' \tag{14}$$

where n' is the total number of moles remaining in the depleted solution phase, and

$$X_1' = \frac{n_1'}{n'} \tag{15}$$

where X_1' is the mole fraction of solute remaining in the solution phase. Therefore, we can write for the change in solution solute mole fraction on adsorption

$$\Delta X = X_1 - X_1' = \frac{n_1}{n} - \frac{n_1'}{n'} \tag{16}$$

or

$$\Delta X = \frac{(n_1' + n_1^s w)}{(n_1' + n_2' + n_1^s w + n_2^s w)} - \frac{n_1'}{(n_1' + n_2')} \tag{17}$$

and accumulating terms and rearranging

$$\Delta X = \frac{n_1'^2 + n_1'n_2' + n_1'n_1^s w + n_2'n_1^s w - n_1'^2 - n_1'n_2' - n_1'n_1^s w - n_1'n_2^s w}{(n_1' + n_2')\ (n_1' + n_2' + n_1^s w + n_2^s w)} \tag{18}$$

$$\Delta X = \frac{n_2'n_1^s w - n_1'n_2^s w}{(n_1' + n_2')n} \tag{19}$$

Rearranging

$$\frac{n\ \Delta X}{w} = \frac{n_2'n_1^s - n_1'n_2^s}{n_1' + n_2'} \tag{20}$$

$$\frac{n\ \Delta X}{w} = n_1^s\left(\frac{n_2'}{n_1' + n_2'}\right) - n_2^s\left(\frac{n_1'}{n_1' + n_2'}\right) \tag{21}$$

$$= n_1^s\left(\frac{n_2'}{n'}\right) - n_2^s\left(\frac{n_1'}{n'}\right) \tag{22}$$

$$= n_1^s X_2' - n_2^s X_1' \tag{23}$$

Also $X_2' = (1 - X_1')$, so in terms of X_1', the mole fraction of solute remaining in solution,

$$\frac{n\ \Delta X}{w} = n_1^s(1 - X_1') - n_2^s X_1' \tag{24}$$

The term $n\,\Delta X/w$ plotted as adsorption provides an isotherm composed of the sum of the two individual isotherms of components 1 and 2. A problem exists in separating the two isotherms. Since there are two unknowns, n_1^s and n_2^s, without more information relating them no solution is possible.

However, in the case of very dilute solutions an approximation can be made. When X_1' is very small the number of moles of component 1 adsorbed is approximately

$$n_1^s \simeq \frac{n\Delta X}{w} \tag{25}$$

Even if n_2^s is large, the product $n_2^s X_1'$ is small enough in relation to $n_1^s(1 - X_1')$ to be dropped. Furthermore

$$n_1^s(1 - X_1') \simeq n_1^s \tag{26}$$

because $(1 - X_1')$ is approximately one. The situation is well approximated for values of $X_1' \leq 10^{-2}$, a range of concentrations which conveniently includes most surfactant behavior.

Measurement of Concentration Change

The number of moles of solute adsorbed on a solid from dilute solution can be obtained from a measurement of the change in solute concentration which in this case is the concentration of a specific surfactant at a very small concentration, i.e., usually much less than 10^{-4} mole fraction. Any number of the various techniques are available, e.g., refractometry, colorimetry, titrimetric analysis, densitometric analysis, the use of radio active tracers, gravimetric analysis or the measurement of the solution- air interfacial tension.

The concentration of a surfactant in aqueous solution changes the liquid-air interfacial tension of that solution in an orderly reproducible manner. The liquid-air interfacial tension can be measured reproducibly and the changes in interfacial tension with surfactant concentration are usually on the order of 10 dyn/cm per order of magnitude change in mole fraction which is sufficiently large to establish excellent precision as the reproducible error in the interfacial tension is in the range of $\pm$ 0.20 dyn/cm.

The adsorption process removes surfactant molecules from the bulk solution, thus causing a decrease in concentration and a subsequent increase in the interfacial tension. By carefully measuring the change in the liquid-air interfacial tension (γ_{LA}) versus surfactant concentration at a known temperature and comparing these data with similar data obtained in the presence of a known weight of coal of a known size range, surfactant adsorption curves can be developed.

Thus, the number of moles of surfactant adsorbed per unit weight of coal, n_1^s, at constant temperature (room temperature) was plotted as a function of the surfactant concentration, x, of the aqueous solution into which the coal was placed. This was reported as the room temperature surfactant adsorption isotherm.

The interfacial tension technique was also used by Garner, McKie, and Knight [33] to determine the adsorption of aliphatic alcohols on charcoal, and by Fowkes [34] in the adsorption of surfactants on cotton fibers.

VI. MATERIALS

Coal

The coal that was used for all the subsequent experiments was obtained from a sample of Pittsburgh bed coal collected in the U.S. Bureau of Mines (now U.S. Department of Energy) Bruceton coal mine, Pittsburgh, Penna. The sample was prepared by the Bureau by stage crushing through a roll crusher and a hammer mill to obtain a nominal size distribution of 35 mesh (420 μm diameter) x 0.

The "as received" sample was wet-screened to give a sufficient amount of 35 x 60 mesh (420 x 250 μm diameter) particles to conduct all of the dewatering and adsorption experiments. It was recognized that the phenomena under investigation were dependent on particle size distribution, but to examine this variable at this time was beyond the scope of the study.

An analysis [35] of the 35 x 60 mesh product coal showed that it contained 93% by weight coal and 7% mineral matter. The ash content of the total was found to be 8.47 $\pm$ 0.43%. The ash content of the coal product from a gravity separation at 1.50 specific gravity was 4.62 $\pm$ 0.05%. The internal moisture content of the separated coal was 1.62 $\pm$ 0.01%. The internal moisture content of the total sample was 1.71 $\pm$ 0.06%.

Surfactants

Five surfactants were chosen for this investigation: three anionic, one cationic and one non-ionic. The choice was arbitrary as there was no well based understanding of the interaction of surfactants with coal, yet it was felt that at least one representative from each class should be examined for comparison. The two additional anionic surfactants were chosen for reasons which became obvious as the investigation proceeded.

1. Aerosol A-196 (anionic)

Aerosol A-196 is the trade name for sodium dicyclohexyl sulfosuccinate produced by the American Cyanamid Company. The empirical formula is $C_{16}H_{25}SO_7Na$. The structural formula is shown in Figure 11. Figure 12 shows a photograph of the molecular model of the anionic portion from a side and top view. The main hydrocarbon portion of this molecule consists of the two cyclohexyl groups which are joined to the sulfosuccinate core. The molecular weight of Aerosol A-196 is 384.4 atomic mass units. The sample supplied to the laboratory was in the form of an extruded solid. It contained approximately eighty-five percent by weight of active ingredient with the balance as water. All concentrations reported for solutions of this surfactant were corrected to present the actual concentration of active ingredient only. Other impurity concentrations were not determined.

2. Triton X-114 (non-ionic)

Triton X-114 is the trade name for a product of the Rohm and Haas Company which is octylphenoxypolyethoxy ethanol. The empirical formula is C_8H_{17}- -$(OCH_2CH_2)_{7-8}OH$. The expanded structural formula is

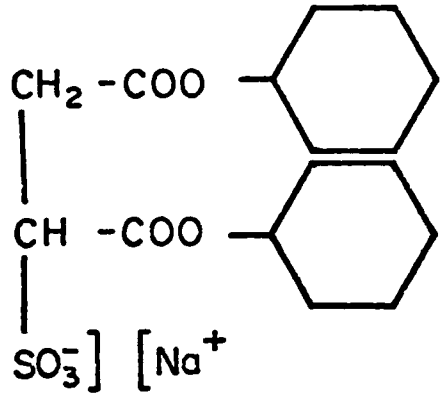

FIGURE 11. STRUCTURAL FORMULA OF AEROSOL A-196 (SODIUM DICYCLOHEXYL SULFOSUCCINATE).

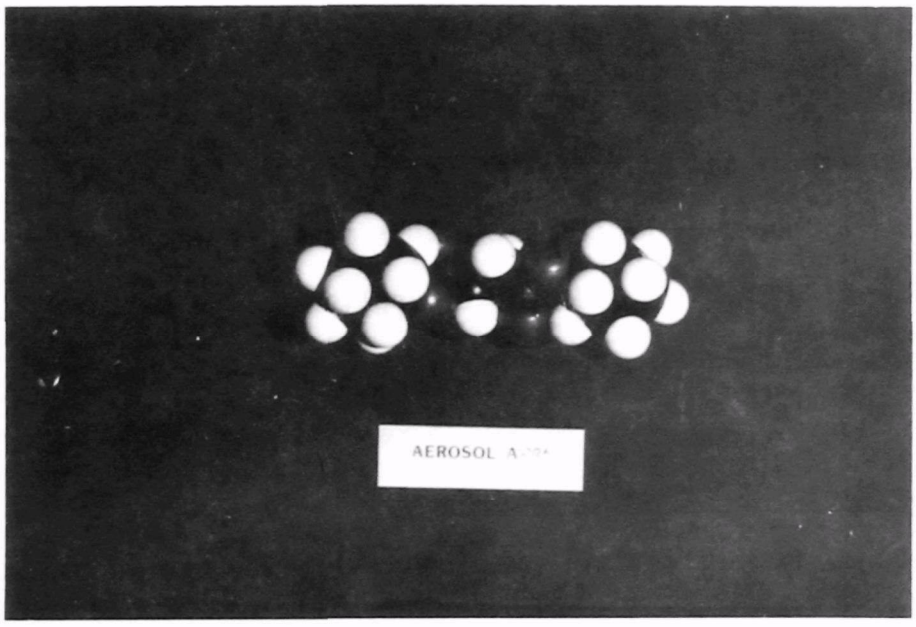

TOP VIEW

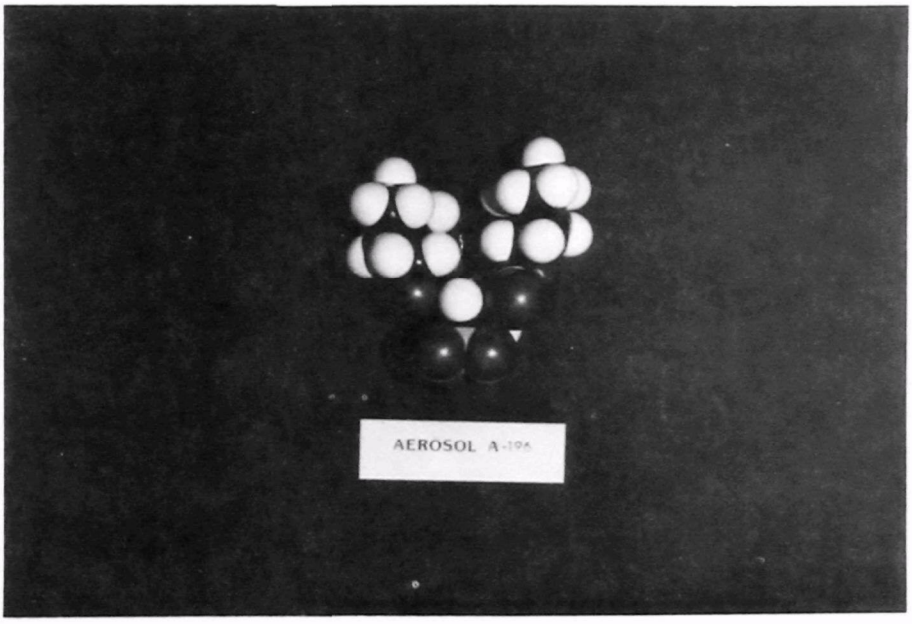

SIDE VIEW

FIGURE 12. MOLECULAR MODEL OF A DICYCLOHEXYL SULFOSUCCINATE ION, (SIDE AND TOP VIEW).

shown in Figure 13 and Figure 14 is a photograph of a molecular model where the polyoxyethylene chain is slightly coiled. The average molecular weight of Triton X-114 is 536 atomic mass units. The product contains a number of homologs containing either seven or eight units of polyoxyethylene $(CH_2CH_2O)_n$. The sample supplied to the laboratory was reported to be one hundred percent active ingredient in the form of a clear pale liquid. Any impurity concentrations were not determined.

3. Dodecyl Pyridinium Chloride (cationic)

The cationic surfactant dodecyl pyridinium chloride has an empirical formula of $C_{17}H_{30}NCl$. The structural formula is shown in Figure 15 and Figure 16 is a photograph of a molecular model of the cationic portion, i.e. $C_{12}H_{25}N$ 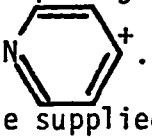 . The molecular weight is 283.9 atomic mass units. The sample supplied to the laboratory was reported to be one hundred percent active ingredient which was in the form of a straw colored powder. Sample purity was not investigated.

4. Sodium Dodecyl Sulfate (anionic)

Another anionic surfactant used was sodium dodecyl sulfate, also known as sodium lauryl sulfate. Use of this surfactant is frequently reported in the literature. The empirical formula is $C_{12}H_{25}SO_4Na$. The structural formula is shown in Figure 17 and Figure 18 is a photograph of a molecular model of the anionic portion. Its molecular weight is 288.4 atomic mass units. The sample was supplied to the laboratory in the form of a white powder. It was of laboratory grade from the Fisher Scientific Company. Impurity content was not analyzed.

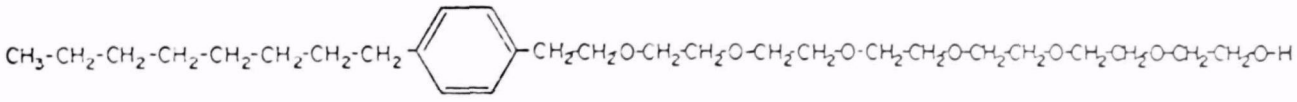

FIGURE 13. STRUCTURAL FORMULA OF TRITON X-114 (OCTYLPHENOXYPOLYETHOXY ETHANOL).

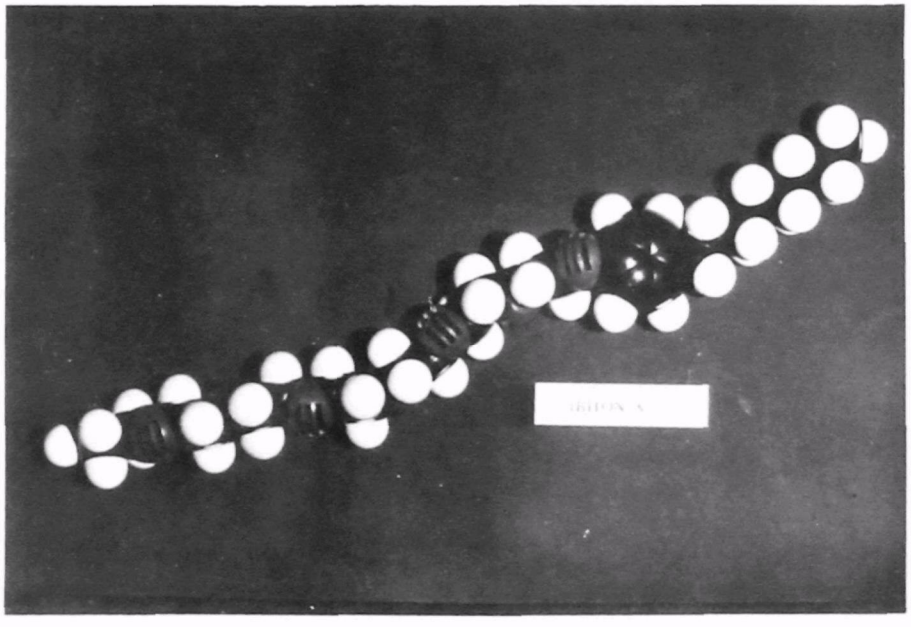

FIGURE 14. MOLECULAR MODEL OF TRITON X-114.

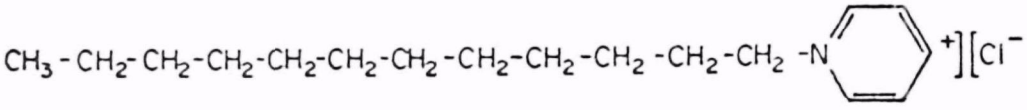

FIGURE 15. STRUCTURAL FORMULA OF DODECYL PYRIDINIUM CHLORIDE.

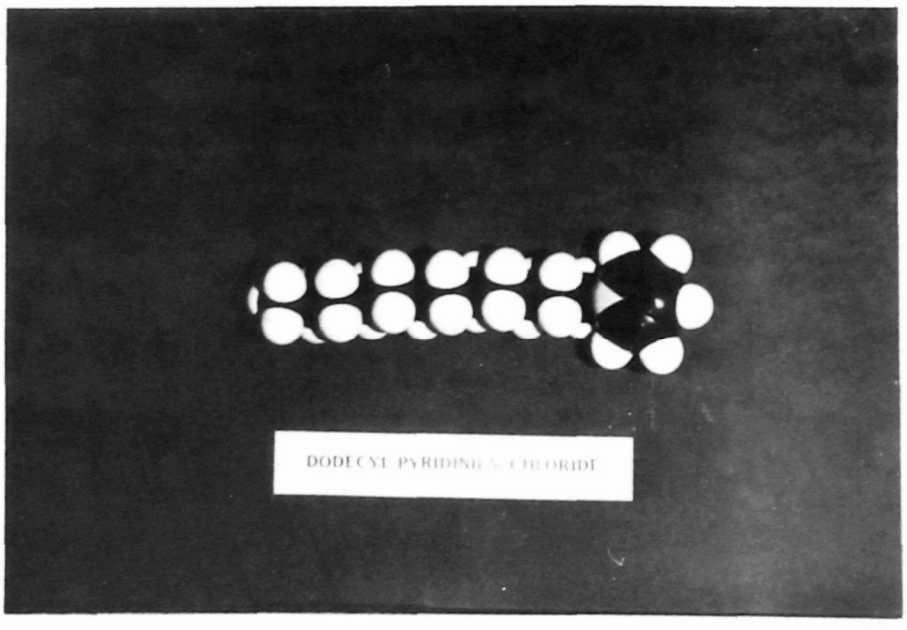

FIGURE 16. MOLECULAR MODEL OF A DODECYL PYRIDINIUM ION.

$$CH_3\text{-}CH_2\text{-}CH_2\text{-}CH_2\text{-}CH_2\text{-}CH_2\text{-}CH_2\text{-}CH_2\text{-}CH_2\text{-}CH_2\text{-}CH_2\text{-}CH_2\text{-}SO_4^-]\,[Na^+$$

FIGURE 17. STRUCTURAL FORMULA OF SODIUM DODECYL SULFATE.

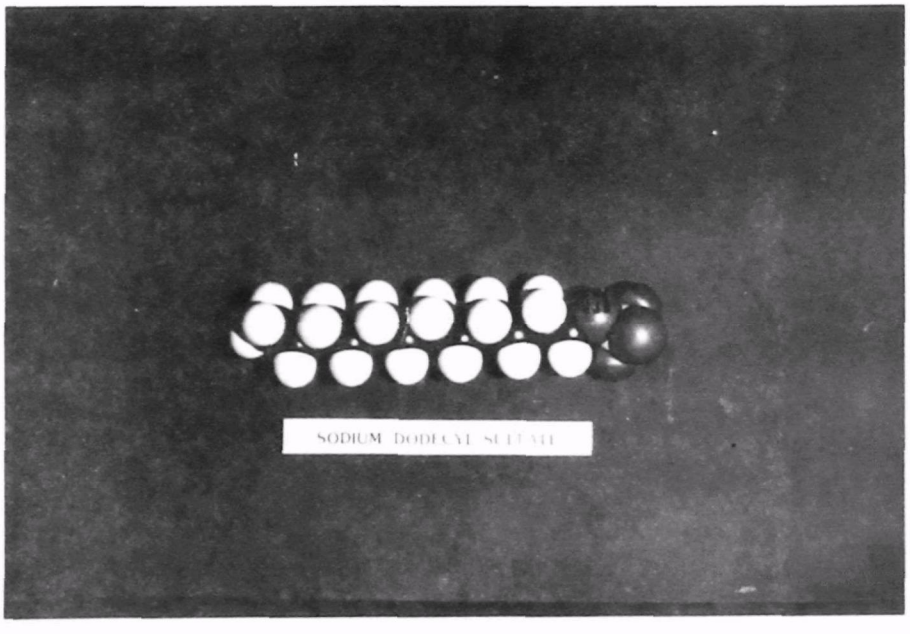

FIGURE 18. MOLECULAR MODEL OF A DODECYL SULFATE ION.

5. Aerosol-OT (anionic)

Aerosol-OT, another anionic surfactant, was chosen also because of its reputation as a commercial wetting agent. Aerosol-OT is the trade name for sodium di(2-ethylhexyl) sulfosuccinate manufactured by the American Cyanamid Company. The empirical formula is $C_{20}H_{37}SO_7Na$. The structural formula is shown in Figure 19. Figure 20 is a photograph of a molecular model of the anionic portion from a side and top view. This surfactant is essentially the same as Aerosol A-196 except for the configuration of the hydrocarbon groups. The molecular weight of Aerosol-OT is 444.5 atomic mass units. The sample supplied to the laboratory was in the form of a soft waxy solid. The sample was reported to be one hundred percent active ingredient, i.e., no water or alcohol as a suspending medium. Purity of the sample was not investigated.

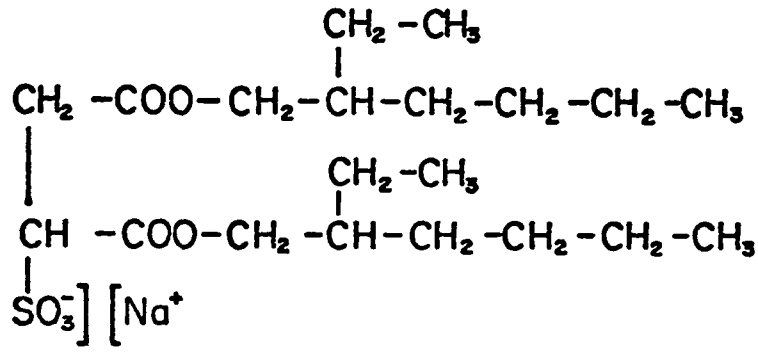

FIGURE 19. STRUCTURAL FORMULA OF AEROSOL-OT (SODIUM DI (2-ETHYLHEXYL) SULFOSUCCINATE).

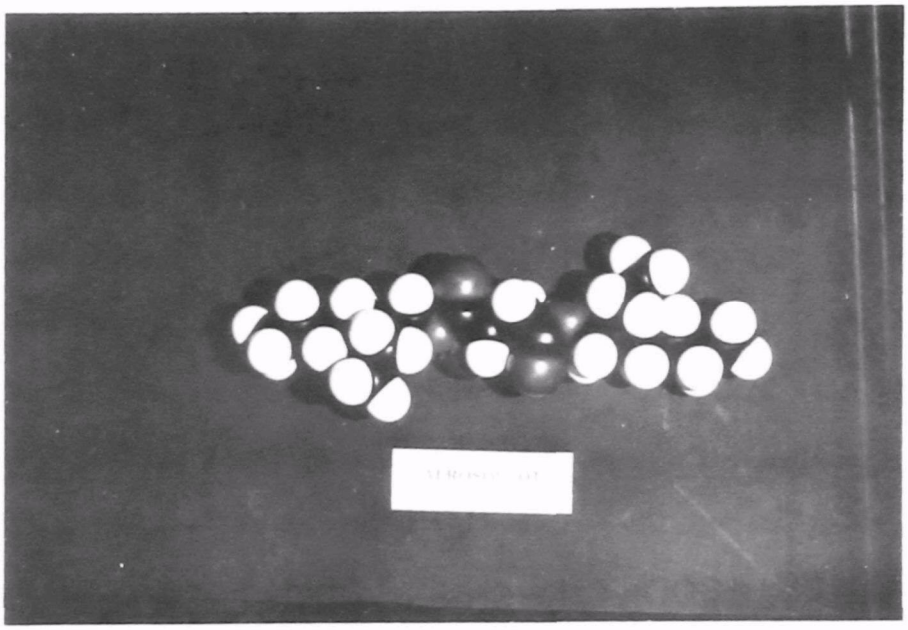

TOP VIEW

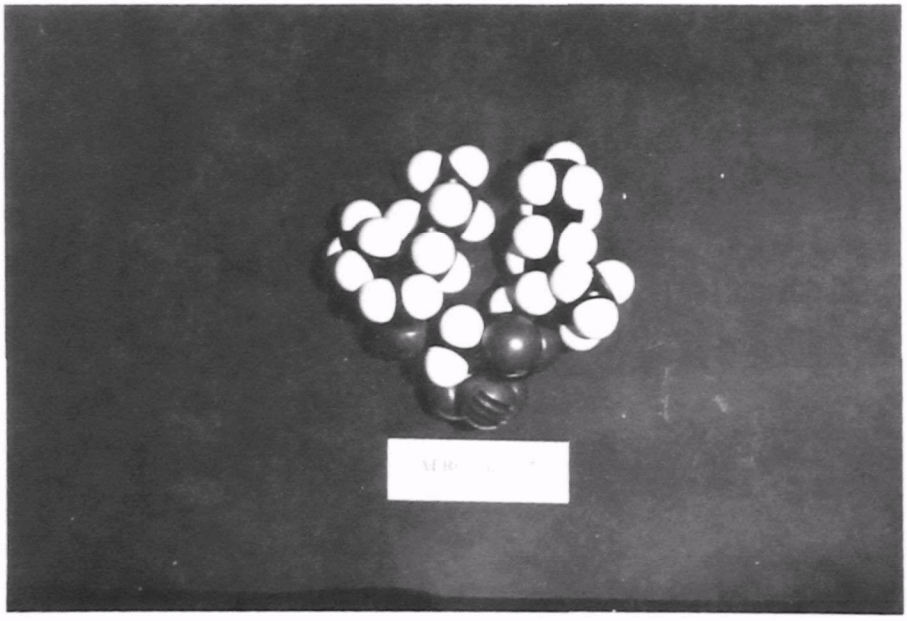

SIDE VIEW

FIGURE 20. MOLECULAR MODEL OF A DI (2-ETHYLHEXYL) SULFOSUCCINATE ION, (SIDE AND TOP VIEW).

VII. EXPERIMENTAL

Introduction

The purpose of the placement of surfactants on the surface of coal was to modify its hydrophobicity and allow for more complete dewatering of that modified coal. Let us now turn to the dewatering measurements that were performed. Two techniques were utilized: one we call equilibrium, in which the saturated coal bed was dewatered over many hours with very small incremental changes in applied pressure differential across the bed, such that at any instant the dewatering process could be stopped, and reinitiated without a change in dewatering rate with pressure. This method, which has been also used for the testing of soils, consisted of continuously recording the equilibrium retained water content of a partially saturated bed of fine coal particles across which a measured pressure differential existed and as the pressure differential was increased in small increments a curve of retained water content as a function of applied pressure differential was obtained. The pressure differential was obtained by the application of air-pressure to the top of the bed.

The second method, called non-equilibrium, relied on a fixed bed pressure differential across the bed established by the application of a vacuum such that the bed moisture could be measured at fixed times of exposure. The non-equilibrium dewatering experiments that were conducted were used for evaluating only the final water contents of a dewatered bed as a function of surfactant concentration in the water. A gravity drained slurry was dewatered by the application of constant vacuum from below for various time intervals. Hence the final water

content was determined at certain exposures (pressure x time). This technique was employed to increase and support other dewatering data at certain surfactant concentrations.

Although the "non-equilibrium (vacuum) dewatering" technique was developed by the author and the data accumulation directed by same, it should be recognized at the outset that a large fraction of the data collected in the experiments under this heading were done so by Chi [36] of this laboratory. The details of the experiments and the results were included as these data developed an exceedingly strong support for the proposed molecular model of surfactant-coal surface interaction that was the focal point of this dissertation.

Pressure Dewatering (equilibrium)

The equilibrium dewatering experiments were performed on 30 gram samples of the narrow size distribution coal which were formed into a cylindrical bed approximately 2.5 cm deep and 4.5 cm in diameter. The coal bed was formed from a slurry in a test cell, mixed and allowed to settle and drain by gravity in a test cell apparatus which is shown schematically in Figure 21. The cell was made from Teflon and designed so that it could be readily disassembled. Teflon was chosen to aid in cleaning the cell walls of any surfactant films and to reduce wall wetting during the experiments. The bottom of the test cell was fitted with a wire mesh support screen and a filter paper disc which was changed for each experiment to prevent clogging. The filter paper was purchased from the Carl Schleicher and Schuell Co. and was No. 595. A dewatered coal bed could be removed intact in the form of a plug, since the top and bottom cell caps were removable. This minimized any evaporation before the coal sample was weighed for final retained moisture content. Approximately 98 to 99% by weight of the original coal charge ($\sim$ 30 grams) remained intact for the weighing process.

The cell was supported on a torsion balance arrangement made from stainless steel tubing which was shaped into a "T" configuration as shown in Figure 22. Mass changes in the cell due to dewatering were detected by a linear variable differential transformer (LVDT) which was in contact with the end of the lever arm of the torsion balance at the same point as the dewatering cell. The output of the LVDT was amplified and observed as the y coordinate of an x-y recorder. Before

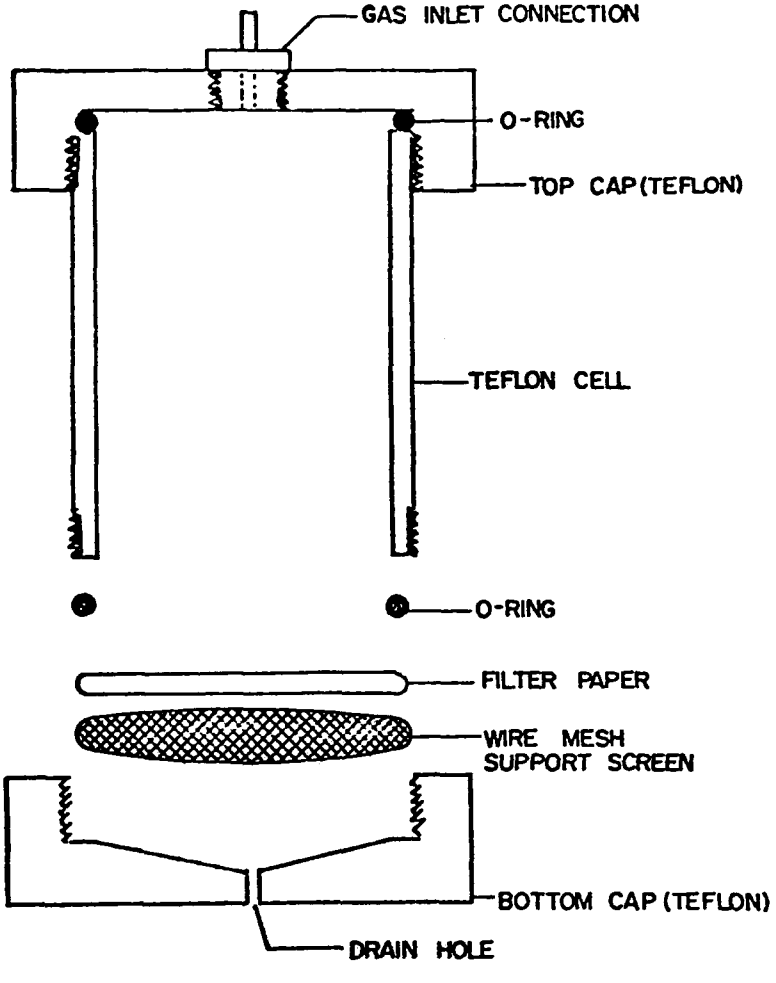

FIGURE 21. TEFLON DEWATERING CELL

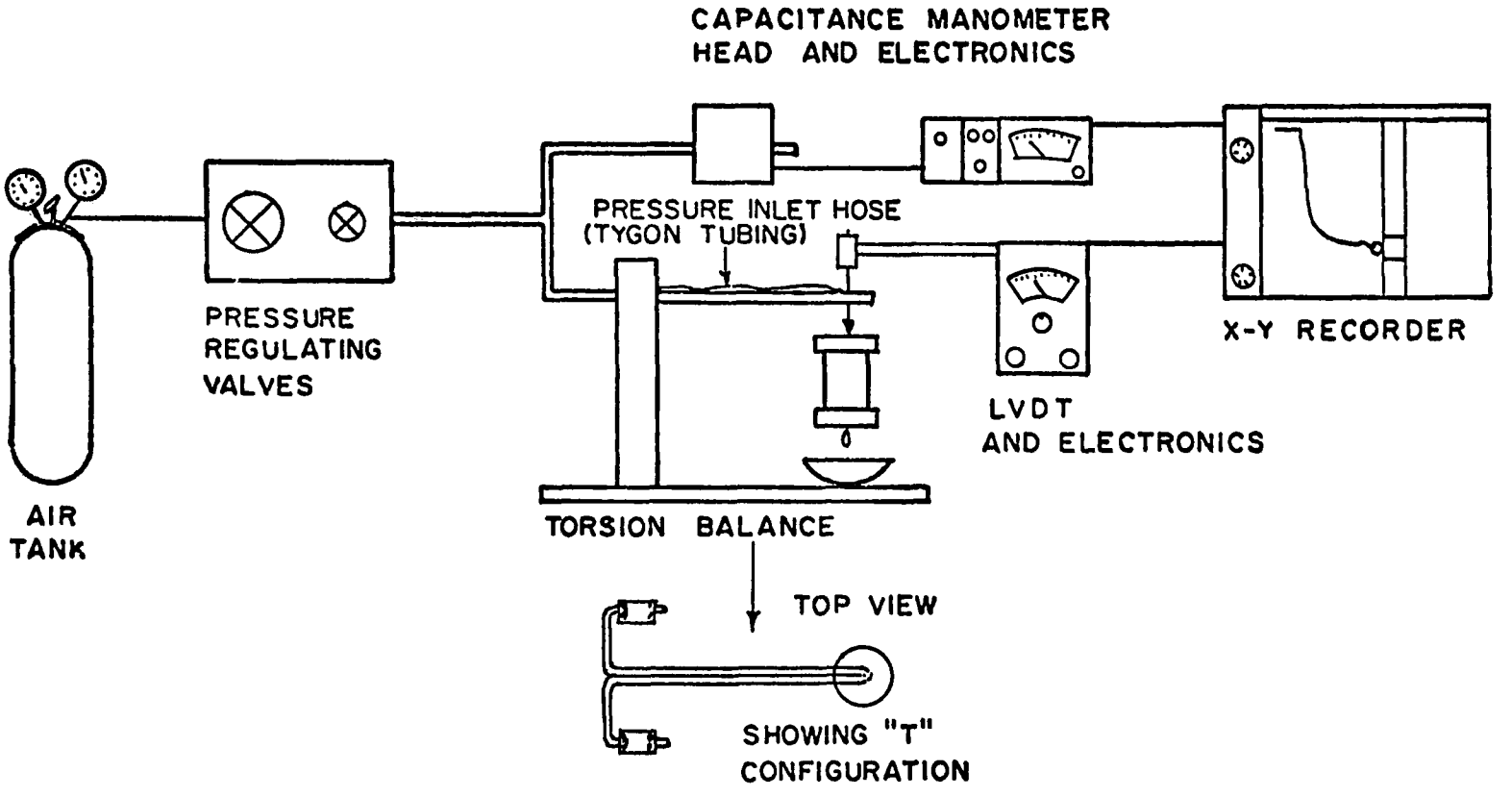

FIGURE 22. PRESSURE DEWATERING APPARATUS.

each experiment the system was calibrated by placing a twenty gram weight on the cell. With this arrangement the system was sensitive to weight changes of 0.05 gm or less than 0.17 wt% retained water. Figure 22 also shows the gas pressure inlet line, which is connected to the compressed dry air tank and pressure regulators and leak valves. The pressure differential applied across the coal bed was measured by an MKS Baratron capacitance manometer with differential pressure head. One end of the pressure gauge was left open to the atmosphere, while the other end read the pressure present over the coal bed. In this way effects due to changes in ambient barometric pressure were eliminated and the actual pressure differential across the coal bed was continuously recorded. The electronics of the manometer provide a 10 volt full scale reading output. The output was read as the x coordinate on the x-y recorder. With this arrangement the recorder was accurate to 0.25 mm Hg.

A dewatering experiment was conducted as follows. Thirty grams of coal was placed in the cell. A slurry was formed and the solution allowed to drain from the cell. This was repeated with fresh solution until the expelled solution had approximately the liquid-air interfacial tension of the prepared solution. This procedure assured that the concentration of the liquid phase in the bed was the known concentration of the prepared solution, i.e. the coal was fully in equilibrium with the surfactant solution of that γ_{LA} value. The top cap of the cell was then affixed and when drainage ceased, i.e., no weight change in the cell occurred for about one hour, the x-y recorder was calibrated and the x-y recorder scales adjusted accordingly. The pressure lines

were opened and the leak valves adjusted so that the pressure above the cell increased at an extremely slow rate of less than 0.25 mm Hg/hr. The system was established so that when the applied pressure became only equal to the capillary pressure, dewatering ceased. The system could remain at equilibrium in this state for over a period of one day or until the pressure over the coal was increased very slightly. When no further dewatering was observed even after the pressure had risen considerably or when air breakthrough took place, the experiment was terminated. At that point the cell was removed and the dewatered coal plug transferred to an open preweighed petri dish and immediately weighed on an analytical balance. The coal was then allowed to air dry at room temperature for over 24 hours. This time was greater than that needed for the coal to dry to constant weight, but was chosen for convenience and to allow the inherent moisture content to form in equilibrium with the ambient humidity (the conditions under which the dry coal was originally weighed). The sample was reweighed and the final moisture content calculated on a weight percent basis as follows:

$$\text{wt\% retained } H_2O = \frac{\text{wt\% retained } H_2O}{\text{wt\% of dry coal + wt\% of retained } H_2O} \times 100\% \ .$$

The accuracy obtained by using the analytical balance was $\pm$ 0.005 wt%. With the final wt% of water, the original weight of coal in the cell and the calibration of the x-y recorder, the weight percent of retained water was back calculated at various values of applied pressure differential ΔP, from the continuous dewatering curve of weight vs. ΔP. This data then gave the equilibrium dewatering curves.

Vacuum Dewatering (non-equilibrium)

The vacuum dewatering experiments were performed on five 15 gram samples of the 35 x 60 mesh coal. Each sample was formed into a cylindrical bed in a glass crucible, the bottom of which consisted of a porous fritted glass disc. The formed beds were approximately 2.2 cm deep and 3.7 cm. in diameter. The pore size of the disc was reported as 4 to 5.5 microns. A schematic diagram of the apparatus is shown in Figure 23. The crucible was connected securely to a vacuum flask by means of a rubber stopper in which there was a hole slightly smaller in diameter than the crucible bottom. This produced a vacuum-tight fit. The vacuum connect nipple of the flask was connected, through vacuum tubing and a stopcock, to an oil vacuum pump. The vacuum pump could evacuate the flask to a pressure of less than 10^{-2} Torr, so that the pressure differential across the coal bed, with the stopcock open and the pump in operation, was approximately 1 atmosphere.

The vacuum dewatering experiments were conducted in the following manner. A known amount of coal (15 g) was placed in the crucible and a quantity of distilled water was added to form a coal slurry. This was allowed to gravity drain, and then, as much as possible of the remainder of the water was removed by application of the vacuum. This was repeated with more water until all coal particles of the sample were readily wet by the water. At this point the actual dewatering experiment commenced. A saturated bed was formed and the vacuum was applied for a five minute interval after which the crucible was removed and quickly weighed, without disturbing the bed of coal. Any

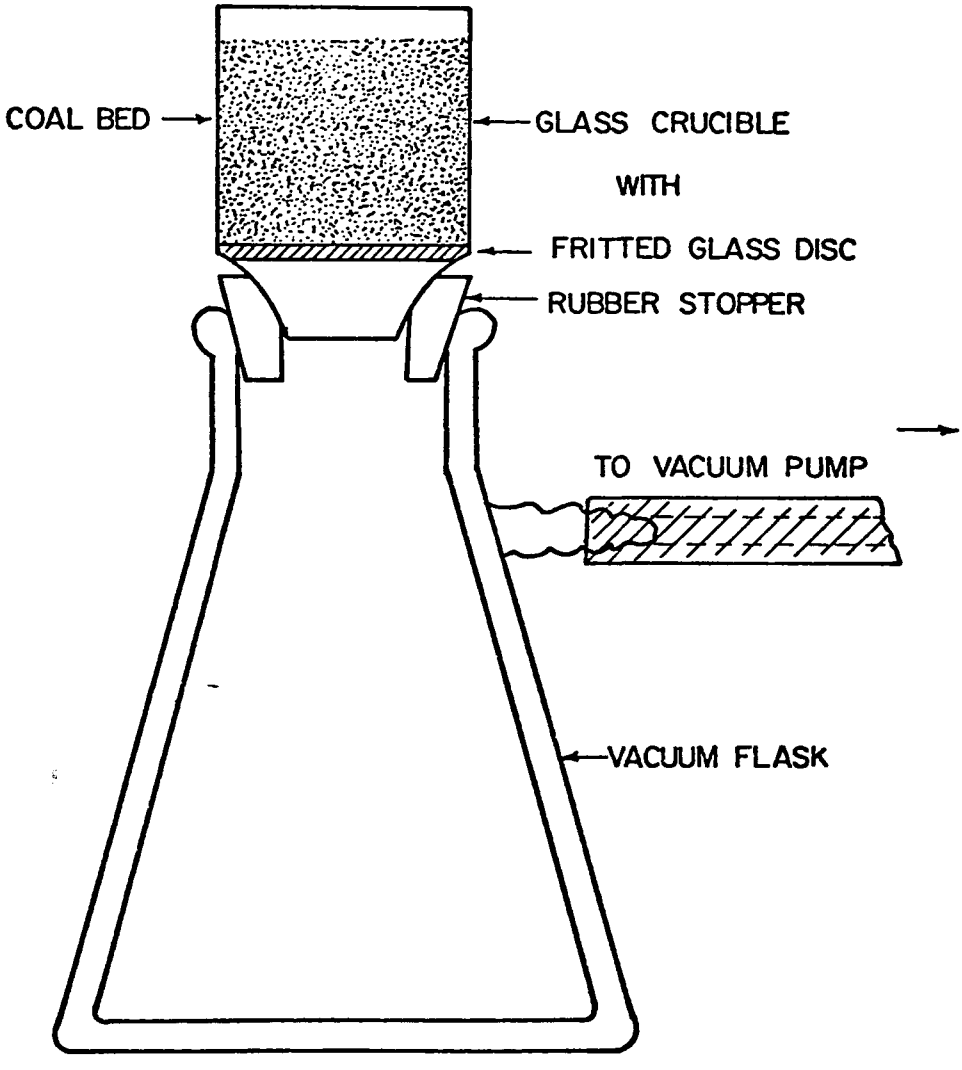

FIGURE 23. VACUUM DEWATERING APPARATUS

excess water collected on the bottom of the crucible was wiped off before the weighing process. Immediately after being weighed the crucible was placed back on the vacuum system for another five minute interval and the process repeated. The procedure was continued for four intervals. This procedure served to standardize each specific coal bed as to its water retention as a function of time under a constant applied pressure differential.

The entire procedure was then repeated, but instead of only distilled water, a prepared aqueous surfactant solution was used. A quantity of the surfactant solution was added to the wet coal bed to form the slurry. Again it was allowed to gravity drain and the remainder of the liquid was removed by application of the vacuum. However, this was repeated with fresh solution until the recovered solution was of the same concentration as that put in as determined by measurement of the liquid-air interfacial tension of the solution. Again, at this point the actual dewatering procedure was initiated. The bed was saturated with solution and exposed to the vacuum for the five minute time intervals, after each of which the crucible was weighed as before. The dewatering procedure was then repeated again, only the next time the concentration of surfactant in the solution was increased to some predetermined value.

The dewatering procedure was conducted at each increased value of surfactant concentration which was chosen as the experiment progressed. The initial starting concentrations were chosen on the basis of information from the pressure dewatering experiments, the liquid-air interfacial tension behavior of each surfactant, and the adsorption experiments.

Only one coal bed was used for the entire series of experiments with each surfactant. This was to insure that the only variable was that of the increasing concentration of surfactant.

From these data, isochronal plots of the amounts of liquid (which, due to the extremely small concentrations of surfactant, was essentially water) retained by the coal beds, under a constant pressure differential, as a function of surfactant concentration could be generated. These curves were plotted at 5, 10, 15, and 20 minute cumulative exposure times.

Liquid-Air Interfacial Tension Measurements (γ_{LA})

All liquid-air interfacial tension, γ_{LA}, measurements were made by the du Nouy ring method [37] which involves the determination of the force required to detach a ring or loop of platinum-iridium wire from the surface of a liquid. A commercial apparatus, the Fisher Surface Tensiomat Model 21, was used. The instrument makes use of a torsion wire in determining the maximum pull on the ring.

The determination of γ_{LA} for a liquid was accomplished in the manner described in the instruction manual for the instrument [38]. The procedure can be briefly outlined as follows. The liquid under investigation was placed in an appropriate beaker, which was then placed on the sample stage of the instrument, under the ring. The ring was then submerged into the liquid and the instrument adjusted to give a zero reading. The instrument was then manipulated to properly withdraw the ring from the surface of the liquid. When detachment occurred the "apparent" reading on the instrument dial was noted.

The "apparent" readings of the tensiometer must be multiplied by a correction factor in order to obtain an absolute value. The correction factor takes into account the densities of the two phases, the interfacial tension between which is being measured, and the meniscus volume, the volume of the distended liquid.

The correction factor was calculated for each reading according to the procedure outlined in the instrument instruction manual [38]. Certain values unique to the instrument used which were contained in the correction factor were the ratio of the ring radius, R, to the

radius of the wire, r, which was

$$R/r = 53.5697$$

and the circumference, c, of the ring which was 5.980 cm.

Also recorded with each γ_{LA} reading was the temperature of the liquid being measured.

Before its initial use the instrument was carefully calibrated according to the recommended procedure such that the dial of the instrument read directly in dynes per centimeter. An additional check which was also performed periodically, was the determination of the liquid-air interfacial tension of a sample of spectrographic grade benzene. The γ_{LA} values of the benzene were found to be 28.20 $\pm$ 0.09 dyn/cm at 25.0^{o}C. An interpolated value from the 57th edition of the Handbook of Chemistry and Physics [39] is 28.21 dyn/cm and rounded off to the accuracy of the present instrument, which was 0.05 dyn/cm, is 28.20 dyn/cm in excellent agreement.

To eliminate, or at least to prevent the spread of any surface contaminants such as fingerprint oils etc. and especially any adhering traces of the surfactants, which exhibit such a high degree of surface activity at such small concentrations, the platinum-iridium ring and all glassware involved in the measurement of the interfacial tensions were thoroughly cleaned before each change in the test liquid.

The ring was thoroughly rinsed in distilled water and then heated in the oxidizing portion of a gas flame.

The glassware, inclusive of all solution transfer pipettes, was thoroughly rinsed in distilled water. Then the glassware was immersed in a warm, $60^{o}C$ - $70^{o}C$, standard cleaning solution of sodium dichromate in concentrated sulfuric acid, for at least 5 minutes. The glassware was then rinsed in tap water and then finally in distilled water.

This same glassware cleaning procedure was also used for cleaning the teflon cell used throughout the pressure dewatering experiments, the crucible used in each vacuum dewatering experiment, and on a routine basis for all other laboratory glassware that came into use.

Liquid-Air Interfacial Tensions of Aqueous Surfactant Solutions

To determine the behavior of the liquid-air interfacial tension as a function of concentration for aqueous solutions of each surfactant under investigation, a concentrated stock solution of each surfactant was initially prepared. The solutions were gravimetrically prepared and stored in 100 ml stoppered, volumetric flasks. Distilled water was used as solvent in all cases. Precise aliquots of these solutions were then pipetted into premeasured quantities of distilled water, already in the appropriate beaker used in determining γ_{LA}. For ultra low concentrations the use of a 10 μl pipette was necessitated. The quantities of solution on which the interfacial tensions were measured were on the order of 30 to 50 ml. It should be noted that all glass surfaces, e.g., of the pipettes, were fully saturated with the prepared solutions prior to liquid transfer. This eliminated concentration variations due to any surfactant adsorption on the glassware.

All surfactant solution-air interfacial tension values reported were the result of ten readings each, over a period of about 30 minutes. This procedure was followed to allow the surfaces to come to equilibrium and to estimate and subsequently avoid any transient aging effects (see Appendix A). Constant readings, though, were usually achieved after allowing a freshly mixed solution to equilibrate for about 5 minutes and then allowing about 3 minutes between individual readings. The standard deviations of the γ_{LA} values reported from this procedure were in the range of 0.20 dyn/cm.

The density of the surfactant solutions, needed to calculate the

correction factor for the γ_{LA} readings, was taken as that of pure water because of the extreme dilutions involved. The density of the solutions was chosen as 0.9970 g/ml [40]. The density of the other phase constituting the interface, which was ambient air, was chosen as 1.1845 x 10^{-3} g/cm^3 [41].

Surfactant Adsorption Experiments

The surfactant adsorption experiments were conducted on coal samples of twenty grams each. A dilute solution containing a precisely known amount of distilled water and surfactant was prepared to which the coal sample was added, then the coal, water, surfactant slurry (with an average value of about 30 wt% solids and about 50 to 100 ml solution) was repeatedly thoroughly stirred and allowed to settle. This procedure was followed to insure complete adsorption on all particles. The liquid-air interfacial tension of the supernatant solution was then measured as described above for the surfactant solutions alone. The concentration of the solution was then changed by dilution with precise amounts of distilled water or by the addition of precise aliquots of the more concentrated stock solution prepared for each surfactant. This was repeated over as much of the same concentration range as investigated above when coal was not present in the solution for each surfactant.

In the case of two surfactants tested the increase in the interfacial tension of the solutions, whose proportions of constituents were mandated by physical experimental parameters, was not great enough at the higher concentrations for the determination of a concentration change. However, determination of the change in concentration was possible by gravimetric analysis of the solution [36]. For this, most of the solution was decanted from the beaker containing the coal slurry, then weighed and allowed to evaporate at 100°C, then reweighed. This process was repeated for a solution which was not exposed to the coal. Comparison of the findings gave the concentration change. The solution

was decanted, not filtered, because it was found that the filter paper used sorbed too much of the surfactant.

VIII. RESULTS

Pressure Dewatering (equilibrium)

The results of the pressure dewatering experiments are shown in Figures 24-36, where the amount of solution, on a weight percent basis with the coal, retained by the coal bed is plotted as a function of the applied pressure differential across the bed. As explained in the Experimental section, the actual data was in the form of a continuous x-y recorder trace of the weight loss versus the applied pressure differential, and that this information had to be transformed into a weight percent versus applied pressure differential curve so that all the curves could be compared on an equal basis. The data points shown in Figures 24-36 are points at which the conversion from weight to weight percent was calculated from the actual data to enable the construction of the "normalized" curves shown. These then are only data transfer points.

Table II lists the important data for the experiments. That is the weight of the coal sample used in each experiment; the measured solution-air interfacial tension of the dewatering solution; the concentration of the solution as derived from the respective curves calibrating the interfacial tension with surfactant concentration; and the applied pressure differential at which the dewatering curve had its steepest slope, as determined graphically from the curve.

Figures 37-41 are isobaric plots of the residual amount of solution left in the dewatered coal beds, at the given pressure as a function of the surfactant concentration. The data was taken from the third stage of the dewatering curves of Figures 24-36, where the

retained amounts of solution are becoming asymtotic to some final value as the pressure is increased. Isobaric plots of the dewatering data in this region give an indication of how this portion of the dewatering is affected by the surfactants. The data is plotted on the same concentration scale as that for the solution-air interfacial tension plots of each surfactant. The values of the isobaric residual water contents, i.e. at zero concentration of surfactant, are also indicated on the vertical axes of the graphs.

TABLE II

DATA FOR PRESSURE DEWATERING EXPERIMENTS

FIGURE NUMBER	SOLUTION	COAL SAMPLE WEIGHT (g)	SURFACTANT CONCENTRATION (mole fraction)	SOLUTION-AIR INTERFACIAL TENSION γ_{LA}(dyn/cm)	PRESSURE DIFFERENTIAL AT MAXIMUM SLOPE ΔP(max)(mmHg)
24	Distilled Water	30.0887	0	69.85	17.5
25	Aerosol A-196	30.3165	1.32×10^{-6}	66.90	17.5
26	Aerosol A-196	30.0242	2.02×10^{-6}	65.60	18.0
27	Aerosol A-196	30.0012	1.42×10^{-4}	52.30	17.5
28	Triton X-114	30.2416	3.20×10^{-7}	41.50	16.0
29	Triton X-114	30.2550	1.45×10^{-6}	30.95	6.5
30	Dodecyl Pyridinium Chloride	30.1446	4.75×10^{-5}	44.15	12.0
31	Sodium Dodecyl Sulfate	30.0003	7.20×10^{-6}	41.40	16.8
32	Sodium Dodecyl Sulfate	30.0073	2.10×10^{-5}	35.35	12.0
33	Aerosol-OT	30.3150	3.00×10^{-6}	40.65	10.3
34	Aerosol-OT	30.0090	1.20×10^{-5}	31.65	5.0
35	Aerosol-OT	30.0013	1.85×10^{-5}	28.90	7.0
36	Aerosol-OT	30.0043	2.00×10^{-5}	28.50	6.0

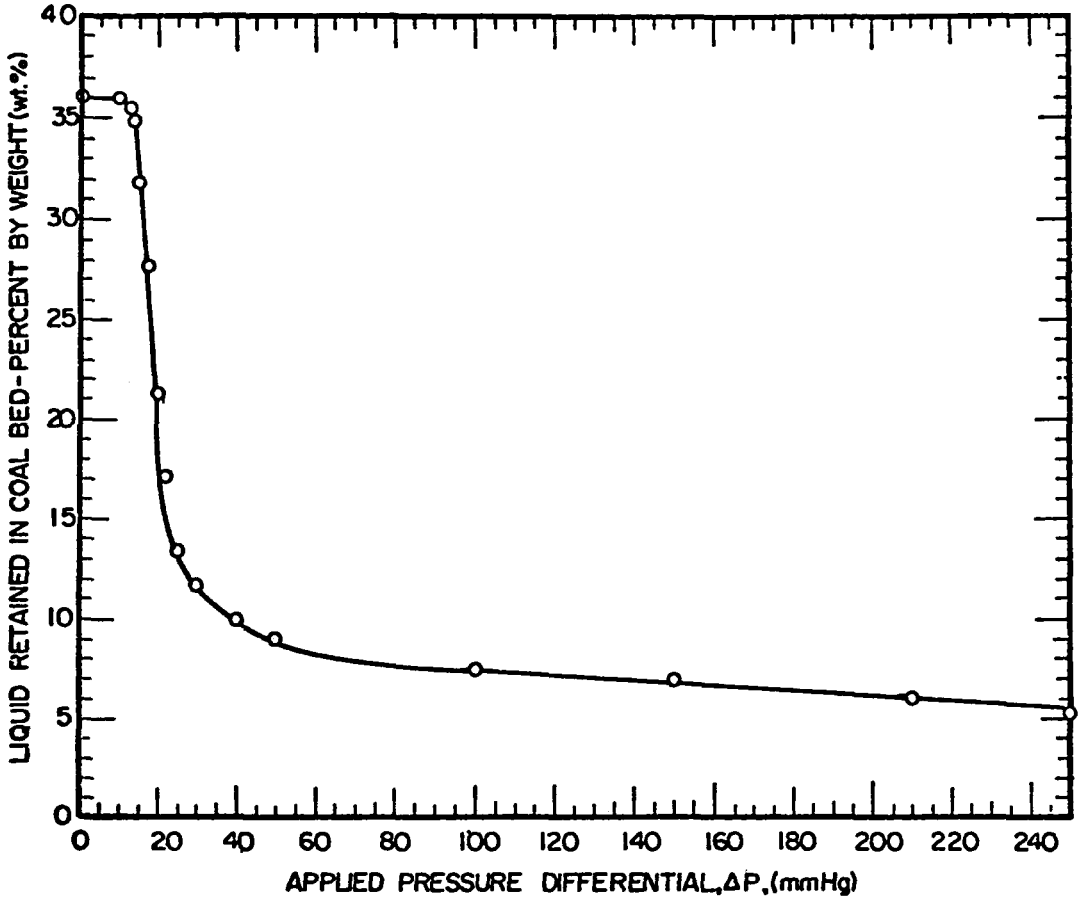

FIGURE 24. PRESSURE DEWATERING CURVE OBTAINED FOR A 35 x 60 MESH COAL BED CONTAINING DISTILLED WATER.

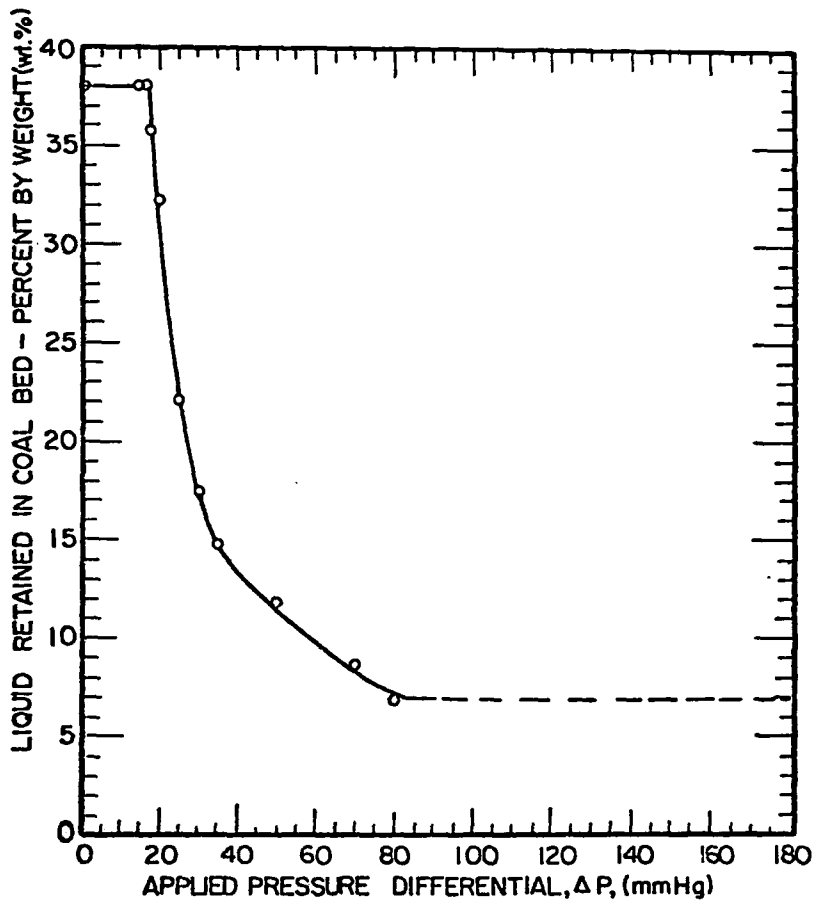

FIGURE 25. PRESSURE DEWATERING CURVE OBTAINED FOR A 35 x 60 MESH COAL BED CONTAINING AN AQUEOUS SOLUTION OF AEROSOL A-196; $c = 1.32 \times 10^{-6}$ MOLE FRACTION.

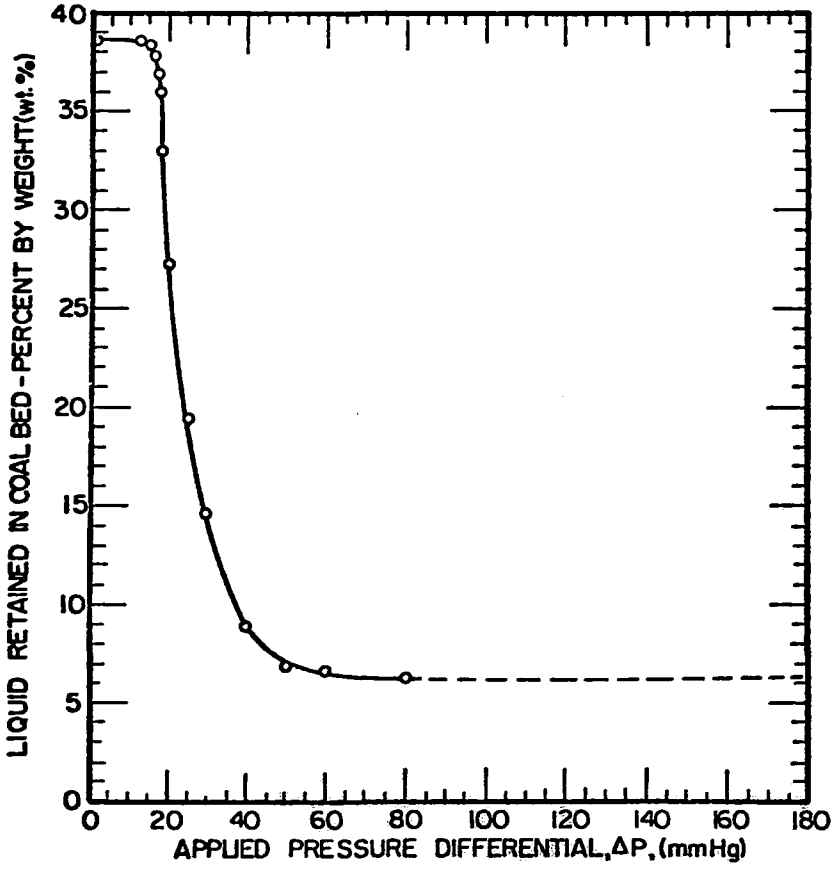

FIGURE 26. PRESSURE DEWATERING CURVE OBTAINED FOR A 35 x 60 MESH COAL BED CONTAINING AN AQUEOUS SOLUTION OF AEROSOL A-196; $c = 2.02 \times 10^{-6}$ MOLE FRACTION.

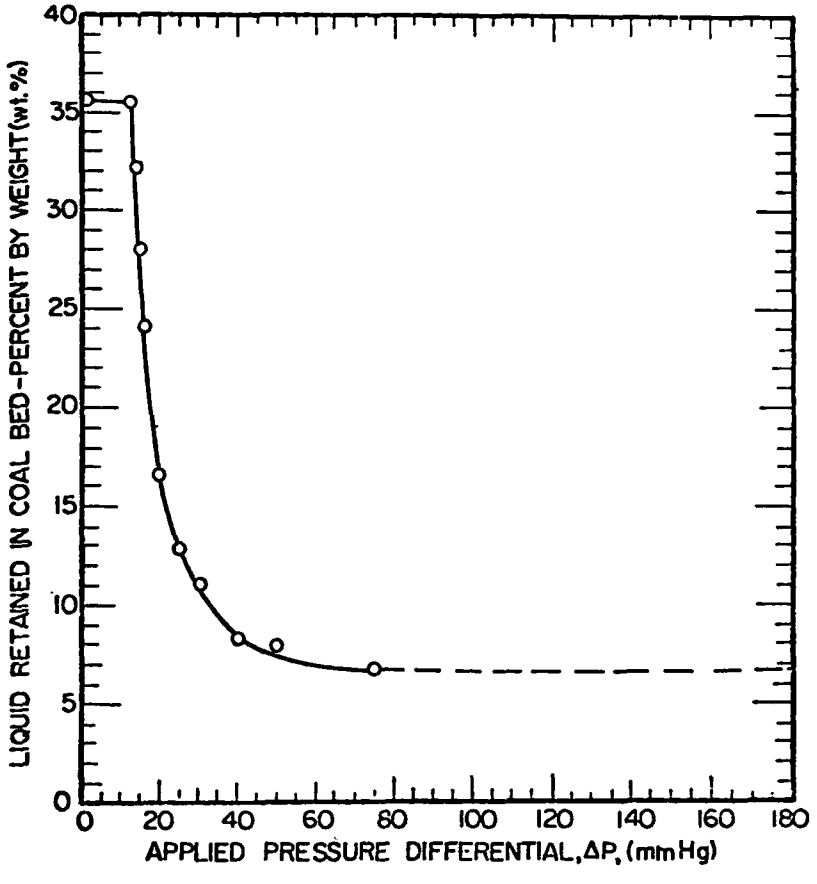

FIGURE 27. PRESSURE DEWATERING CURVE OBTAINED FOR A 35 x 60 MESH COAL BED CONTAINING AN AQUEOUS SOLUTION OF AEROSOL A-196; $c = 1.42 \times 10^{-4}$ MOLE FRACTION.

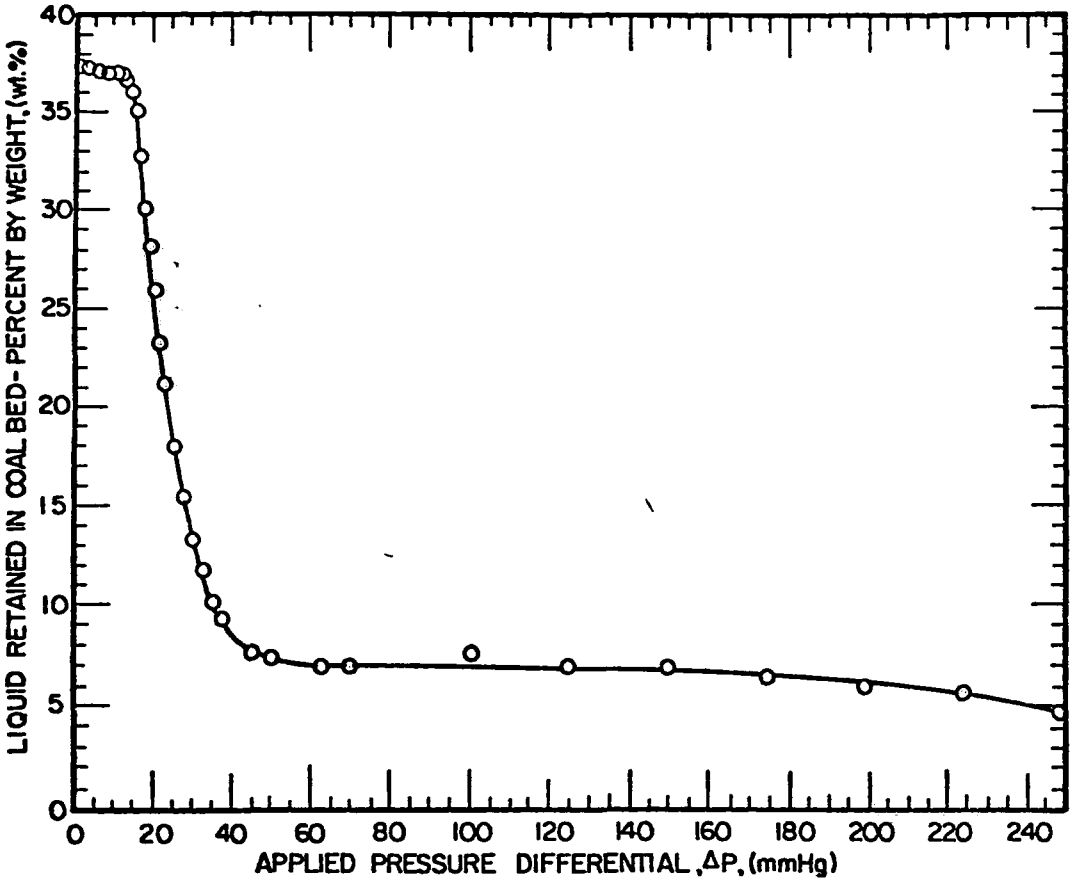

FIGURE 28. PRESSURE DEWATERING CURVE OBTAINED FOR A 35 x 60 MESH COAL BED CONTAINING AN AQUEOUS SOLUTION OF TRITON X-114; $c = 3.20 \times 10^{-7}$ MOLE FRACTION.

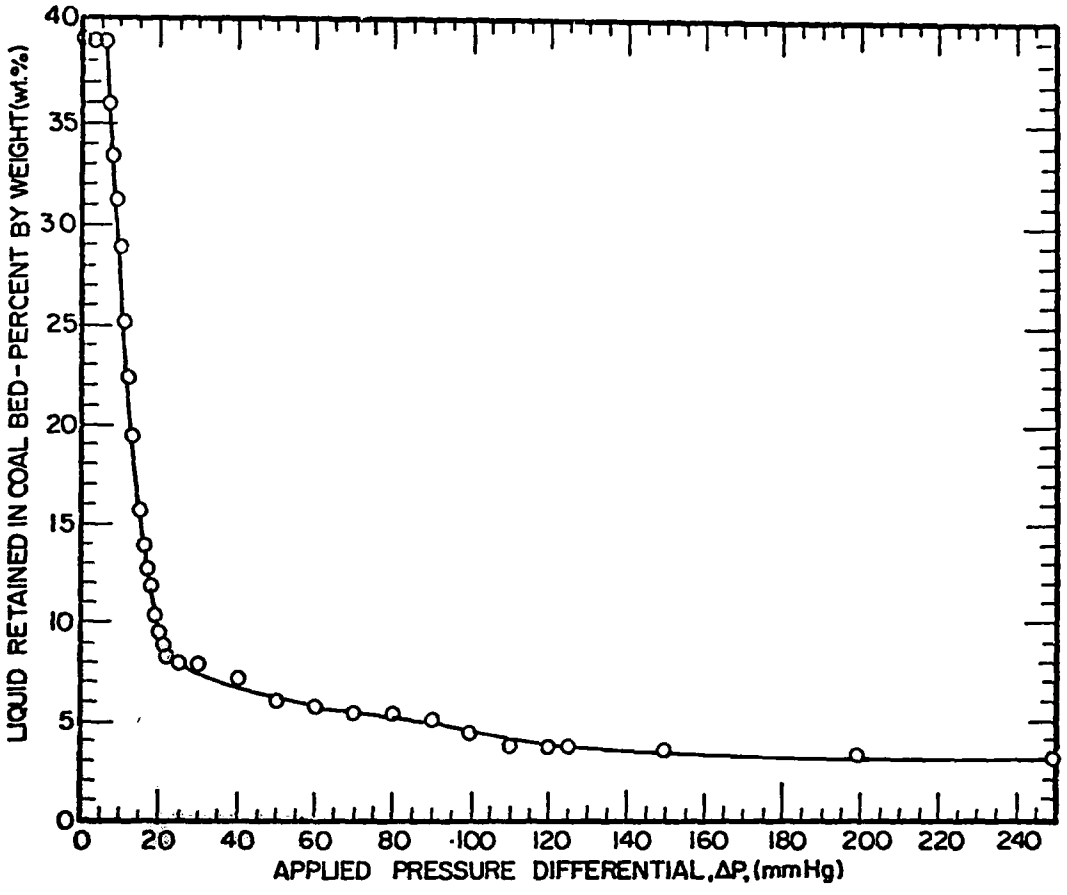

FIGURE 29. PRESSURE DEWATERING CURVE OBTAINED FOR A 35 x 60 MESH COAL BED CONTAINING AN AQUEOUS SOLUTION OF TRITON X-114; $c = 1.45 \times 10^{-6}$ MOLE FRACTION.

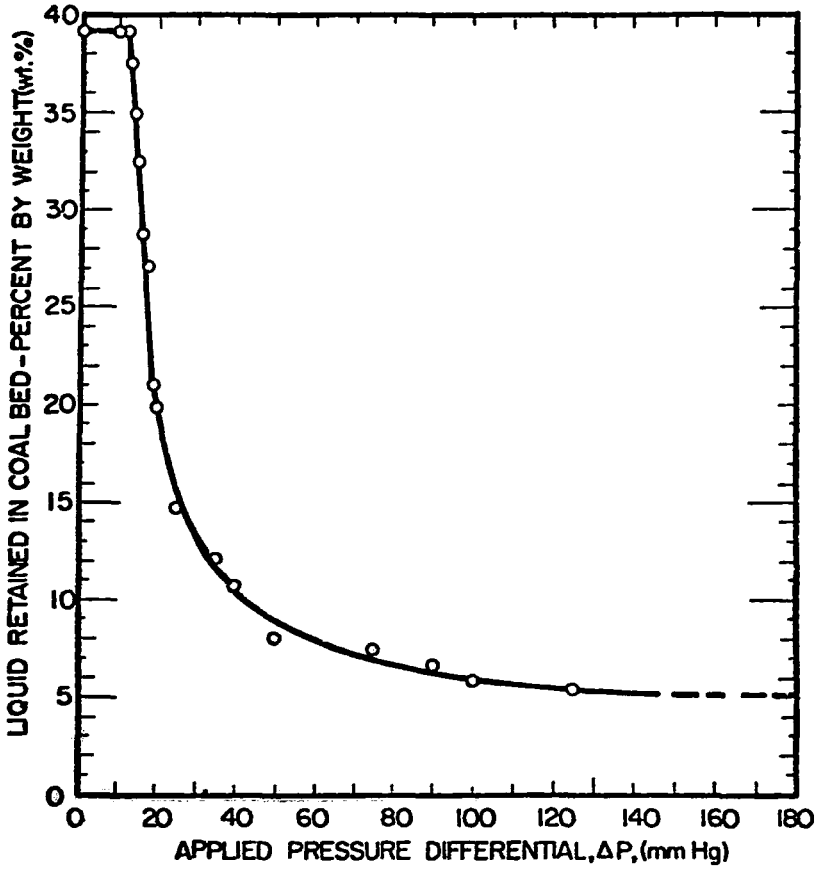

FIGURE 30. PRESSURE DEWATERING CURVE OBTAINED FOR A 35 x 60 MESH COAL BED CONTAINING AN AQUEOUS SOLUTION OF DODECYL PYRIDINIUM CHLORIDE; $c = 4.75 \times 10^{-5}$ MOLE FRACTION.

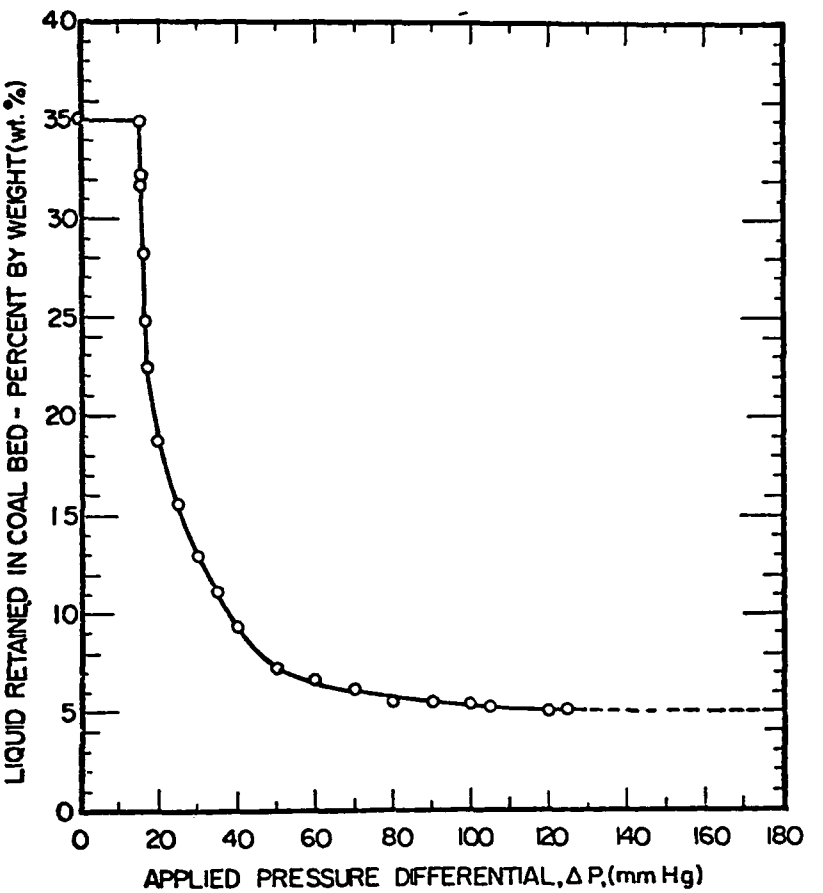

FIGURE 31. PRESSURE DEWATERING CURVE OBTAINED FOR A 35 x 60 MESH COAL BED CONTAINING AN AQUEOUS SOLUTION OF SODIUM DODECYL SULFATE: $c = 7.20 \times 10^{-6}$ MOLE FRACTION.

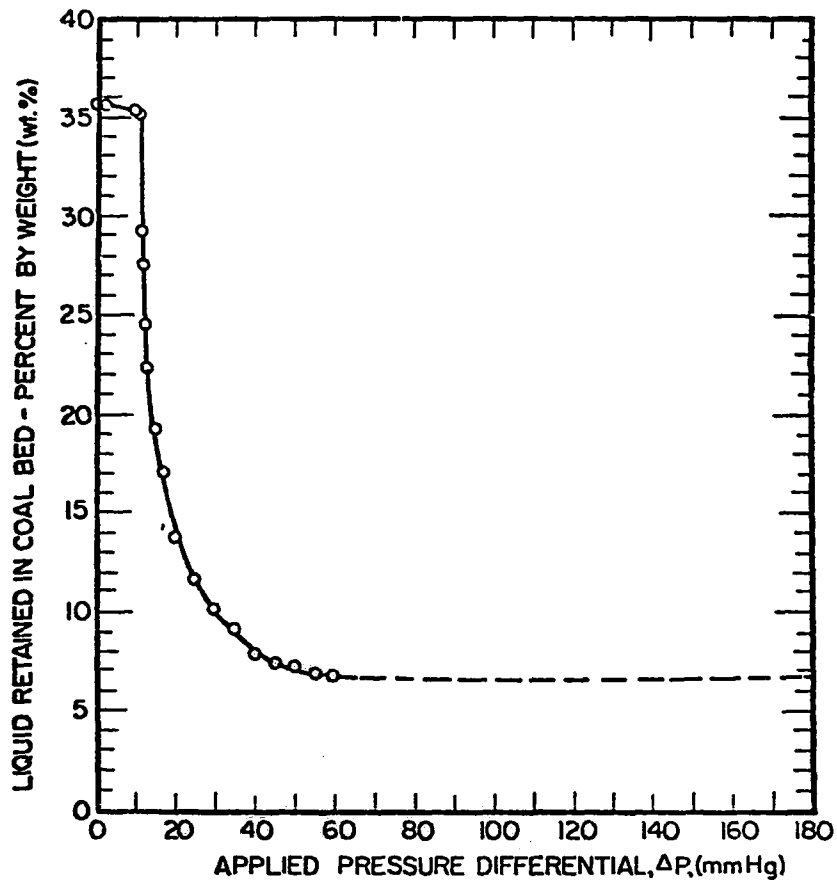

FIGURE 32. PRESSURE DEWATERING CURVE OBTAINED FOR A 35 x 60 MESH COAL BED CONTAINING AN AQUEOUS SOLUTION OF SODIUM DODECYL SULFATE: $c = 2.10 \times 10^{-5}$ MOLE FRACTION.

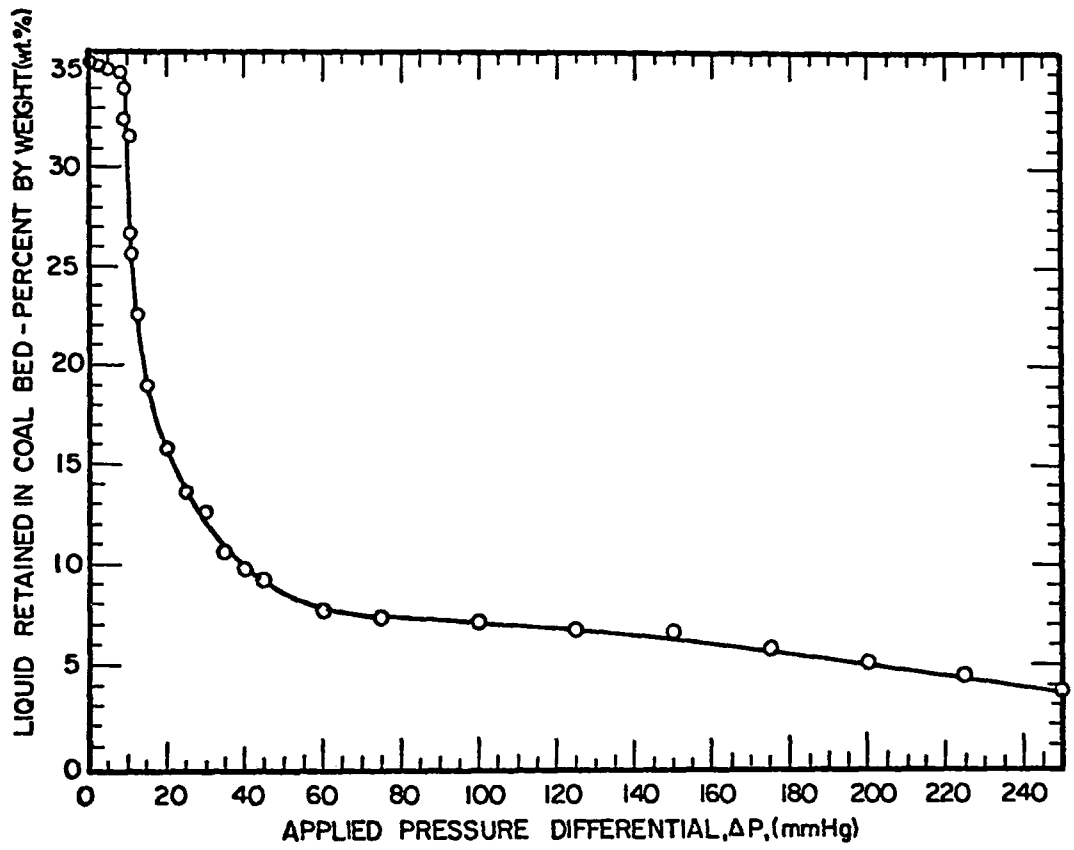

FIGURE 33. PRESSURE DEWATERING CURVE OBTAINED FOR A 35 x 60 MESH COAL BED CONTAINING AN AQUEOUS SOLUTION OF AEROSOL-OT; $c = 3.00 \times 10^{-6}$ MOLE FRACTION.

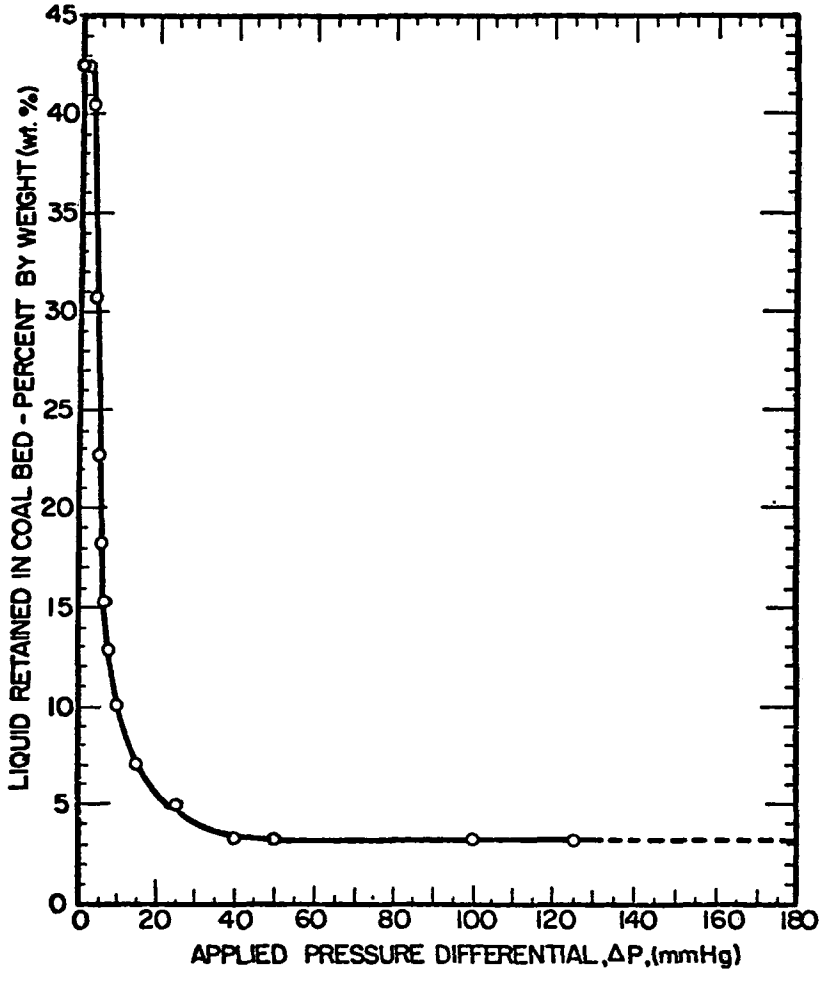

FIGURE 34. PRESSURE DEWATERING CURVE OBTAINED FOR A 35 x 60 MESH COAL BED CONTAINING AN AQUEOUS SOLUTION OF AEROSOL-OT; $c = 1.20 \times 10^{-5}$ MOLE FRACTION.

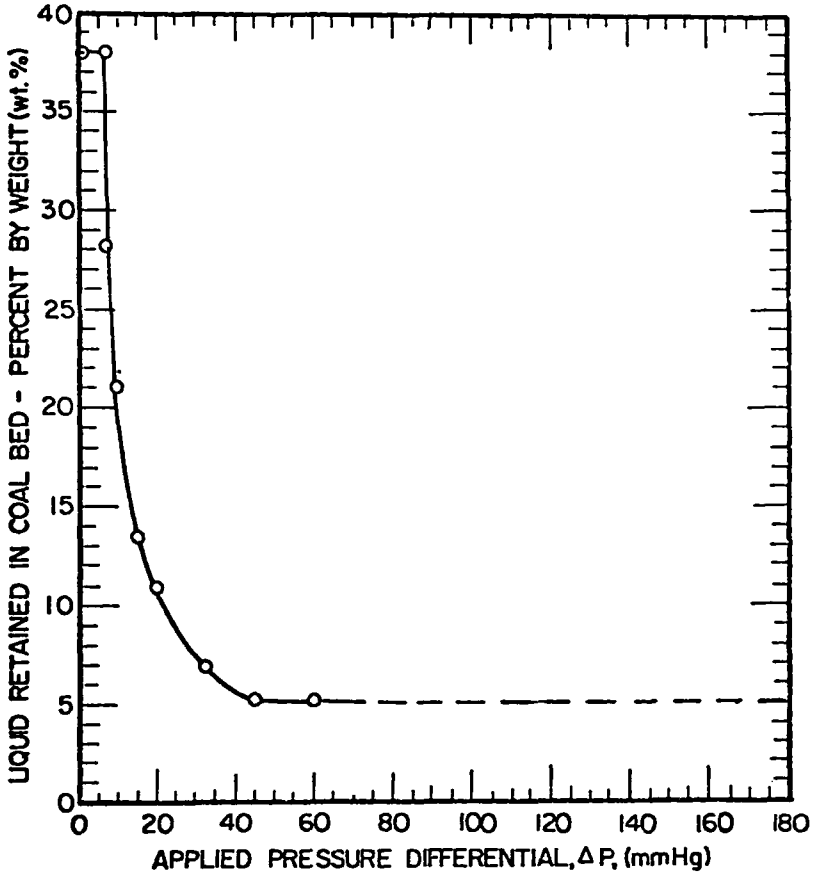

FIGURE 35. PRESSURE DEWATERING CURVE OBTAINED FOR A 35 x 60 MESH COAL BED CONTAINING AN AQUEOUS SOLUTION OF AEROSOL-OT; $c = 1.85 \times 10^{-5}$ MOLE FRACTION.

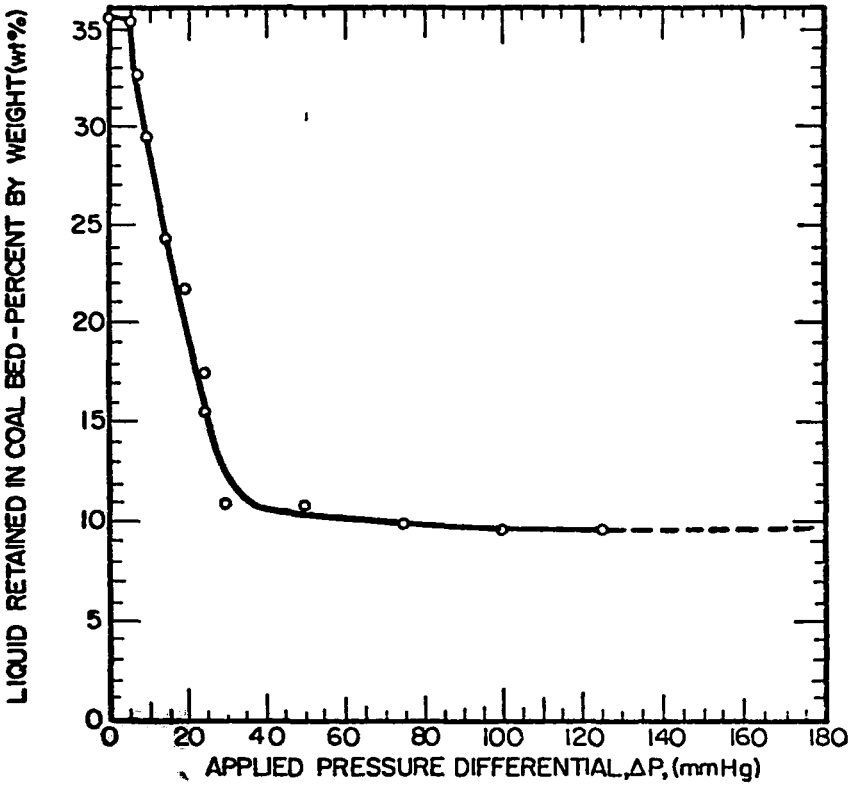

FIGURE 36. PRESSURE DEWATERING CURVE OBTAINED FOR A 35 x 60 MESH COAL BED CONTAINING AN AQUEOUS SOLUTION OF AEROSOL-OT; $C = 2.00 \times 10^{-5}$ MOLE FRACTION.

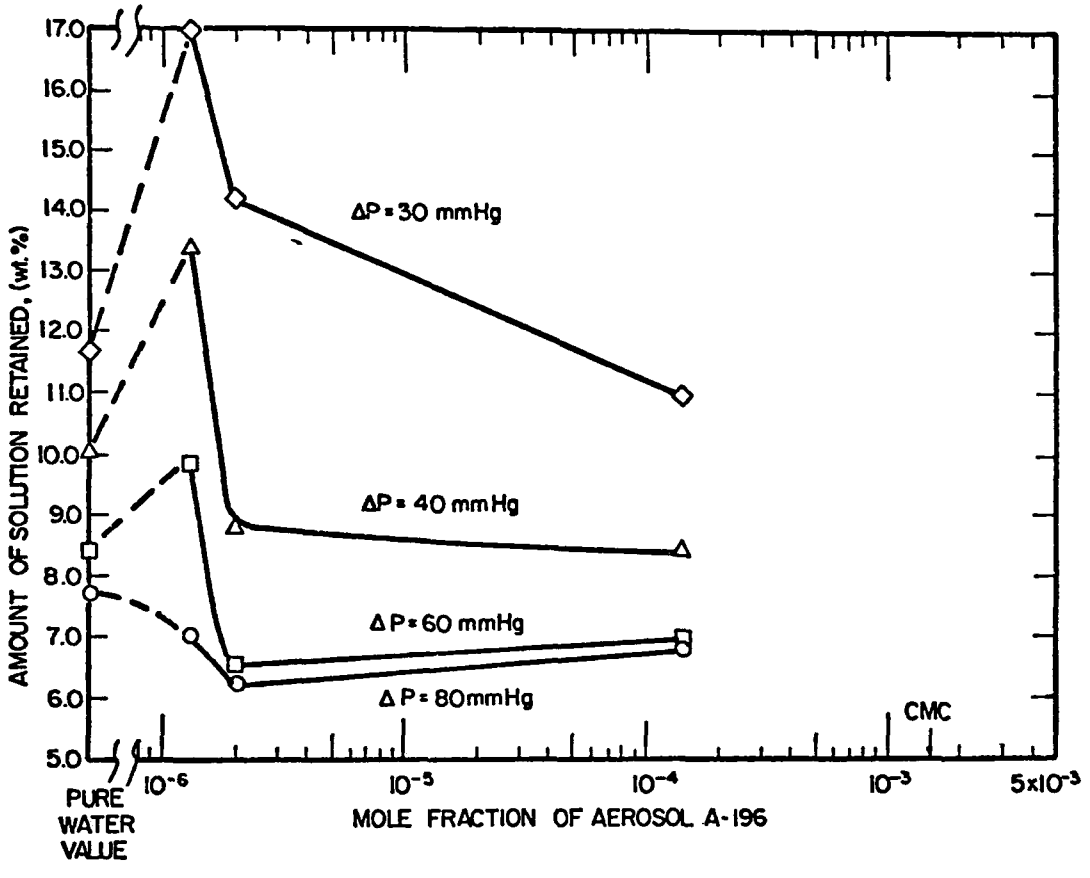

FIGURE 37. EFFECT OF AEROSOL A-196 ON THE AMOUNT OF AQUEOUS SOLUTION RETAINED BY THE PRESSURE DEWATERED COAL BED. (ISOBARIC DATA; COAL SIZE: 35 x 60 MESH).

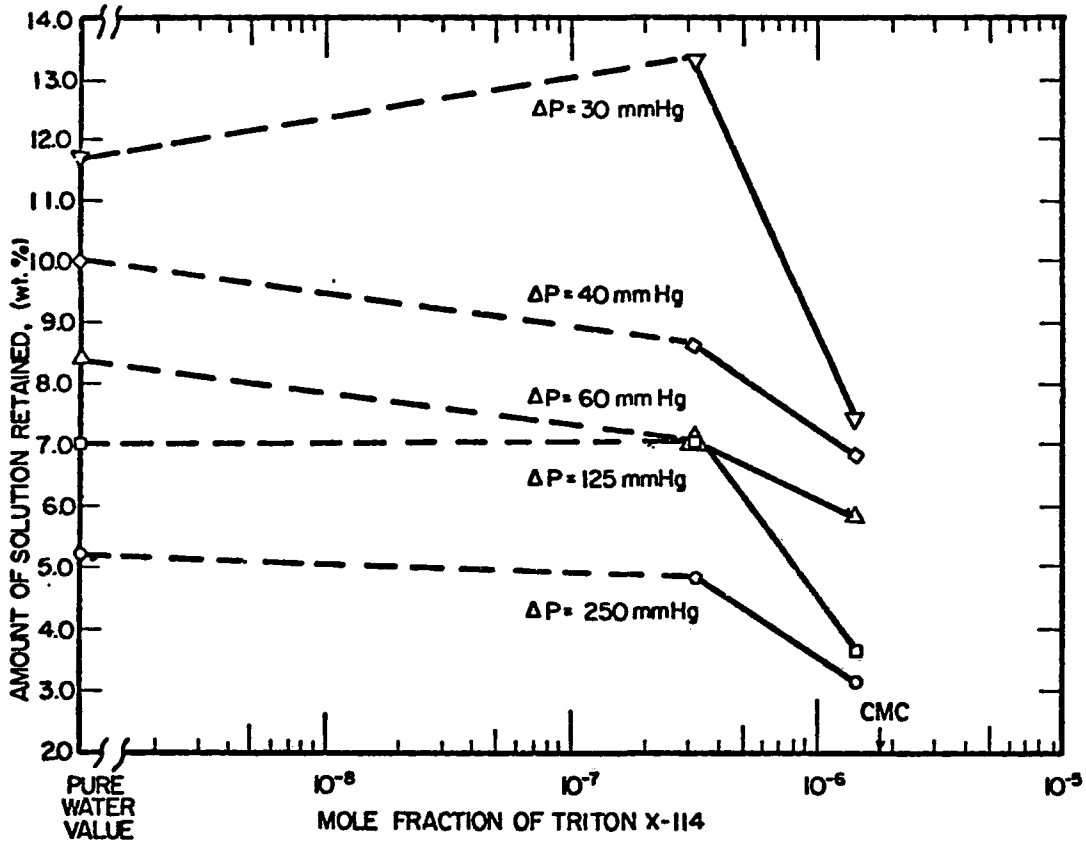

FIGURE 38. EFFECT OF TRITON X-114 ON THE AMOUNT OF AQUEOUS SOLUTION RETAINED BY THE PRESSURE DEWATERED COAL BED. (ISOBARIC DATA; COAL SIZE: 35 x 60 MESH).

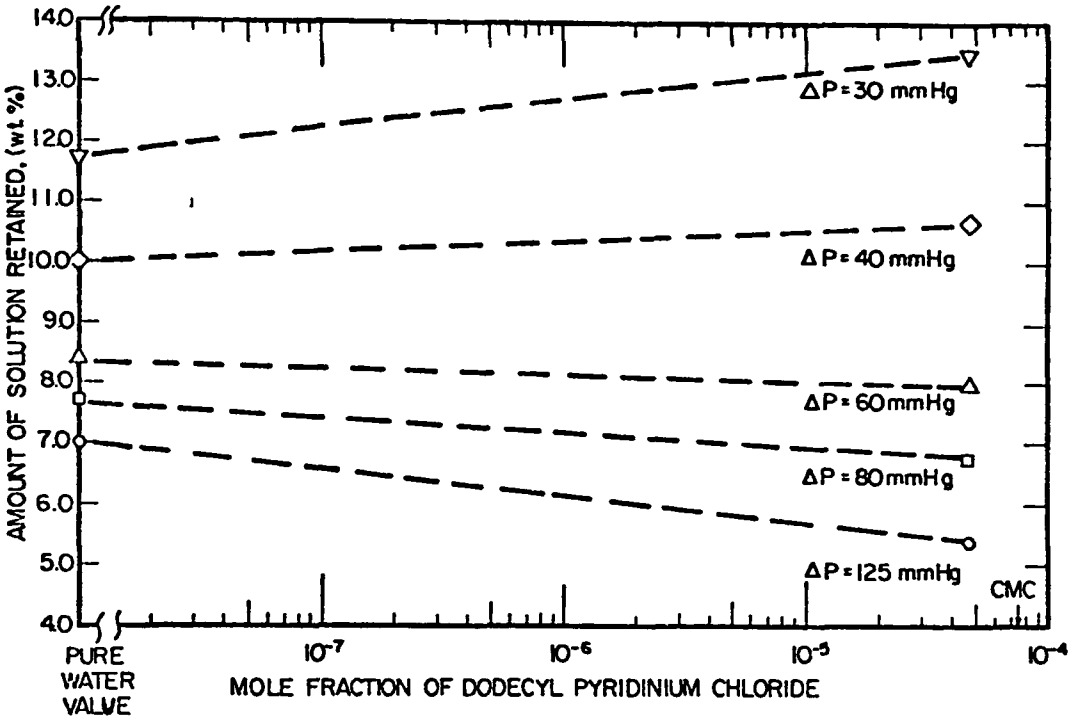

FIGURE 39. EFFECT OF DODECYL PYRIDINIUM CHLORIDE ON THE AMOUNT OF AQUEOUS SOLUTION RETAINED BY THE PRESSURE DE-WATERED COAL BED. (ISOBARIC DATA; COAL SIZE: 35 x 60 MESH).

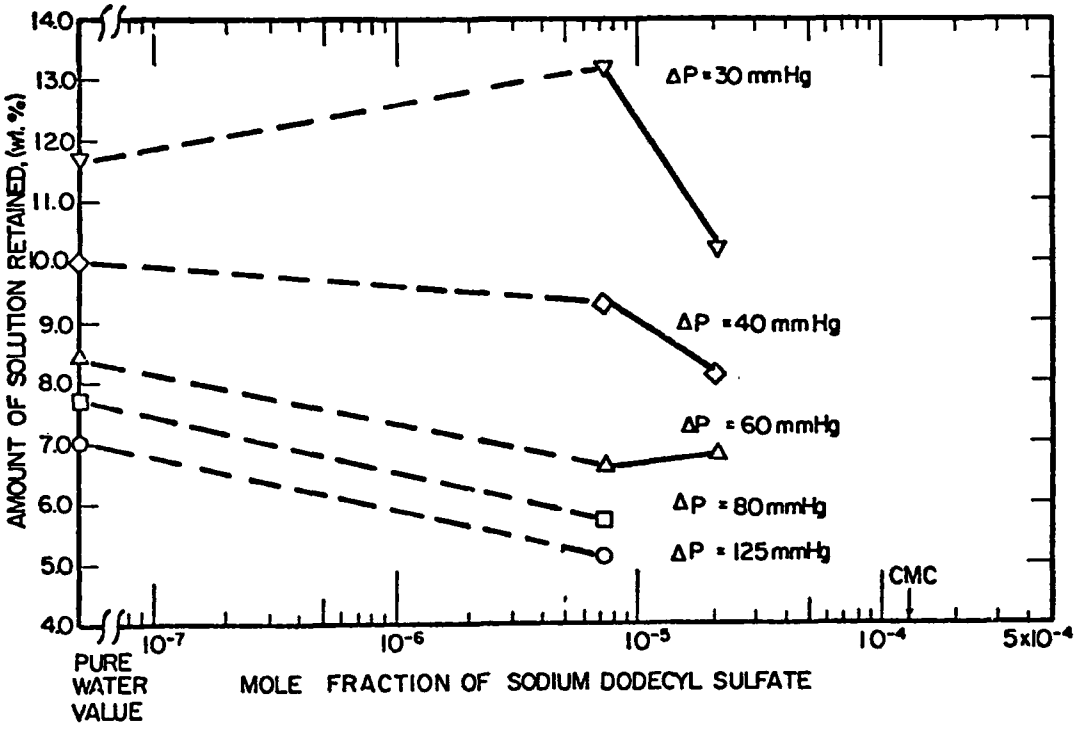

FIGURE 40. EFFECT OF SODIUM DODECYL SULFATE ON THE AMOUNT OF AQUEOUS SOLUTION RETAINED BY THE PRESSURE DE-WATERED COAL BED. (ISOBARIC DATA; COAL SIZE: 35 x 60 MESH).

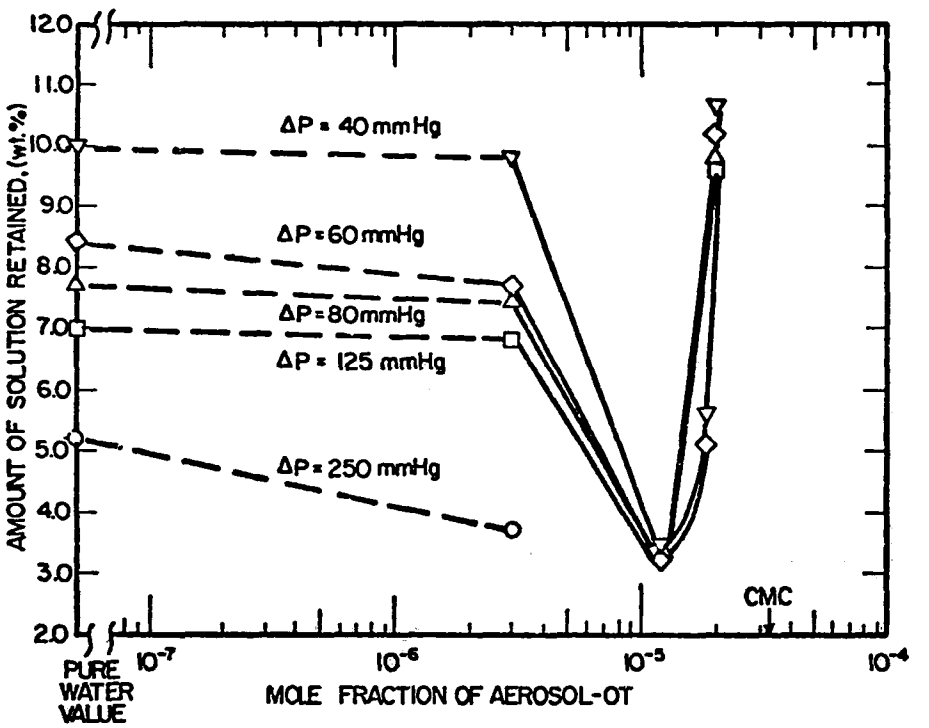

FIGURE 41. EFFECT OF AEROSOL-OT ON THE AMOUNT OF AQUEOUS SOLUTION RETAINED BY THE PRESSURE DEWATERED COAL BED. (ISOBARIC DATA; COAL SIZE: 35 x 60 MESH).

Vacuum Dewatering (non-equilibrium)

The results of the vacuum dewatering experiments [36] are plotted in Figures 42-46. The data are presented in graphs which cover the same range of concentration as presented in the data on the solution-air interfacial tension of Figures 47-51 for perspective. The data for each surfactant is plotted isochronally as stated previously and gives the amount of retained solution as a function of surfactant concentration. The values of retained water content, i.e. at zero concentration of surfactant, at each time value are indicated at the lowest concentration listed on the graphs since a zero is not plottable on a log scale. The data is presented for Aerosol A-196, Triton X-114, dodecyl pyridinium chloride, sodium dodecyl sulfate, and Aerosol-OT respectively. Table III lists the weight of the coal sample used with each surfactant.

TABLE III

WEIGHT OF COAL SAMPLES USED IN

VACUUM DEWATERING EXPERIMENTS

SURFACTANT	COAL SAMPLE WEIGHT (g)
Aerosol A-196	15.2636
Triton X-114	15.6285
Dodecyl Pyridinium Chloride	15.4668
Sodium Dodecyl Sulfate	15.7705
Aerosol-OT	15.1406

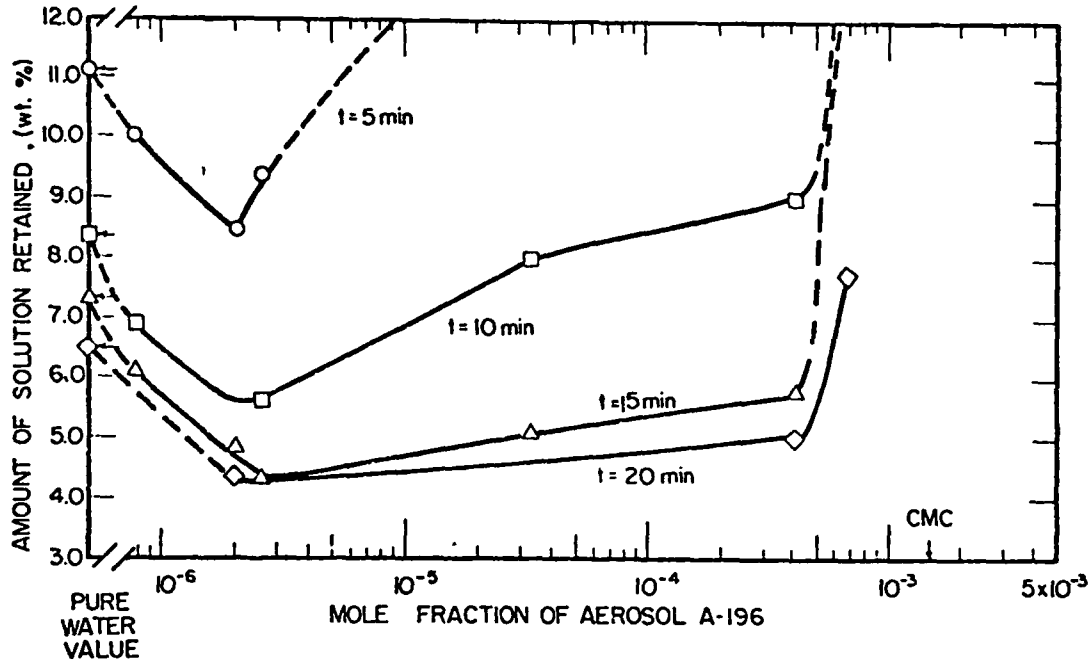

FIGURE 42. EFFECT OF AEROSOL A-196 ON THE RESIDUAL AQUEOUS SOLUTION CONTENT OF THE VACUUM DEWATERED COAL BED. (ISOCHRONAL DATA AT ΔP = 1 ATM; COAL SIZE: 35 x 60 MESH).

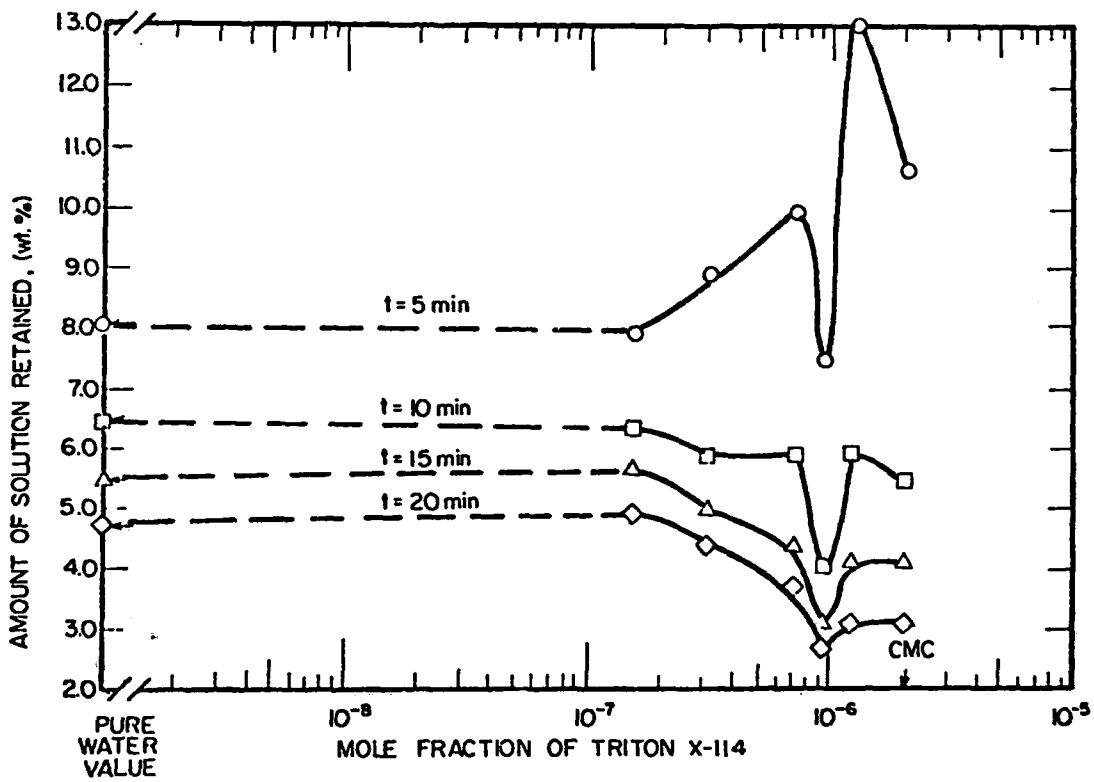

FIGURE 43. EFFECT OF TRITON X-114 ON THE RESIDUAL AQUEOUS SOLUTION CONTENT OF THE VACUUM DEWATERED COAL BED. (ISOCHRONAL DATA AT ΔP = 1 ATM; COAL SIZE: 35 x 60 MESH).

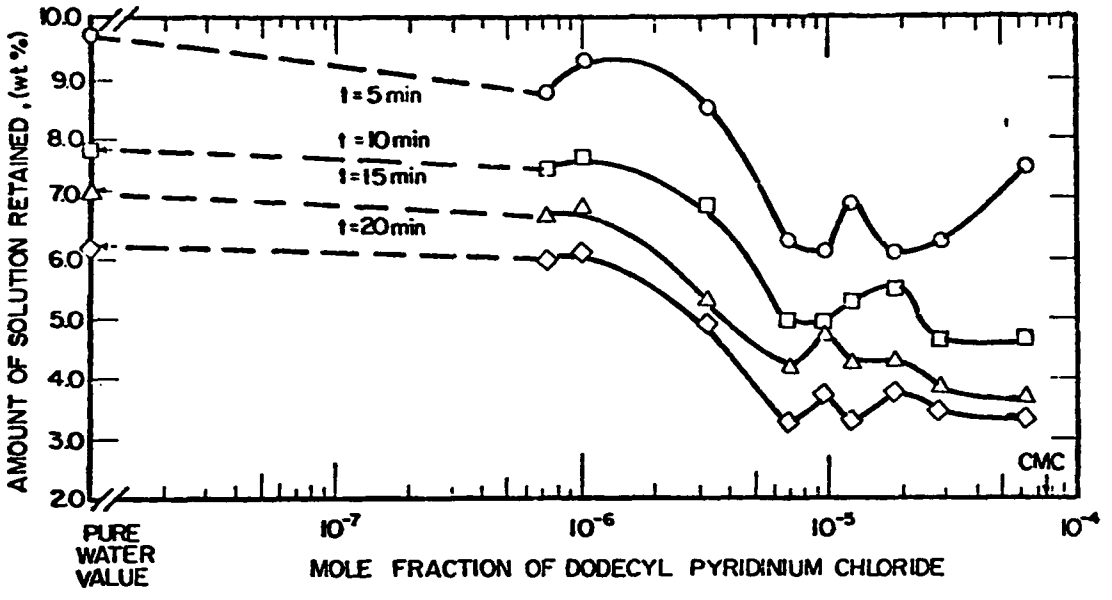

FIGURE 44. EFFECT OF DODECYL PYRIDINIUM CHLORIDE ON THE RESIDUAL AQUEOUS SOLUTION CONTENT OF THE VACUUM DEWATERED COAL BED. (ISO-CHRONAL DATA AT ΔP = 1 ATM; COAL SIZE: 35 x 60 MESH).

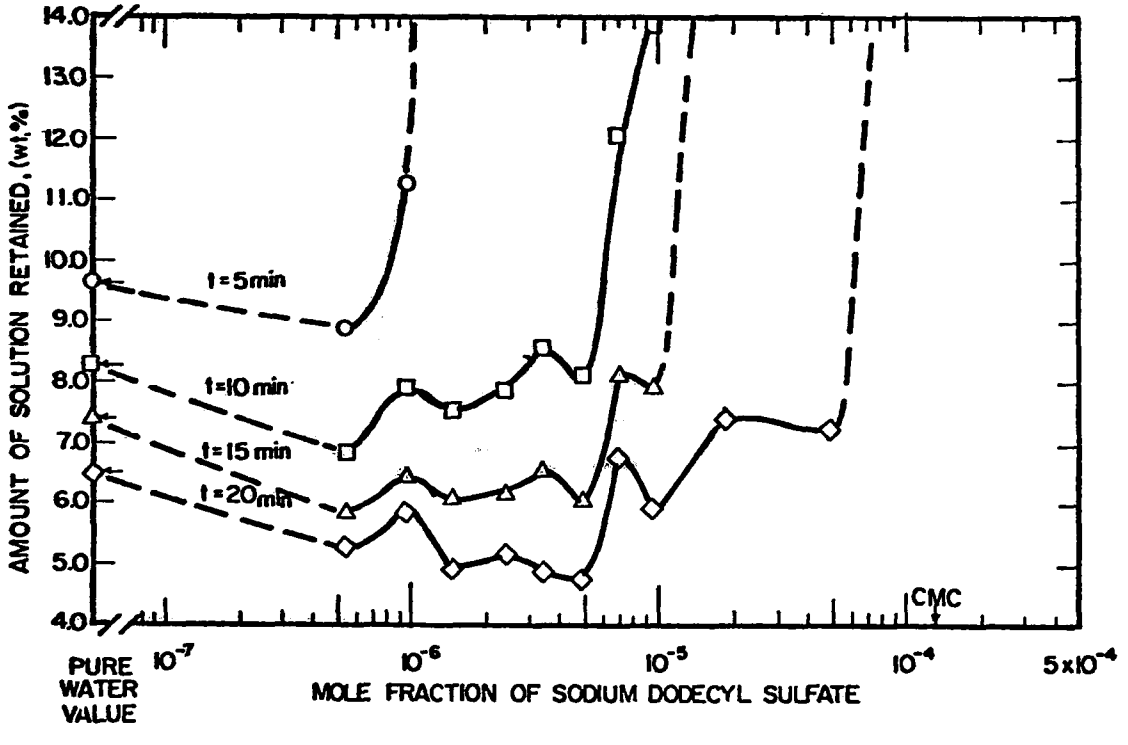

FIGURE 45. EFFECT OF SODIUM DODECYL SULFATE ON THE RESIDUAL AQUEOUS SOLUTION CONTENT OF THE VACUUM DEWATERED COAL BED. (ISO-CHRONAL DATA AT ΔP = 1 ATM; COAL SIZE: 35 x 60 MESH).

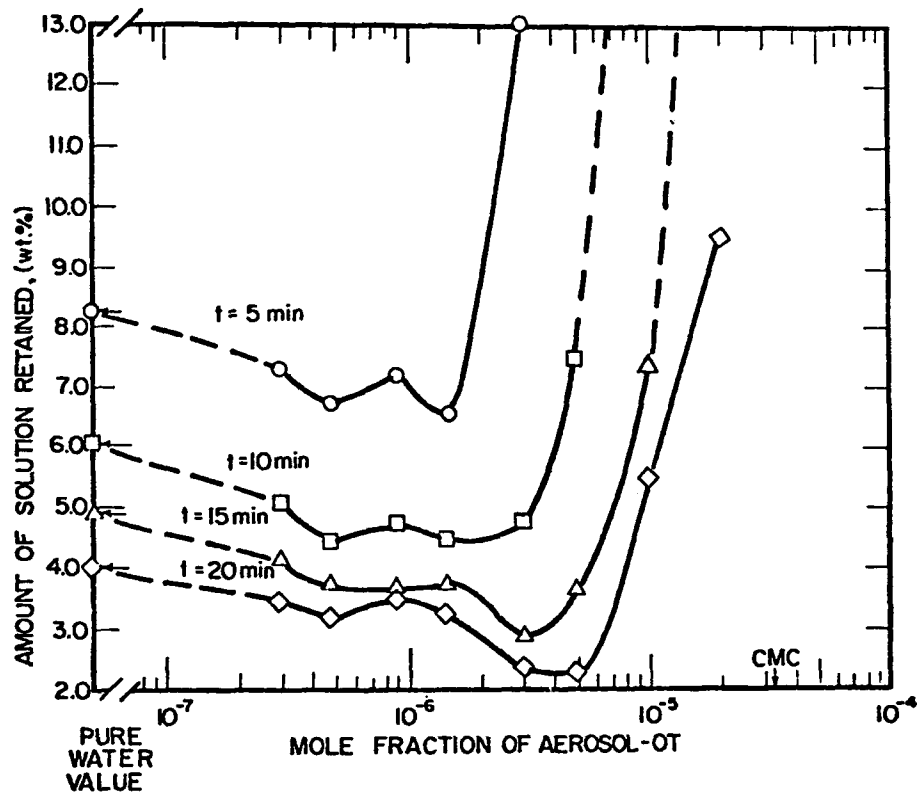

FIGURE 46. EFFECT OF AEROSOL-OT ON THE RESIDUAL AQUEOUS SOLUTION CONTENT OF THE VACUUM DEWATERED COAL BED. (ISOCHRONAL DATA AT ΔP = 1 ATM; COAL SIZE: 35 x 60 MESH).

Liquid-Air Interfacial Tension (γ_{LA}) - Concentration Curves

It has been stated that it was necessary to determine the liquid-air interfacial tension of the aqueous surfactant solutions as a function of concentration so that this could be used as a convenient analytical procedure for determination of the changes in solution concentration on adsorption. Figures 47-51 are the experimentally determined curves for each of the five surfactants studied in this investigation at room temperature, 25°C. The concentration scales are logarithmic to encompass the full range of concentrations investigated. Listed in Table IV are the critical micelle concentrations (CMC) determined by the radical change in slope of the curves at the higher concentrations. It is at this point that the surfactants begin a form of precipitation or aggregation phenomena as described above. Also reported in Table IV are the values of the maximum slope

$$\left.\frac{d\,\gamma_{LA}}{d\,\ln C}\right|_{max}$$

of each curve for later use in determing the area of the adsorbed surfactant molecules.

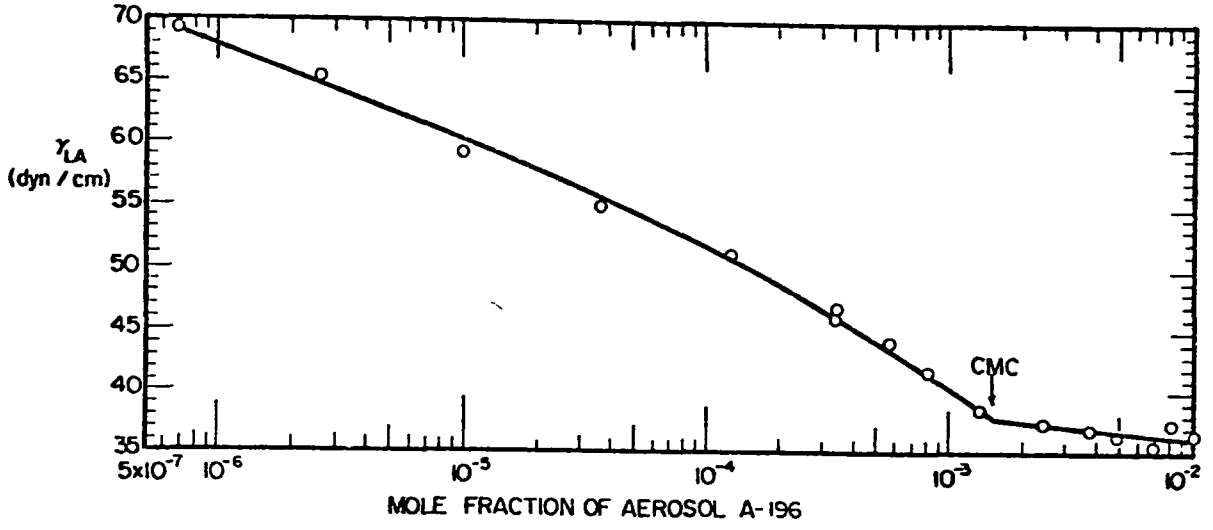

FIGURE 47. LIQUID-AIR INTERFACIAL TENSION OF AQUEOUS SOLUTIONS OF AEROSOL A-196 AT 25°C. [36]

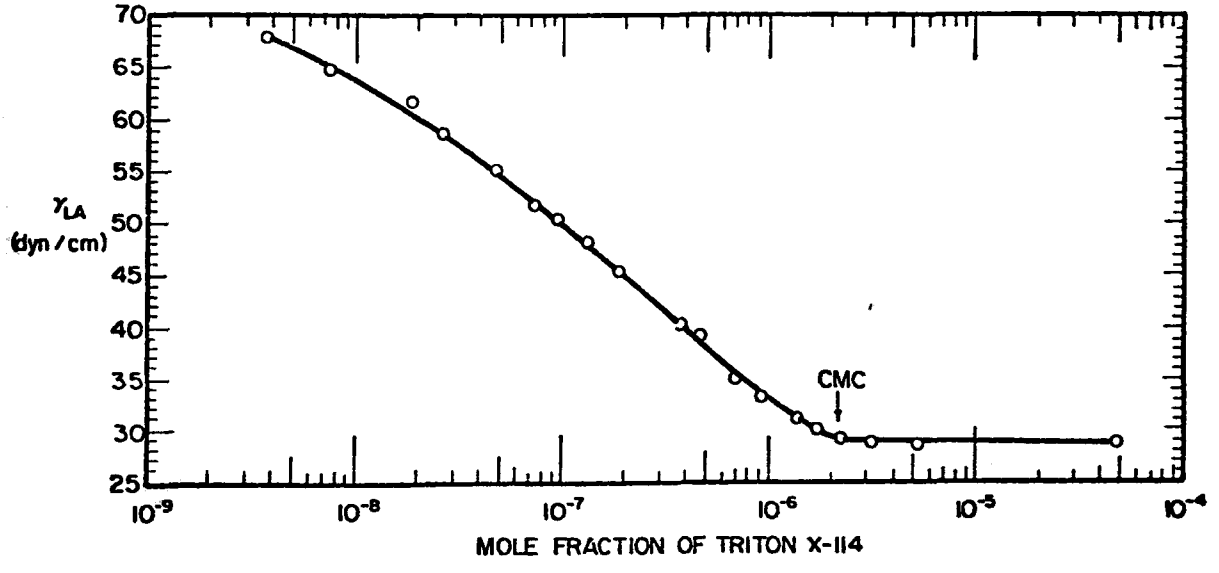

FIGURE 48. LIQUID-AIR INTERFACIAL TENSION OF AQUEOUS SOLUTIONS OF TRITON X-114 AT 25°C.

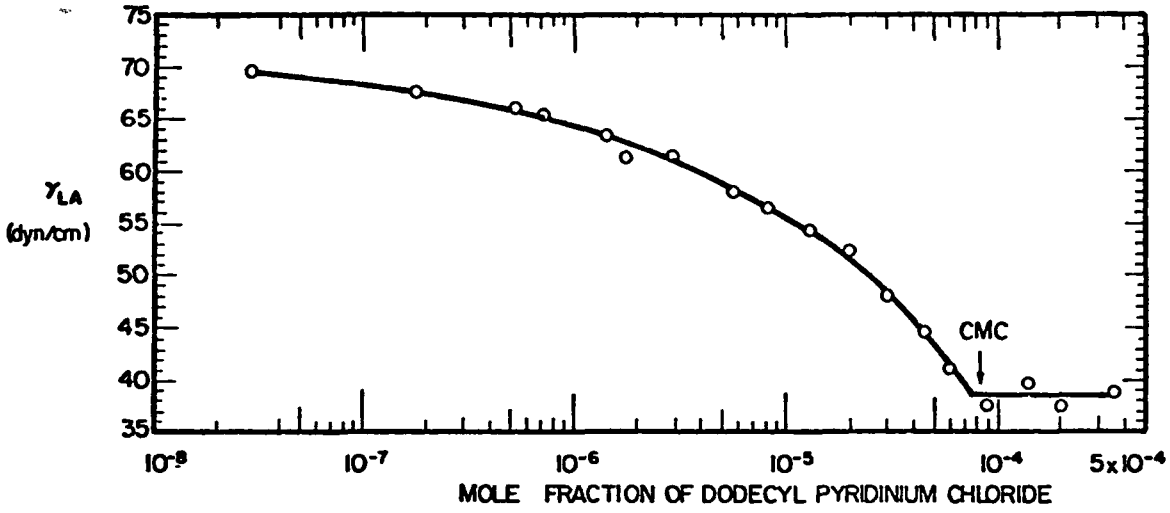

FIGURE 49. LIQUID-AIR INTERFACIAL TENSION OF AQUEOUS SOLUTIONS OF DODECYL PYRIDINIUM CHLORIDE AT 25°C.

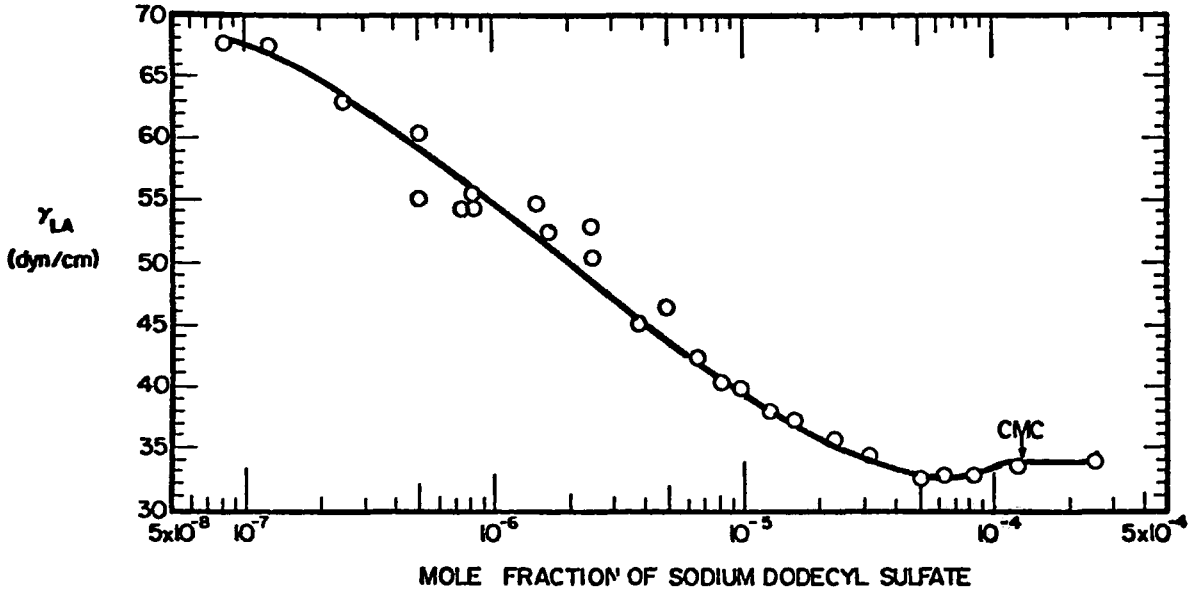

FIGURE 50. LIQUID-AIR INTERFACIAL TENSION OF AQUEOUS SOLUTIONS OF SODIUM DODECYL SULFATE AT 25°C.

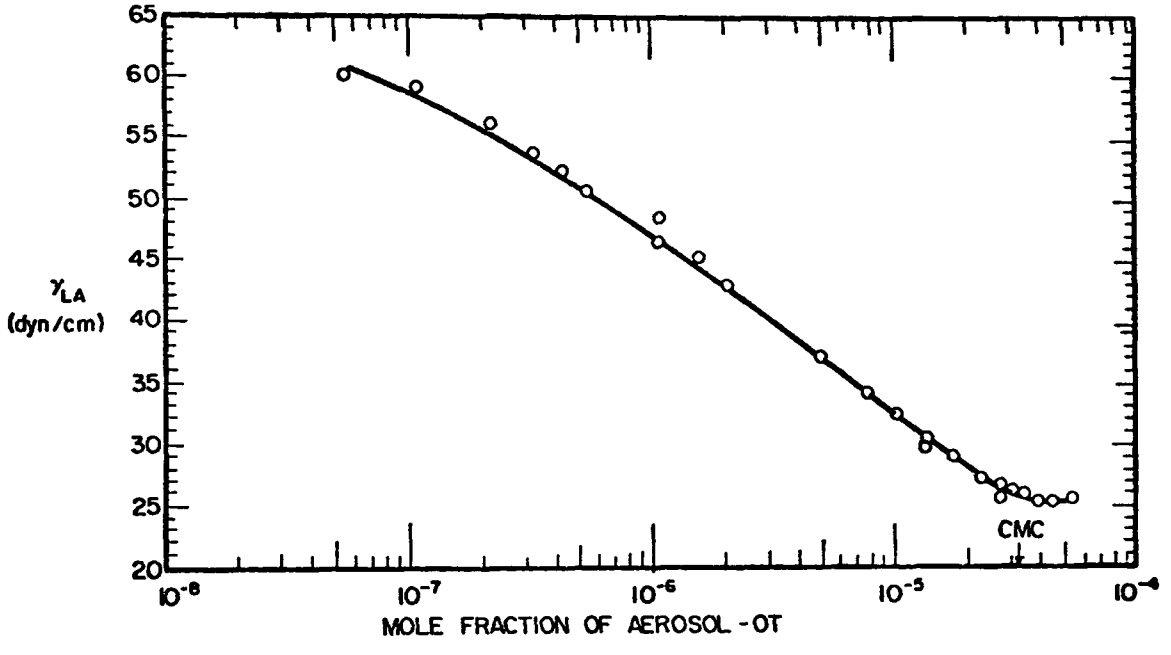

FIGURE 51. LIQUID-AIR INTERFACIAL TENSION OF AQUEOUS SOLUTIONS OF AEROSOL-OT AT 25°C.

TABLE IV

CRITICAL MICELLE CONCENTRATION AND MAXIMUM SLOPE

DETERMINED FROM THE γ_{LA}-lnC CURVES OF EACH SURFACTANT

SURFACTANT	CMC (mole fraction)	$\left.\frac{d\,\gamma_{LA}}{d\,\ln C}\right\|_{max}$ (dyn/cm per order of magnitude increase in concentration)
Aerosol A-196	1.50×10^{-3}	- 6.06
Triton X-114	2.10×10^{-6}	- 7.29
Dodecyl Pyridinium Chloride	7.60×10^{-5}	-11.93
Sodium Dodecyl Sulfate	1.30×10^{-4}	- 7.00
Aerosol-OT	3.20×10^{-5}	- 6.45

Influence of Coal on the Interfacial Tension of Distilled Water

Before conducting the adsorption experiments the liquid-air interfacial tension, γ_{LA}, of twenty-eight milliliters of distilled water (γ_{LA} = 70.50 $\pm$ 0.20 dyn/cm) in which there was approximately twenty grams of coal was monitored [36] for five days to determine whether or not the coal or any of its components were dissolving into the water, which might alter the subsequent interfacial tension measurements. The γ_{LA} value of the water over the slurry remained constant over this time. The settled mixture was agitated regularly to insure homogeneity in the liquid phase. The results are given below in Table V.

The coal sample apparently presented no significant impurities to the contacting liquid phase which could cause a significant γ_{LA} variation. One should note, however, that traces of calcium (or other alkali or alkaline earth elements) might effect reactions with the small concentrations of surfactants in this study. This would be particularly the case at surfactant concentrations below 10^{-6} mole fraction. The γ_{LA} vs. concentration data, however, did not indicate major inflections, which would be expected, if the surfactants were caused to precipitate.

TABLE V

INFLUENCE OF COAL ON THE

INTERFACIAL TENSION OF DISTILLED WATER

DAY	TEMPERATURE (^{o}C)	γ_{LA} (dyn/cm)	H_2O REMAINING IN BEAKER (g)
1	25.5	70.50	27.6730
2	25.5	71.00	27.0302
3	25.0	70.65	26.3224
4	25.0	70.75	25.1628
5	25.5	70.65	24.2422
		mean 70.70 ± 0.20	

Weight of coal = 20.0099 g.

Original weight of water = 28.0000 g.

Adsorption Isotherms

The decrease in surfactant concentration occurring due to the adsorption of the surfactant on the coal was determined by measurement of the liquid-air interfacial tension, γ_{LA}, of the solution over the coal slurry. The "missing" number of surfactant molecules necessary to decrease the concentration to some final value were presumed to be adsorbed on the coal surface. Figures 52-56 are plots of the change in interfacial tension as a function of the original concentration of surfactant in solution when twenty grams of coal were present in that solution. In order to compare these data with those of the standard liquid-air interfacial tensions, the points from the adsorption experiments are shown superimposed on their respective interfacial tension-concentration curves without coal. A smooth curve cannot be drawn through these points since they are not normalized. That is, each point provides only the numerical determination of the change in concentration of the solution, a value which must be multiplied by the total number of moles of solution present and divided by the weight of the adsorbent coal, such that a comparison to other values may be made on an equal basis. Normalization in this manner provides a value for the number of moles of surfactant adsorbed per gram of coal and when this value is plotted against the overall concentration of surfactant present in the coal-water-surfactant solution an adsorption isotherm is generated.

Tables B1-B5 shown in Appendix B provide the data for each surfactant in order to determine the adsorption isotherms. Figures 57-61 are the adsorption isotherms.

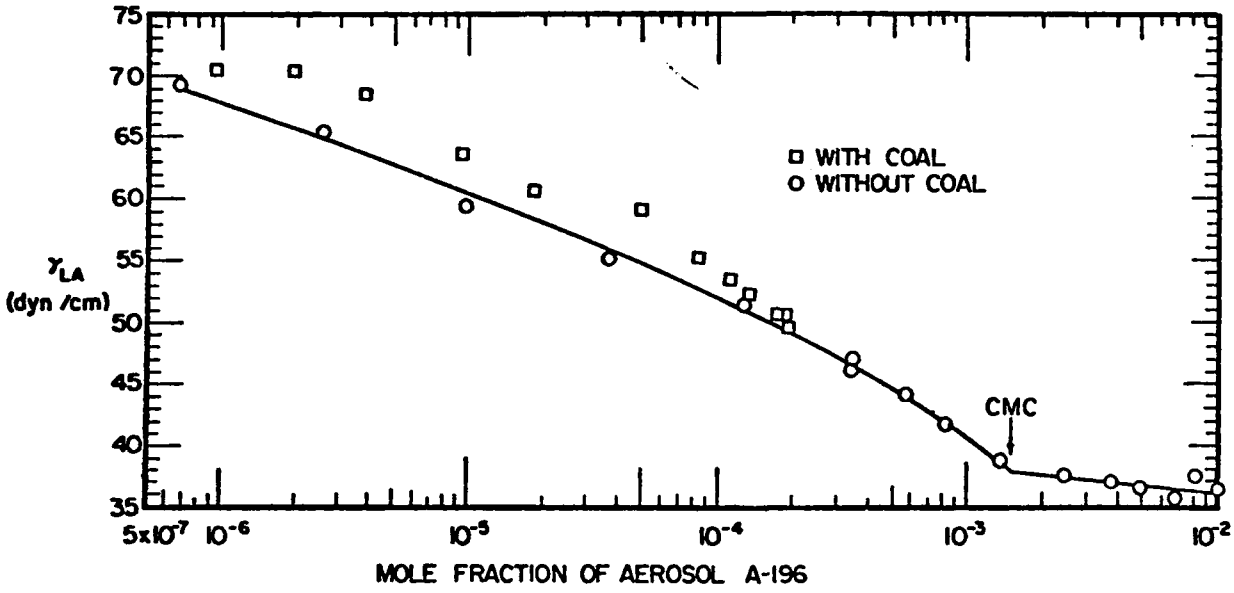

FIGURE 52. LIQUID-AIR INTERFACIAL TENSION OF FIXED AMOUNTS OF AQUEOUS SOLUTIONS OF AEROSOL A-196 IN CONTACT WITH AN ADSORBENT COAL SAMPLE, TOGETHER WITH THE DATA TAKEN WITHOUT THE COAL PRESENT, FOR DETERMINATION OF THE CHANGE IN SOLUTION CONCENTRATION ON ADSORPTION.

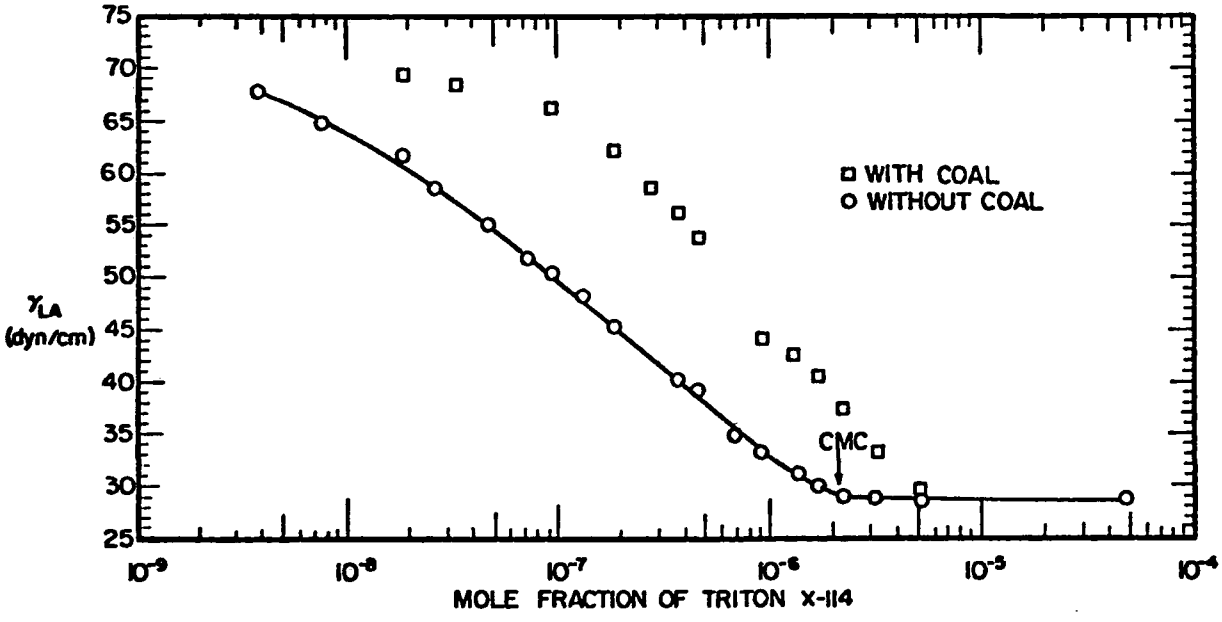

FIGURE 53. LIQUID-AIR INTERFACIAL TENSION OF FIXED AMOUNTS OF AQUEOUS SOLUTIONS OF TRITON X-114 IN CONTACT WITH AN ADSORBENT COAL SAMPLE, TOGETHER WITH THE DATA TAKEN WITHOUT THE COAL PRESENT, FOR DETERMINATION OF THE CHANGE IN SOLUTION CONCENTRATION ON ADSORPTION.

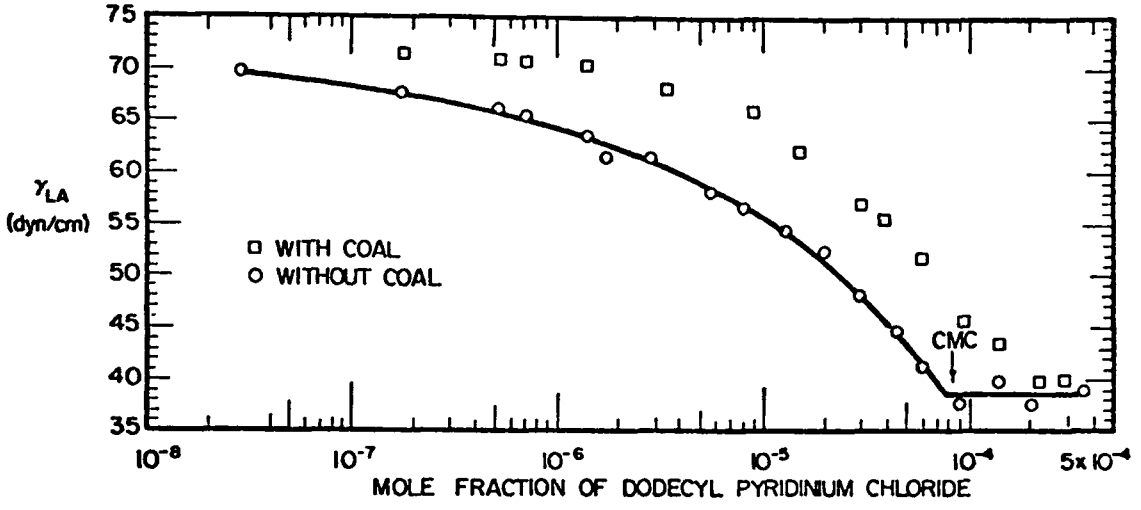

FIGURE 54. LIQUID-AIR INTERFACIAL TENSION OF FIXED AMOUNTS OF AQUEOUS SOLUTIONS OF DODECYL PYRIDINIUM CHLORIDE IN CONTACT WITH AN ADSORBENT COAL SAMPLE, TOGETHER WITH THE DATA TAKEN WITHOUT THE COAL PRESENT, FOR DETERMINATION OF THE CHANGE IN SOLUTION CONCENTRATION ON ADSORPTION.

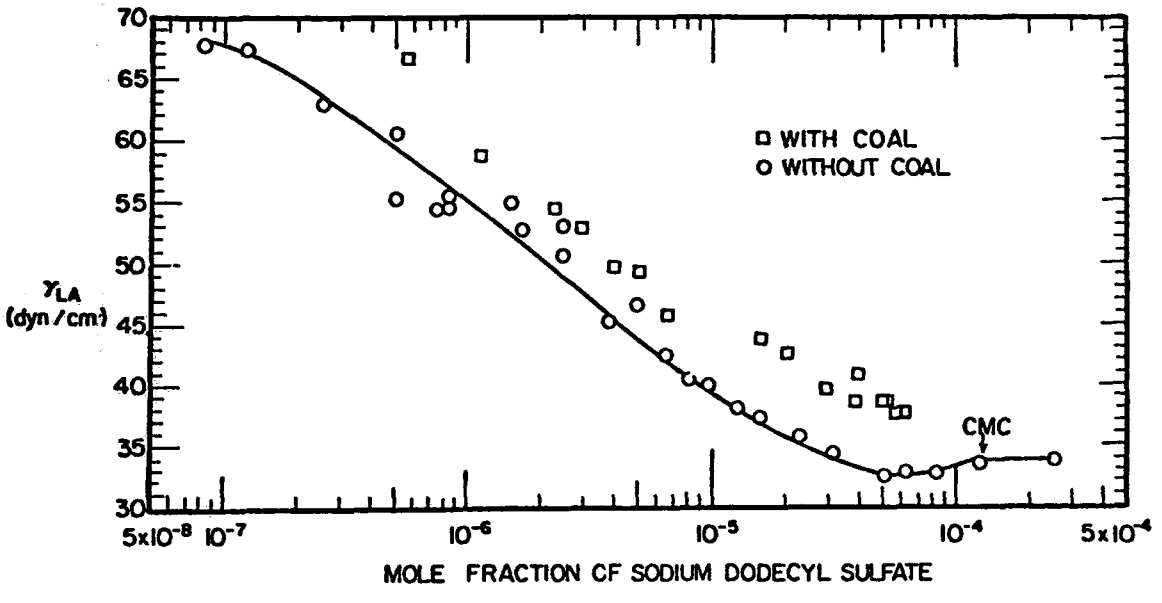

FIGURE 55. LIQUID-AIR INTERFACIAL TENSION OF FIXED AMOUNTS OF AQUEOUS SOLUTIONS OF SODIUM DODECYL SULFATE IN CONTACT WITH AN ADSORBENT COAL SAMPLE, TOGETHER WITH THE DATA TAKEN WITHOUT THE COAL PRESENT, FOR DETERMINATION OF THE CHANGE IN SOLUTION CONCENTRATION ON ADSORPTION.

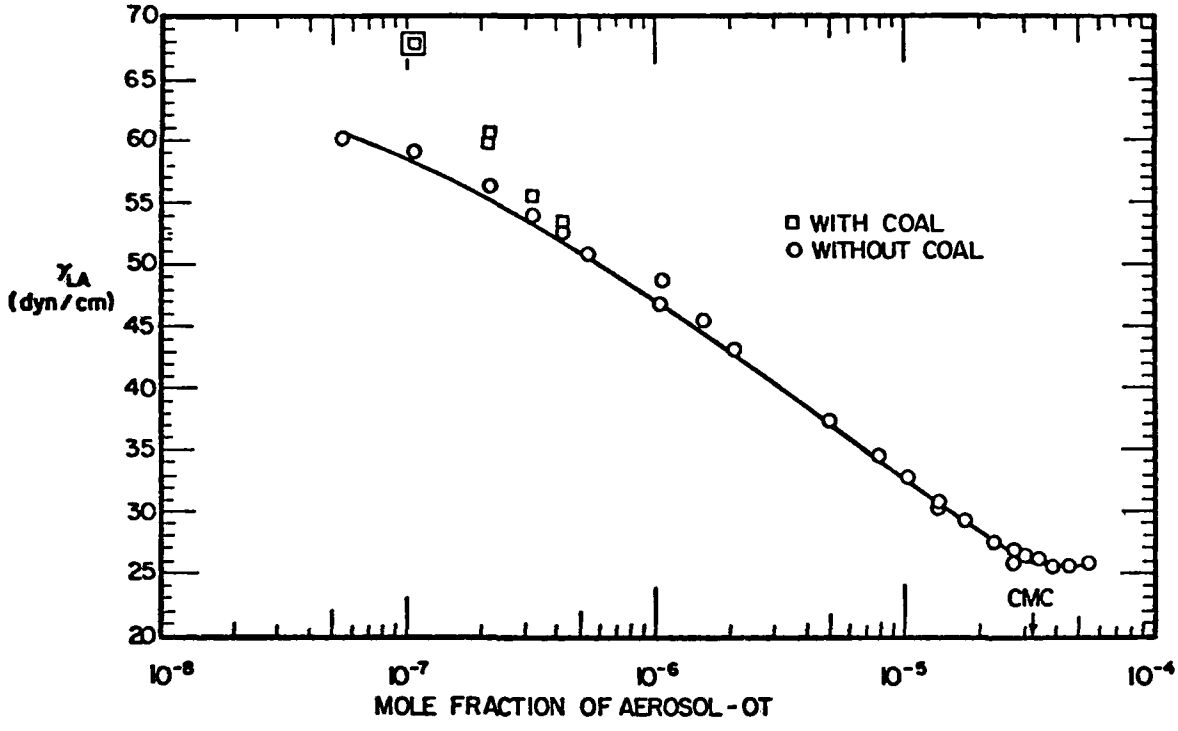

FIGURE 56. LIQUID-AIR INTERFACIAL TENSION OF FIXED AMOUNTS OF AQUEOUS SOLUTIONS OF AEROSOL-OT IN CONTACT WITH AN ADSORBENT COAL SAMPLE, TOGETHER WITH THE DATA TAKEN WITHOUT THE COAL PRESENT, FOR DETERMINATION OF THE CHANGE IN SOLUTION CONCENTRATION ON ADSORPTION.

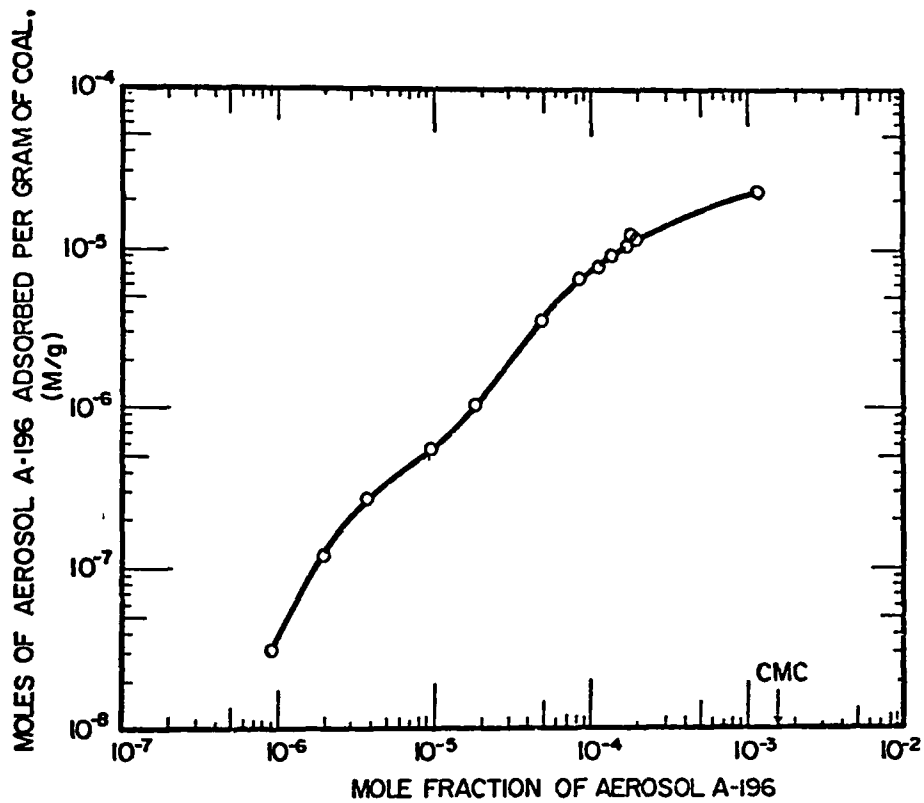

FIGURE 57. ADSORPTION ISOTHERM FOR AEROSOL A-196 ON 35 x 60 MESH COAL FROM AQUEOUS SOLUTION AT 25°C.

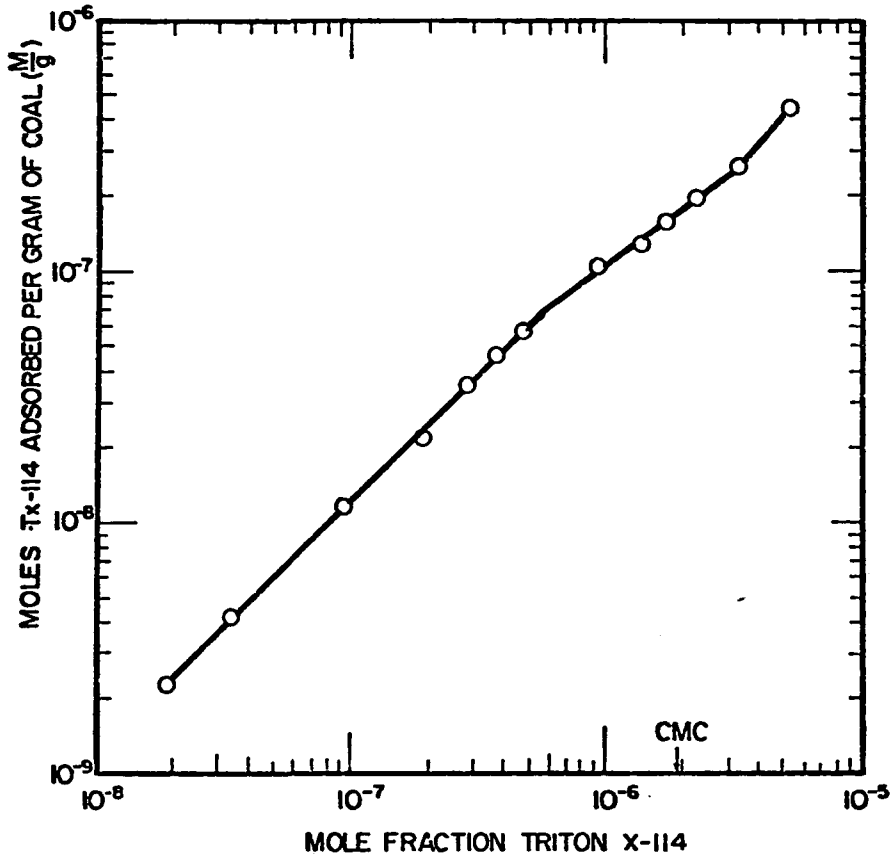

FIGURE 58. ADSORPTION ISOTHERM FOR TRITON X-114 ON 35 x 60 MESH COAL FROM AQUEOUS SOLUTION AT 25°C.

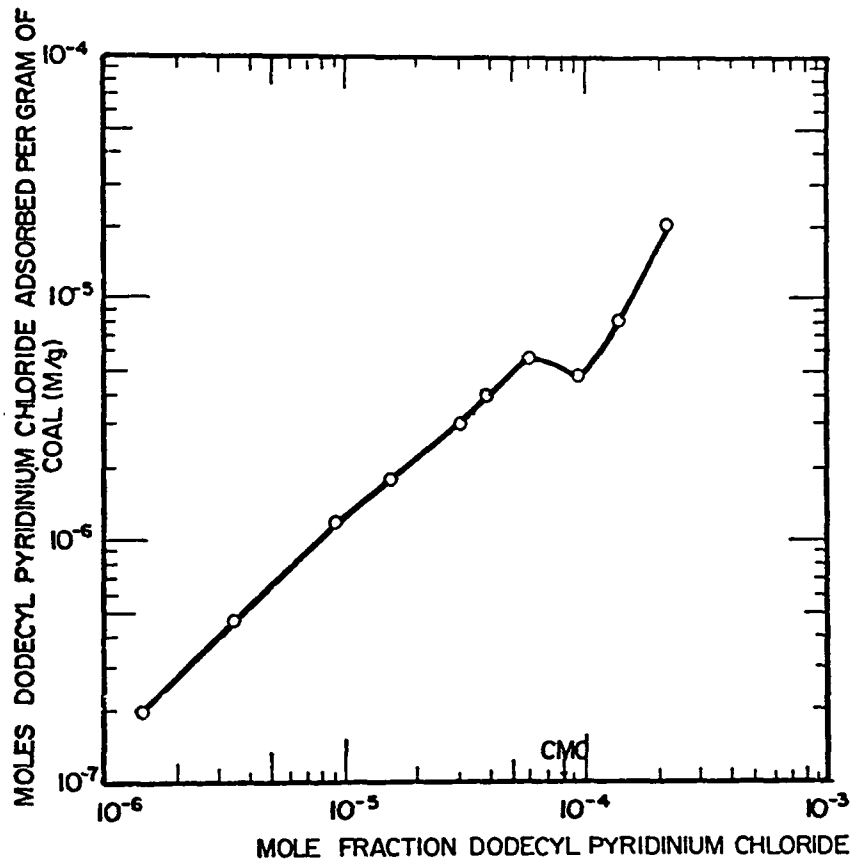

FIGURE 59. ADSORPTION ISOTHERM FOR DODECYL PYRIDINIUM CHLORIDE ON 35 x 60 MESH COAL FROM AQUEOUS SOLUTION AT 25°C.

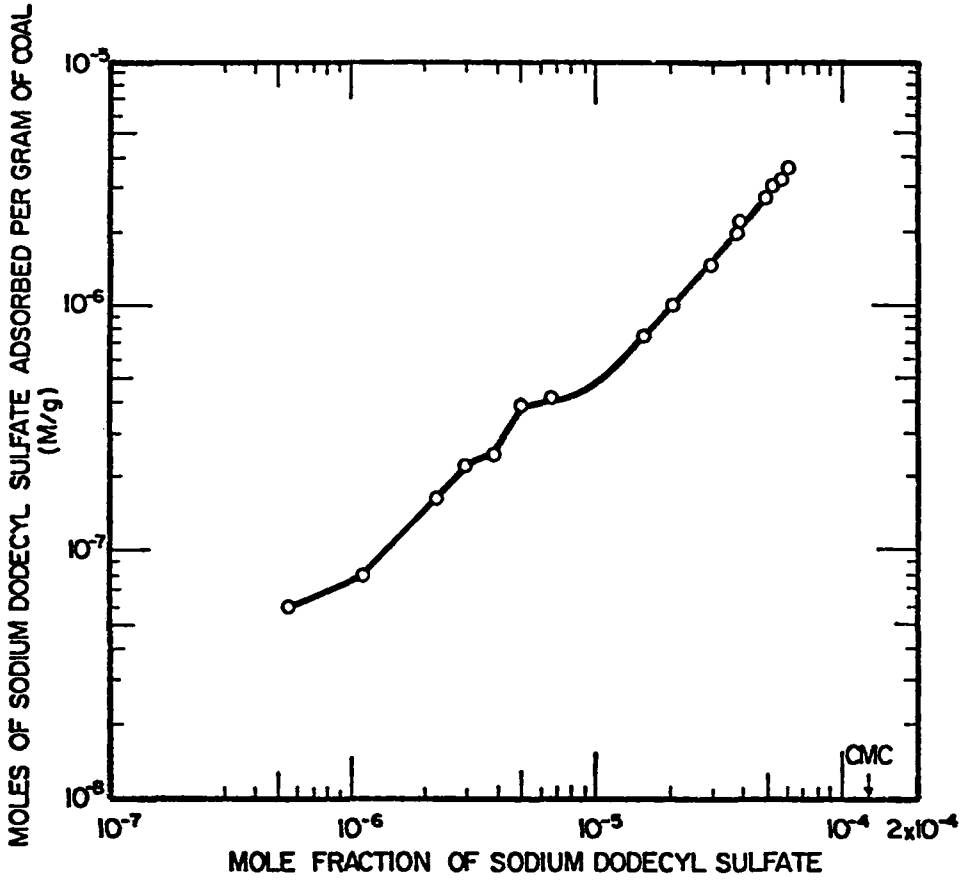

FIGURE 60. ADSORPTION ISOTHERM FOR SODIUM DODECYL SULFATE ON 35 x 60 MESH COAL FROM AQUEOUS SOLUTION AT 25°C.

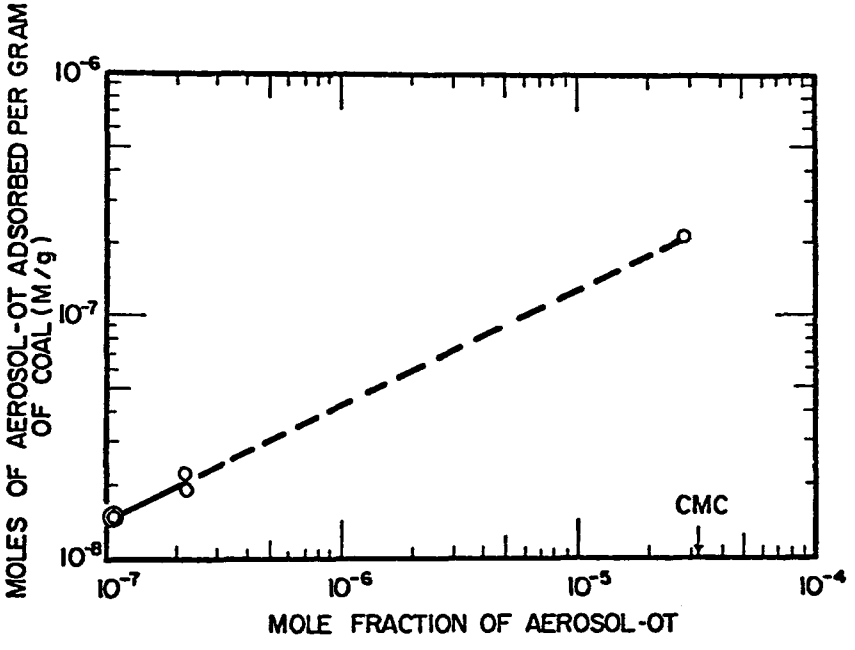

FIGURE 61. ADSORPTION ISOTHERM FOR AEROSOL-OT ON 35 x 60 MESH COAL FROM AQUEOUS SOLUTION AT 25°C.

Standard Free Energy of Adsorption

The standard free energy of adsorption as a function of concentration for each surfactant adsorption isotherm was generated through the use of Equation (6)

$$\Gamma = 2r\ C \exp\left[-\ \Delta G^{o}_{ADS}/RT\right]$$

In calculating the values for ΔG^{o}_{ADS}, R was taken as 1.987 cal/mole^{o}K and T as 298°K. The radii, r, of the adsorbed molecules were determined from the areas per molecule found through the use of the slopes of the interfacial tension curves for each surfactant. The areas were assumed to be circular so that $A = \pi r^2$.

To determine a value for Γ, which is in units of moles/cm^2, the values of the moles of surfactant adsorbed per gram of coal had to be divided by a specific surface area of the coal. The value used was 500 cm^2/gm for reasons which will become apparent in the discussion section. In any case, the shape of the curve remains constant regardless of the value chosen.

Figures 62-66 are the plots of the standard free energy of adsorption generated from each data point of the adsorption isotherms of each surfactant.

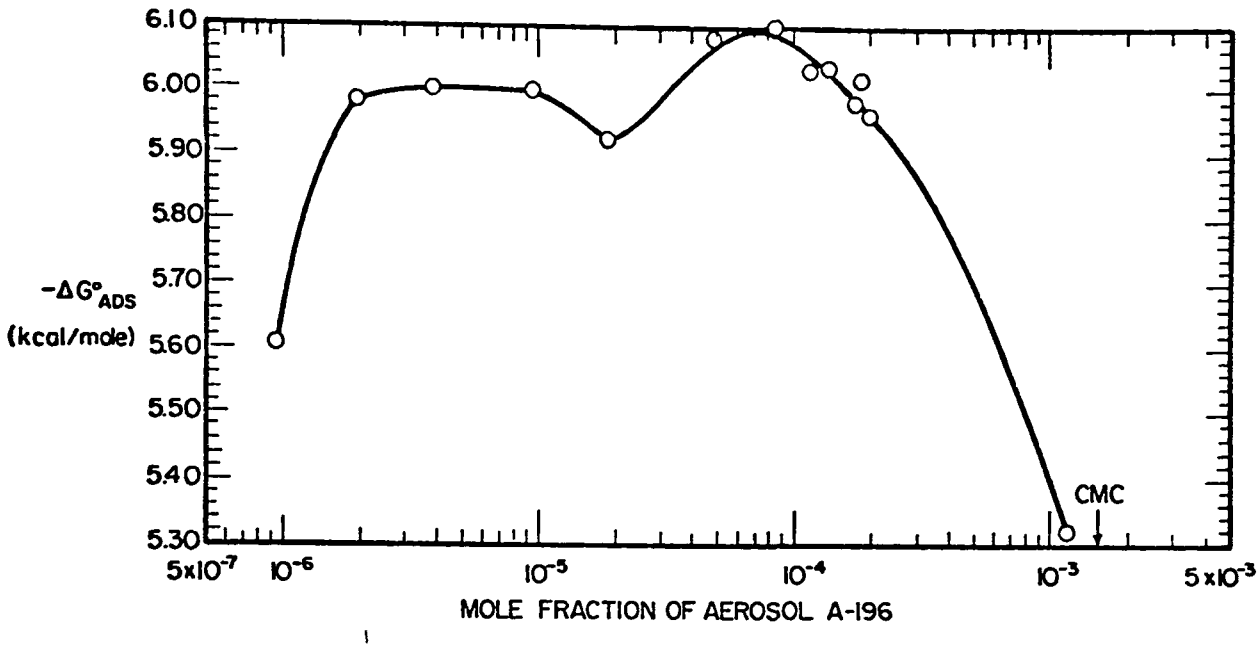

FIGURE 62. STANDARD FREE ENERGY OF ADSORPTION FOR AEROSOL A-196 ON 35 x 60 MESH COAL AT 25°C.

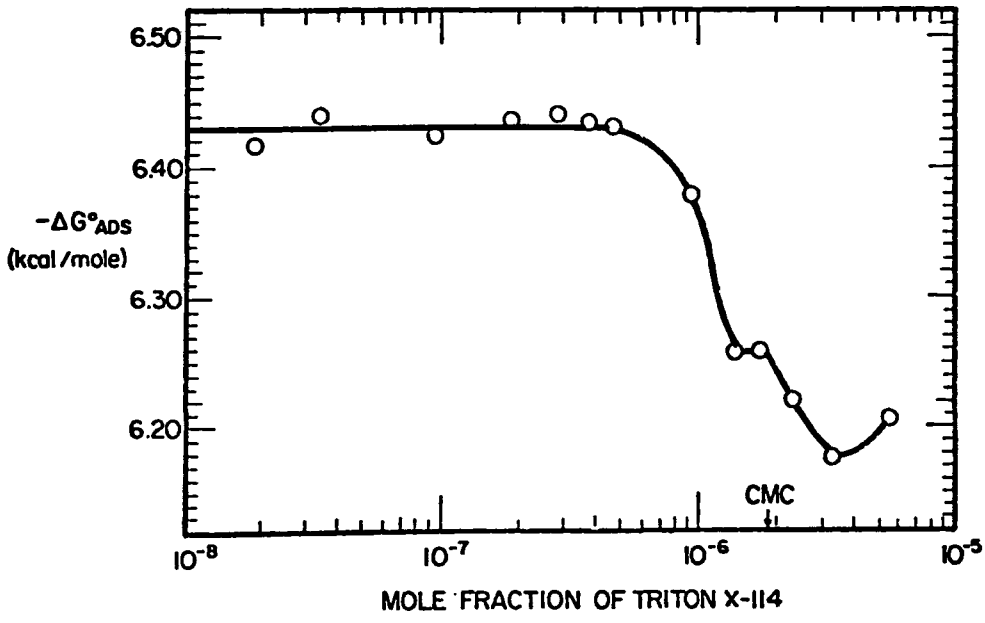

FIGURE 63. STANDARD FREE ENERGY OF ADSORPTION FOR TRITON X-114 ON 35 x 60 MESH COAL AT 25°C.

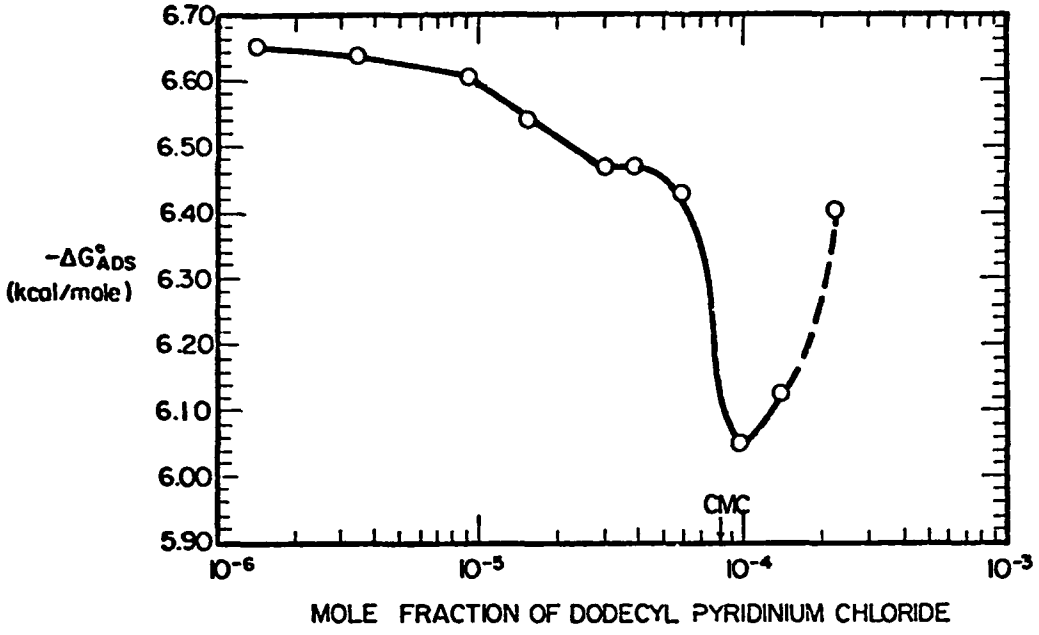

FIGURE 64. STANDARD FREE ENERGY OF ADSORPTION FOR DODECYL PYRIDINIUM CHLORIDE ON 35 x 60 MESH COAL AT 25°C.

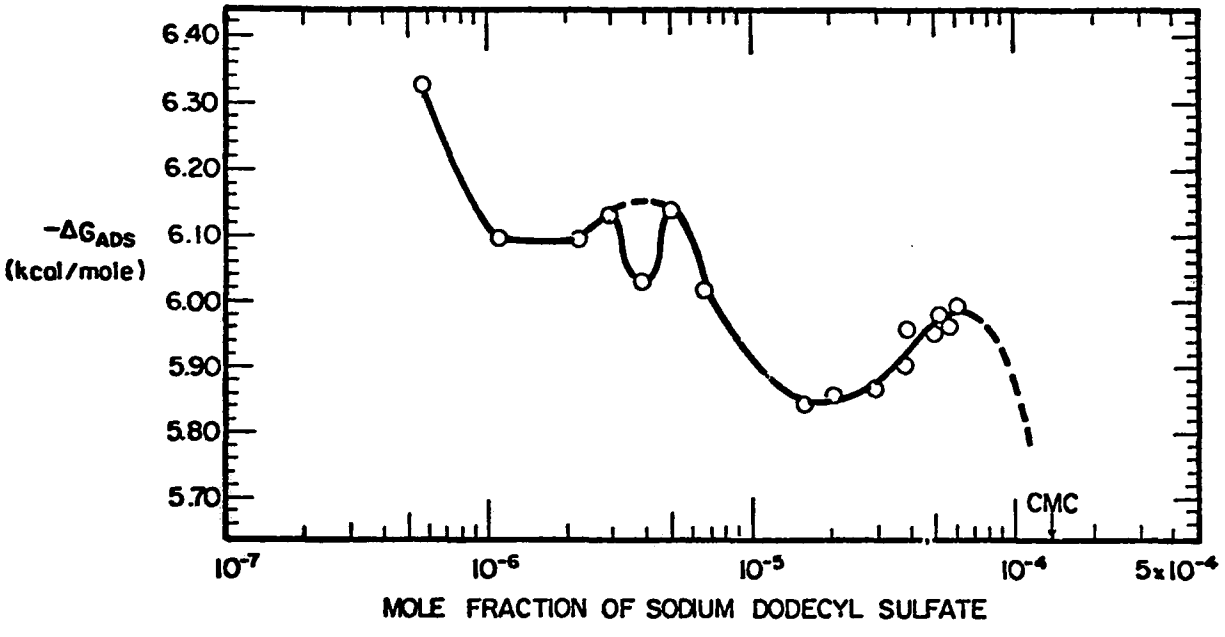

FIGURE 65. STANDARD FREE ENERGY OF ADSORPTION FOR SODIUM DODECYL SULFATE ON 35 x 60 MESH COAL AT 25°C.

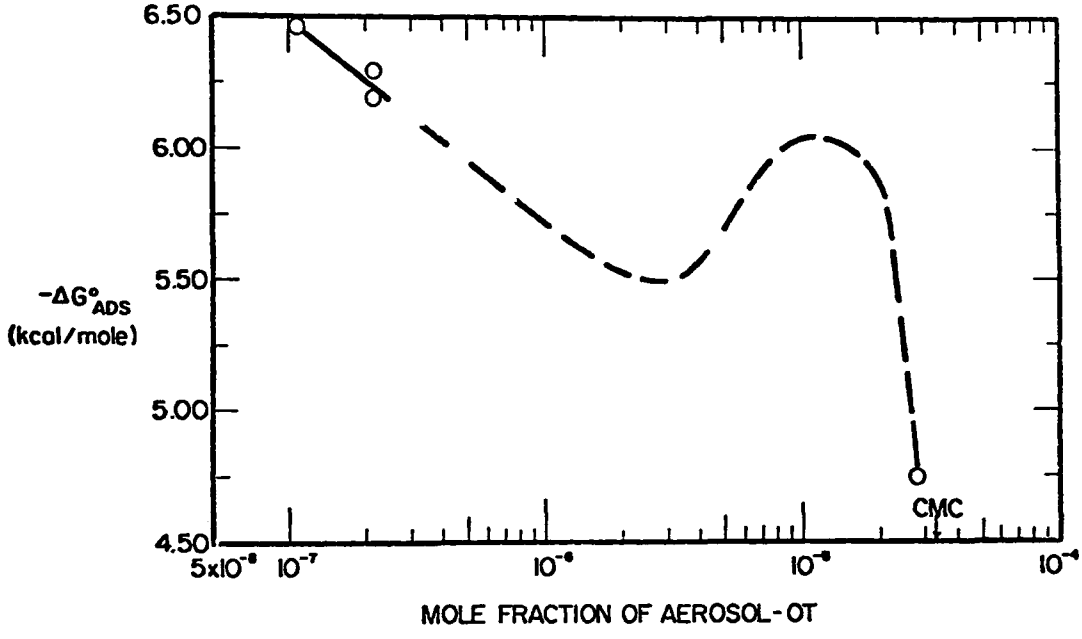

FIGURE 66. STANDARD FREE ENERGY OF ADSORPTION FOR AEROSOL-OT ON 35 x 60 MESH COAL AT 25°C.

IX. DISCUSSION

Interfacial Tension - Concentration Curves

The data for the liquid-air interfacial tension, γ_{LA}, as a function of concentration for each surfactant were not only used as calibration curves to determine unknown concentrations of surfactants, but also to obtain the limits of the range of concentration to be investigated for each surfactant. The lower limit was governed by the onset of observable surface activity as evidenced by a decrease in γ_{LA}. The upper limit, however, was limited by the CMC, since at this point the system under investigation becomes multiphase.

Data past the CMC in each case was limited, therefore, since a precise determination of the CMC was not the objective. Precise determination of the CMC by the surface tension log plot method is dependent upon the extent of the data points used in determining the intersection of the best fit straight lines for the data above and below the change in slope of the curves [42]. This and other techniques for determination of CMC's of aqueous surfactant systems have been reviewed and evaluated by Murkerjee and Mysels [42].

Nevertheless, comparison of the CMC data with values reported in the literature shows good agreement. Table VI lists the CMC's determined in this investigation along with literature values.

Examination of the γ_{LA} - lnC curve for sodium dodecyl sulfate shown in Figure 50 reveals evidence of a minimum slightly below the CMC. Such a minimum has been observed by other investigators [43-47] and has been determined [46] to be due to the presence of some lauryl alcohol impurity, common in most commercially available samples of sodium dodecyl sulfate,and

is reported to disappear when highly purified sodium dodecyl sulfate was used [47].

TABLE VI

CRITICAL MICELLE CONCENTRATIONS

OF AQUEOUS SURFACTANT SOLUTIONS*

SURFACTANT	CMC (mole fraction)	
	THIS WORK	OTHERS
Aerosol A-196	1.50×10^{-3}	———
Triton X-114	2.10×10^{-6}	3.02×10^{-6}[48]
Dodecyl Pyridinium Chloride	7.60×10^{-5}	5.04×10^{-5}[49]; 2.53×10^{-4}[50]
Sodium Dodecyl Sulfate	1.30×10^{-4}	1.44×10^{-4}[51]; 1.52×10^{-4}[52]
Aerosol-OT	3.20×10^{-5}	4.51×10^{-5}[53]; 2.84×10^{-5}[54]

*Room temperature values, 25°C.

Pressure Dewatering

Examination of the dewatering curves of Figures 24-36 reveals that decreasing the interfacial tension of the water in the coal beds at the liquid-air interface through the addition of the surfactants reduced the pressure differentials necessary to accomplish the major portion of the dewatering, which is a trend expected for a capillary system.

Figure 67 is a plot of the interfacial tensions of the solutions expelled from the coal beds versus the respective differentials $\Delta P(max)$ at which the dewatering curve had the maximum slope. The data were listed in Table II. According to the capillary theory discussed above the relationship should be linear if the pore size of each coal bed was the same. The capillary equation, Eq.(5) , in this case can be rewritten as:

$$\gamma_{LA} = \frac{r}{2} \Delta P(max) \qquad (27)$$

The solid line drawn through the data points of Figure 67 is the result of a linear regression analysis of the data, inclusive of the natural data point at the origin. The correlation coefficient of the data, which is a measure of the "degree of fit" of the given points to the straight line, was calculated to be 0.894 which indicates a reasonably good correlation considering the complexity of the system under study.

If then the coal beds can be regarded as a bundle of capillary tubes, then the slope of this line is half of an average effective pore radius, i.e., a pore radius of 42.18 μm.

The least squares line, however, gives an intercept on the γ_{LA} axis

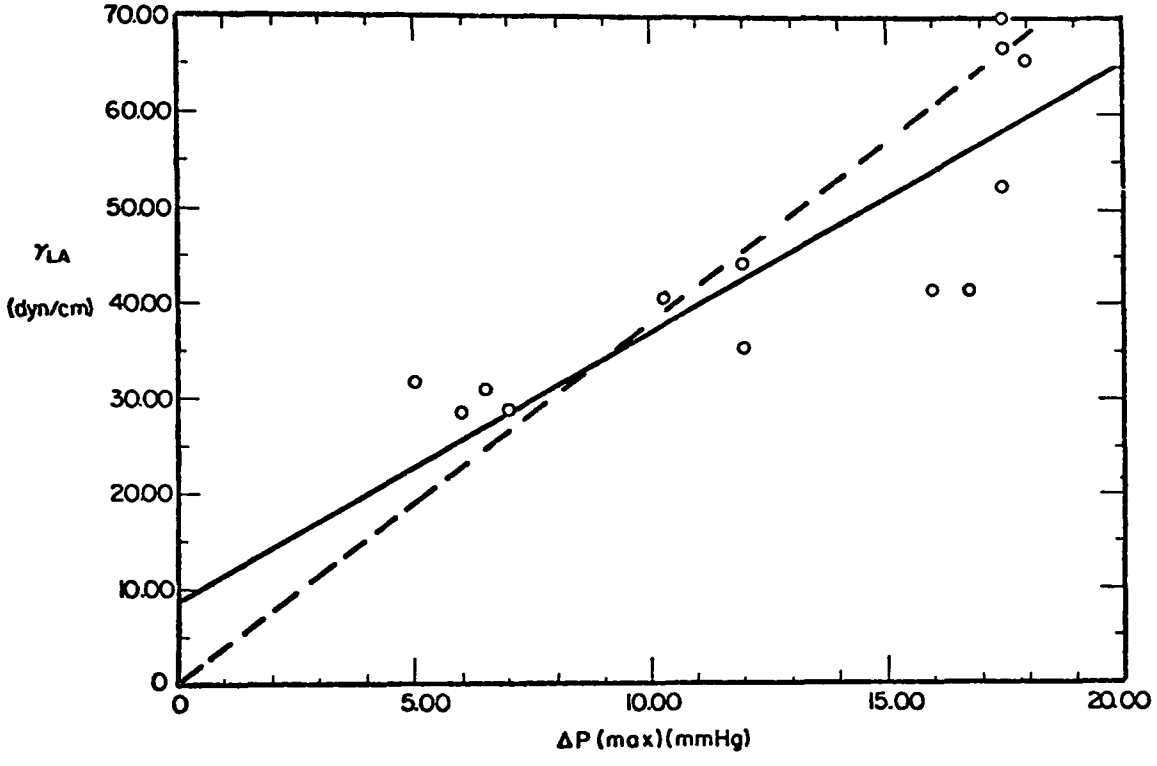

FIGURE 67. RELATIONSHIP BETWEEN THE LIQUID-AIR INTERFACIAL TENSION, γ_{LA}, OF THE AQUEOUS SOLUTION PRESENT IN THE COAL BED AND THE PRESSURE DIFFERENTIAL, ΔP, AT WHICH THE RESPECTIVE DEWATERING CURVE HAD ITS MAXIMUM SLOPE. (——) LINEAR REGRESSION LINE, (---) BEST FIT LINE PASSING THROUGH THE ORIGIN.

of 8.73 dyn/cm. According to the theory though, the line must pass through the origin. It should be noted, however, that the equation as applied assumes that the bed of particles can be regarded as a bundle of capillary tubes of uniform circular cross section; however, in the original derivation from the Laplace equation [55] in which the pressure difference is determined across a curved interface, the surface of a liquid in a capillary, is related to the liquid surface tension and the harmonic mean of the two principal radii of curvature of the interface:

$$\Delta P = \gamma\left(\frac{1}{R_1} + \frac{1}{R_2}\right) \tag{28}$$

Only for the case of a spherical interface, e.g.,the hemispherical meniscus in the capillary, does $R_1 = R_2$ and therefore give

$$\Delta P = \frac{2\gamma}{r} \tag{29}$$

Furthermore, even if the approximation of circular capillaries could be applied to uniformly packed smooth spheres this need not at all be appropriate for coal particles which are neither smooth nor spherical.

Also, the intercept is only an error of about 10% on the γ_{LA} scale, which for a real system with the above assumptions is not unreasonable.

Furthermore the values of $\Delta P(max)$ were chosen as the representative number for each experiment. The slopes of all the dewatering curves were however all askew, with the largest slopes always at the lower ΔP values. The solid line of Figure 67 has only to be offset up the ΔP axis by 3.2

mm Hg for the line to pass through the origin. The determination of the $\Delta P(max)$ value is subject to interpretation. In this case the actual maximum slope was chosen. The other choices however would give values of ΔP higher than the $\Delta P(max)$ and values 3.2 mmHg higher are still contained on the steeply sloping portion of each dewatering curve.

Therefore the fact that the data produce an intercept value is not unreasonable. However to provide a comparison curve, the dashed line of Figure 67 was drawn so as to be the best fit straight line for the data points but passing through the origin. This slope gives a slightly larger pore radius of 57.42 μm.

At this point we can determine a relationship between the effective pore size determined to be in the coal bed and the known particle size of the coal present, by obtaining the ratio of average particle radius to average pore radius.

The actual coal particles size used in these experiments was fixed to range from 420 μm to 250 μm in diameter. Two values for an average particle diameter can be calculated: an arithmetic average and a logarithmic average, since when coal fractures it is known to produce a logarithmic size distribution of the resulting particles. The arithmetic average is 335 μm and the log average is 342 μm which give particle radii of 167.5 and 162 μm respectively. Table VII gives the values of the ratio of particle radii to pore radii calculated for both averages and both pore radii. For uniform spheres arranged in a close packed structure, the ratio would be 4.44. Haines [56] has calculated that for spheres, depending on their packing, the ratio can vary from 2.0 to 6.4. Gray [3] in his study of Betteshanger coal of a similar size distribution obtained a value of about 3.00. The preferred value of Table VII would be 3.84. However, by multi-

TABLE VII

RATIO OF THE AVERAGE COAL PARTICLE RADIUS

TO THE AVERAGE PORE RADIUS OF THE COAL BEDS

AVERAGE PARTICLE DIAMETER (μm)	AVERAGE PARTICLE RADIUS (μm)	AVERAGE PORE RADIUS (μm)	RATIO AVERAGE PARTICLE RADIUS / AVERAGE PORE RADIUS	
335*	167.5	42.18	3.97	With Intercept
324**	162	42.18	3.84***	With Intercept
			3.00	Gray's value
335	167.5	57.42	2.92	Without Intercept
324	162	57.42	2.82	Without Intercept

* Arithmetic average

** Logarithmic average

*** Preferred value

plying the smallest ratio with the smallest pore radii and the largest ratio with the largest pore radii and then doubling the values we can obtain a particle size distribution indicative of the spread of these values. The distribution obtained is 456 μm to 238 μm, which is almost identical to the distribution known to be in the bed, i.e. 420 μm x 250 μm.

The addition of the surfactants to the water contained in a coal bed, therefore, serves to lower the interfacial tension of the water at the liquid-air interface, which in turn lowers the applied pressure differential required to effect dewatering. And, furthermore, the relationship between the interfacial tension of the liquid of the bed and the pressure differentials is consistent with that predicted by the application of a capillary theory to the system.

If the coal beds are reasonably well approximated by a bundle of capillary tubes with an average radius of 42.18 μm then it is possible to calculate the surface area of those capillaries if their contained volume were known. This volume would be the volume of the water contained in a completely saturated bed. The dewatering data however give only a value of the amount of water contained by the bed in a partially saturated or capillary state. This value can be obtained from the weight percent retained water at $\Delta P = 0$ and the weight of the respective coal bed. An area calculated with this data will nevertheless give a reasonable estimate.

The area of the capillaries per gram of coal is related to the contained volume by

$$A = \frac{2V}{rw} \tag{30}$$

where A = specific surface area

V = volume of capillary

r = radius of capillary

w = weight of coal

Table VIII lists the appropriate data and the calculated areas for each bed tested from each dewatering experiment. The volume of the contained solutions were calculated assuming their density was 1 gm/ml, due to their extremely dilute concentration of surfactant. The mean value of specific surface area was found to be 284 cm^2/gm. Gray [3] found an area of 290 cm^2/gm for Betteshanger coal beds of similar size distribution. He found that his value, also determined on a partially saturated coal bed, was 17% lower than a value obtained by permeability methods from flow experiments in which the beds were fully saturated. A correction of 17% brings the mean value of the specific surface area of the coal determined in the present investigation to 342 cm^2/gm. The value is expected to be lower than the actual surface area of the coal because of the assumption of circular capillaries and the fact that the areas between touching particles is not included.

TABLE VIII

DATA FOR CALCULATION OF THE

SPECIFIC SURFACE AREA OF THE COAL BASED ON THE CAPILLARY MODEL

DATA FROM FIGURE	Wt. % @ $\Delta P=0$ (Wt. %)	VOLUME OF SOLUTION V (cm^3)	Wt. COAL W (g)	SPECIFIC SURFACE AREA A (cm^2/g)
24	36.1	17.0	30.0887	268
25	38.0	18.6	30.3165	291
26	38.6	18.9	30.0242	299
27	35.5	16.5	30.0012	261
28	37.4	18.1	30.2416	284
29	38.9	19.3	30.2550	302
30	39.4	19.5	30.1446	306
31	35.1	16.2	30.0003	256
32	35.7	16.6	30.0073	263
33	35.4	16.6	30.3150	260
34	42.4	22.1	30.0090	349
35	38.0	18.4	30.0013	291
36	35.5	16.5	30.0043	261
				mean = 284 ± 27

$284 \frac{cm^2}{g}$ is 17% lower than $342 \frac{cm^2}{g}$

$r = 42.18 \times 10^{-4}$ μm

$V = \pi r^2 h$

$A' = 2\pi r h$

$A = \frac{2V}{rw}$

$A = \frac{A'}{w}$

The Coal-Surfactant Interaction

Let us now consider the dewatering data only in the latter stages of dewatering and its relationship to the retention of liquid on the coal product. This data is best examined on the isobaric plots of percent water retention versus concentration as shown in Figures 37-41 and the non-equilibrium dewatering experiments of Figures 42-46. Examining the two sets of data for anionic Aerosol A-196, Aerosol-OT and sodium dodecyl sulfate, it is observed that the amount of solution retained exhibited a minimum in retained liquid in all three cases as the concentration of surfactant is increased. Also, after this minimum, the amount of solution retained on the coal increased considerably. This is evident particularly on the non-equilibrium dewatering studies. Cationic dodecyl pyridinium chloride, on the other hand, only began to show a decrease in the residual solution content after a certain concentration was reached after which it remained constant. Nonionic Triton X-114 behaved almost in the same fashion except only a slight minimum was observed.

In all five cases the interfacial tensions, plotted over the same concentration range, decreased monatonically with increasing concentration of surfactant to the critical micelle concentration. (The problem of sodium dodecyl sulfate has already been discussed). No minimums or abrupt changes were observed at the concentrations indicated by the residual solution content data.

Therefore, the effect of the addition of surfactants on the residual amount of solution retained by the coal beds cannot be related simply or directly to the lowering of the liquid-air interfacial tensions.

Let us now examine the effect of the surfactants in more detail. As the concentration of the surfactants was increased the amount of solution retained in the coal beds began to decrease at some point in all five cases. This improvement in dewatering can only be explained, if the coal surface became more hydrophobic as the number of surfactant molecules present in the coal-water interface system was increased. The adsorption from solution experiments indicate that each of the surfactant molecules were adsorbed to some extent onto the coal surface, and that amount adsorbed increased with increasing surfactant concentration in solution. For the coal surface to become more hydrophobic as the number of surfactant molecules adsorbed increased, the molecules must have adsorbed with their head groups adjacent to the solid, leaving the hydrophobic hydrocarbon chains extended out into the aqueous phase. Looking at the solid from the liquid, one could imagine a surface becoming more and more dense with hydrophobic hydrocarbon chains.

This preferential orientation of the adsorbed molecules can explain the coal surface becoming more hydrophobic as the concentration of surfactant in solution was increased but seems to be at a loss to explain a minimum, then a reversal, and subsequent increase in the amount of solution retained by the bed in the case of the anionic surfactants. The situation could be reconciled if at the reversal concentrations the surfactant molecules began to adsorb the other way around, presenting their hydrophilic, water soluble, head groups to the water phase, thus making the surface become hydrophilic.

If a situation was known in which the surfactant molecules did aggregate, hydrocarbon chain to hydrocarbon chain, presenting their head groups to the

water phase at a certain concentration, then the change in adsorption behavior might be explained. Fortunately, this is known to happen and has already been described, i.e., micellation; one of the unique properties exhibited by these molecules in bulk aqueous solution. Micellation, however, was found to occur in the bulk surfactant solutions at considerably higher concentrations (CMC's) than those exhibited by the respective minimums when the coal was present. The coal surface may, therefore, be regarded as a form of heterogeneous nucleation site for micelle-like aggregation of the surfactant molecules on the coal surface. If one layer, i.e., some effective monolayer, was adsorbed in the first orientation, it would appear similar to a half micelle in that it is accumulated into a two dimensional sheet across the surface of properly oriented monomers. The excess concentration in the bulk liquid which is required to serve as the driving force for micellation has been reduced by the preferrential orientation of the adsorbed layer.

A type of surfactant adsorption phenomena such as this was treated by Fuerstenau and coworkers [23,32,57] and is called "hemi-micelle" formation. Fuerstenau investigated the adsorption of sodium alkyl sulfonates from aqueous solution onto alumina. The hemi-micelle theory was based on information from adsorption isotherms that were correlated with electrophoretic studies. The adsorption data was analyzed by the Stern-Grahame Theory and exhibited sharp slope changes when plotted on log-log plots. The electrophoretic studies gave information about the potentials in the electric double layer, specifically the zeta potential. The existence of the hemi-micelles was basically proposed to explain the zeta potential sign reversal at the same concentration as a slope change in the adsorption isotherms. Furthermore, Fuerstenau proposed a model for the adsorption be-

havior of the surfactants on the alumina, based also on the change in the standard free energy of adsorption as a function of surfactant concentration in solution, obtained from the adsorption isotherms and the Stern-Grahame adsorption theory. It was concluded that the adsorption progressed through three distinct regions in which the mode of adsorption was controlled by one or another of the components of the total standard free energy of adsorption, ΔG_x^o, becoming more or less dominant. It should be noted here that the solid under investigation, viz., alumina, has a much more well defined surface chemistry than that of heterogeneous coal.

In light of this approach, which seems to reconcile the dilemna of the surfactant adsorption on coal in reverse orientation, let us examine evidence for each surfactant more critically with the assumption that the minimums in the residual solution contents are, in fact, indicative of some effective monolayer coverage or at least the point at which it is energetically favorable to adsorb in the next layer of opposite orientation. With this in hand one can then calculate an effective area covered by the adsorbed molecules, i.e., an effective specific surface area of the coal accessible to the surfactants.

The minimum in residual content of solution in the coal bed for Aerosol A-196 occurred at about 2.0×10^{-6} mole fraction. From the adsorption isotherm the number of moles of surfactant adsorbed per gram of coal at this concentration was 1.25×10^{-7} moles/g, and if this number is multiplied by Avogadro's number, 6.023×10^{23} molecules/mole, we obtain 7.5×10^{16} molecules/g.

The lowering of the liquid-air interfacial tension as a function of concentration is the result of the adsorption of the surfactant molecules at the liquid-air interface, as stated previously in section IV. SURFACTANTS,

above, from which we can obtain a value for the area per adsorbed molecule. This adsorption is treated by means of the Gibbs Equation [58] where the number of molecules adsorbed per square centimeter of interface, Γ, is related to the slope of the interfacial tension versus the log of the concentration curves as

$$\Gamma = \frac{-1}{kT} \frac{d\gamma}{d \ln C} \qquad (31)$$

where k is the Boltzmann constant, T the absolute temperature, γ the liquid-air interfacial tension, and C the surfactant concentration in mole fraction. The maximum slope represents the closest packing of the molecules at the liquid-air interface. The slopes for each surfactant were reported in Table IV with the calibration curves of Figures 47-51. The area per molecule, σ_0, is obtained from the inverse of Γ at the value of the maximum slope:

$$\sigma_0 = -kT \frac{d \ln C}{d\gamma} \qquad (32)$$

The areas per molecule arrived at in this manner are given in Table IX, along with the values observed by other authors as cited in the literature.

We now assume that the area the adsorbed Aerosol A-196 molecule occupies at the liquid-air interface is essentially the same as it might occupy at the solid (coal) - liquid interface. This is reasonable since the molecules are most probably oriented at the coal-liquid interface as they are in the liquid-air interface. Furthermore, the molecules investigated had sufficient steric hinderance as to limit their configurations.

TABLE IX

ADSORBED AREA OF SURFACTANT MOLECULES

SURFACTANT	AREA PER ADSORBED MOLECULE ($Å^2$)	
	THIS WORK	OTHERS
Aerosol A-196	68	———
Aerosol - OT	64	70 [59]; 67 [60]*
Sodium Dodecyl Sulfate	59	52 [61]
Dodecyl Pyridinium Chloride	34	35 [62]
Triton X-114	56	50 [48]
MOLECULE		
CH_3	9	9.6 [63]**
Polyoxyethylene chain (n = 7.5)	177	***
	83	———

*area of the similar molecule Aerosol-OTN (Sodium di-n-octyl sulfosuccinate)

**calculated on the basis of a 3.5Å distance between CH_3 groups

***calculated from n = 2Å [63]

The area of the Aerosol A-196 molecule was found to be 68Å^2. Thus multiplying this by the number of molecules adsorbed per gram of coal we obtain a value of 512 cm^2/gm for the effective specific surface area of the coal size under investigation.

A similar calculation can be conducted for Aerosol-OT, a molecule quite similar to that of Aerosol A-196. The concentration at which Aerosol-OT exhibited the dewatering minimum was chosen as 1.0 x 10^{-5} mole fraction from the isobaric plots shown in Figure 41 since these plots represent an equilibrium situation. The minimums of the non-equilibrium vacuum dewatering curves of Figure 46 appear to be approaching this equilibrium value, as the time of exposure was increased. There was a problem in the determination of the number of moles of surfactant adsorbed at this concentration, however, since it was not possible to obtain adsorption data for this surfactant in this range. Recognizing that all the adsorption isotherms for all of the surfactants were relatively linear when subjected to a log-log plot, a value for the number of moles adsorbed was therefore estimated from a linear interpolation of the data that was available, cf. Figure 61. The value obtained was 1.25 X 10^{-7} moles/g or 7.5 X 10^{16} molecules/g which was the same as the number of molecules/gm of Aerosol A-196. The area of the Aerosol-OT molecule was determined to be 64Å^2, similar to Aerosol A-196 and in good agreement with that found in the literature [59] i.e., 70Å^2. This is also reasonable since the two molecules are almost equal size and shape as illustrated by the molecular models shown in Figures 12 and 20. Using our value, an effective specific surface area of the coal of 482 cm^2/gm is obtained. Using the literature value of 70Å^2, which is also reported [59] as being a value calculated from a molecular model, gives an area of 527 cm^2/gm, both values being in good agreement with that of Aerosol A-196, considering the heterogeneity of the coal

surface.

Before continuing with this study another relation between the concentrations of the observed minimums and the adsorption data should be considered, i.e., the variation of the standard free energies of adsorption with concentration as shown in Figures 62-66. For Aerosol A-196 the concentration in question was 2.0×10^{-6} mole fraction. In Figure 62 this was also where the standard free energy rose to a certain value and remained fairly constant with increased concentration. Fuerstenau [23] concluded that hemi-micelle formation is accompanied by the standard free energy of adsorption becoming sharply more negative then leveling off. The standard free energy of adsorption for Aerosol A-196 remained constant to about 3.0×10^{-4} mole fraction beyond which it dropped towards more positive values indicating a loss of driving force for adsorption. The vacuum dewatering data indicated a severe increase in the amount of retained solution also beyond this concentration. These concentrations, however, are approaching the CMC and micellation in the bulk, precipitated by the early hemi-micellation, may be beginning to compete with the surface phase for molecules. Extended three-dimensional micelles may also be forming at the interface.

Nevertheless, the added correlation of the behavior of the standard free energies more fully supports the model proposed by Fuerstenau for surfactant adsorption on a well defined crystal,alumina. Therefore, let us adopt and elaborate on this model which may be appropriate even for the heterogeneous surfaces found in coal.

Let us now construct a general standard free energy of adsorption curve for the surfactant adsorption on coal. Figure 68 shows this curve along with schematic interpretations of the molecules at the interface.

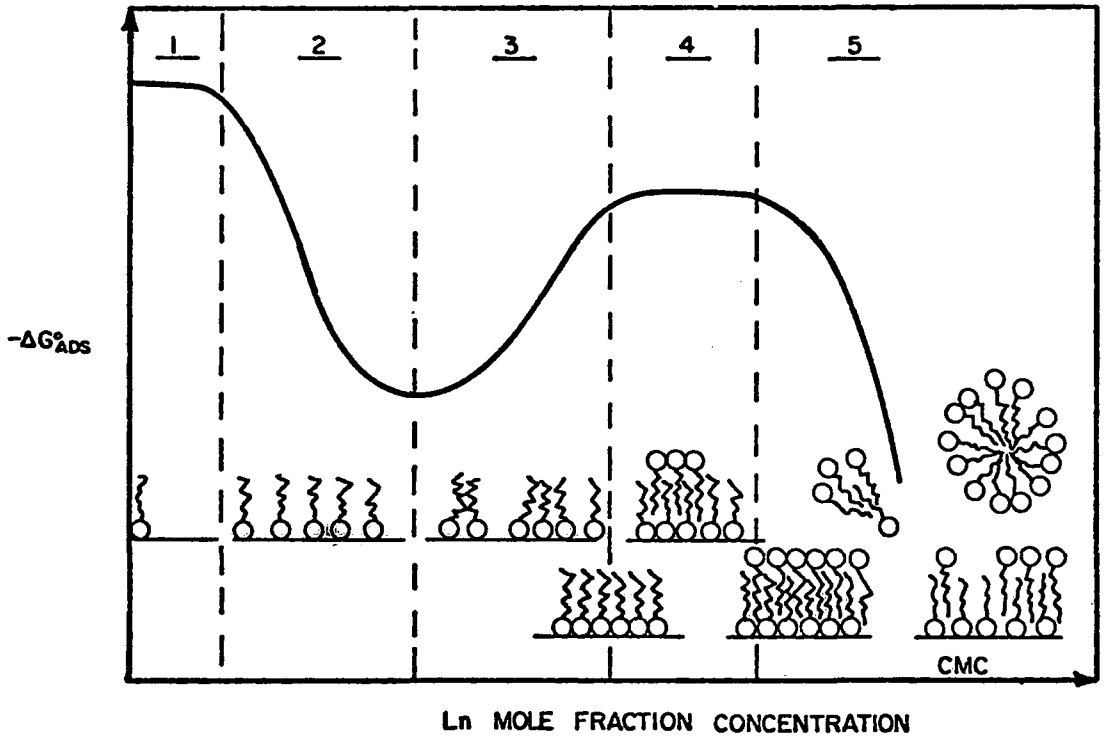

FIGURE 68. GENERAL BEHAVIOR OF THE STANDARD FREE ENERGY OF ADSORPTION FOR SURFACTANT ADSORPTION ON COAL.

At extremely low surfactant concentrations the free energy of adsorption should be approximately constant; the assumptions of Langmuirian type adsorption prevailing. (The Stern-Grahame adsorption equation is actually a form of the Langmuir if the adsorption energy is assumed to remain constant). Specifically, there are no interactions between adsorbing molecules and only the coulombic attraction potentials are operative. This is stage 1 of Figure 68. In addition to any of the specific surface attractive potentials, there is always the hydrophobic repulsion of the hydrocarbon chains by the bulk water molecules driving the surfactant molecules to any interface. This hydrophobic effect has been treated by Tanford [26] and is the result of the water molecules preferring to retain their mutual hydrogen bonding rather than attempt coping with the hydrocarbon chains which offer little bonding capability with the water. It should also be noted that the water molecules and hydroxyl and hydronium ions of the water are also adsorbed on the coal surface. If the coulombic attraction is between the positive solid coal surface and an anionic surfactant, then the surfactant adsorbes by an ion exchange with, for example, a more weakly adsorbed hydroxyl ion. For a cationic surfactant the attraction would be to the adsorbed layer of negative water ions (-OH) and may result in the surfactant adsorbing in the outer Helmholtz plane.

As the number of molecules adsorbed is increased, the electric double layer is being neutralized and the number of adsorption sites is being reduced which results in a more positive trend in free energy. This is shown as stage 2 of Figure 68. A concentration is then reached, stage 3, at which the adsorbed molecules are close enough for the Van der Waals attraction between hydrocarbon chains to become a significant factor.

the water molecules surrounding them and further lower the overall free energy of the system through an elimination of the high energy hydrocarbon-water interface. Due to the great number of $-CH_2-$ groups per surfactant molecule the Van der Waals attraction, on a per molecule basis, is large compared to the coulombic repulsion of the head groups. This has been found to be the case in studies of the standard free energy of bulk liquid micellation [64], in which for example, with dodecyltrimethyl ammonium bromide, the hydrocarbon contribution favored micellation by -14.0 RT and the coulombic contribution opposed it by only +0.84 RT. Therefore, in stage 3, the standard free energy of adsorption increases (i.e. tends toward lower negative values) which favors adsorption.

The beginning of stage 4 occurs when the number of adsorption sites in the first layer become exhausted, and coulombic repulsion due to the increased density of like charges of the adsorbed head groups, now can no longer be offset by the hydrocarbon association. Adsorption in the subsequent layer above the first monolayer now begins with the molecules still bonding hydrocarbon to hydrocarbon but arranged so as not to increase the number of like charges in the first layer, i.e., they adsorb in reverse orientation. This would be the onset of hemi-micelle formation as described by Fuerstenau. The free energy should be constant since adsorption is now occuring on a new surface, one of hydrocarbon chains. Only one type of adsorption mode is operative, i.e., hemi-micelle formation. The actual value of the free energy, therefore, should be similar to the standard free energy of bulk micellation and even somewhat less, i.e., more negative, due to the existence of the nucleated phase.

Stage 5 is initiated when the number of adsorption sites again becomes exhausted, the repulsion of the like head charges building up in the outermost layer becomes dominant and micellation in the bulk liquid is being approached. Therefore,in state 5 the standard free energy becomes more positive.

If we now re-examine the standard free energy of adsorption of Aerosol A-196 we can deduce, in light of the above treatment, that the data reflects the adsorption stages 3,4, and 5 quite clearly. The free energy curve for Aerosol-OT was constructed assuming the above treatment to be appropriate.

The above model was presented envisioning the form of the hemi-micelation as a bilayer arrangement, which as stated previously, is one of the micellar forms possible in a bulk liquid situation. However, as pointed out by Tanford [65] this form is not only possible, but actually optimal specifically for surfactants possessing two hydrocarbon chains per molecule; a category which includes both Aerosol A-196 and Aerosol - OT. Furthermore, Saleeb and Kitchener [59] have speculated on this type of behavior for the adsorption of Aerosol - OT on carbon blacks. An illustration of the possible bilayer for these surfactants is shown in Figure 69.

Let us now return to examining the data for each of the specific surfactants. The last anionic surfactant to be considered is sodium dodecyl sulfate. Examination of the standard free energy curve for this surfactant reveals that it consists of adsorption stages 2, 3, 4 and 5 up to about 10^{-5} mole fraction surfactant. The data from 2.0×10^{-5} mole fraction and higher may be suspect since this is the concentration range in which there was a minimum in the solution-air interfacial tension calibration curve, which was discussed above. However, assuming the free energy model

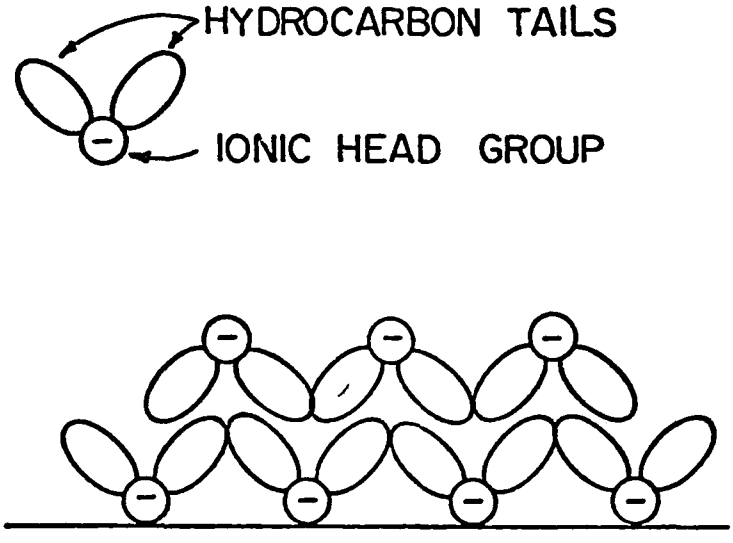

FIGURE 69. POSSIBLE ADSORBED BILAYER OF SURFACTANT MOLECULES WITH TWO HYDROCARBON CHAINS PER MOLECULE.

to be correct, a concentration of 2.0×10^{-6} mole fraction should be the beginning of the hemi-micelle formation. The vacuum dewatering data of Figure 45 are in reasonable agreement, as evidenced by the wide minimum that appears in this range. The existence of such a minimum is consistent with the behavior of the other anionic surfactants. Using these data and proceeding as before, we find the effective specific surface area of the coal to be 533 cm^2/gm which is in excellent agreement with the values obtained for Aerosol A-196 and Aerosol-OT.

Therefore agreement seems to exist among the anionic surfactants as to an effective specific surface area of the coal calculated on the basis of the "hemi-micelle" model.

Let us now examine the data for the cationic surfactant, dodecyl pyridinium chloride. The vacuum dewatering data of Figure 44, shows that the residual solution contents exhibited no minimum, but rather began to decrease at about 2.0×10^{-6} mole fraction and level off at about 7.0×10^{-6} mole fraction. The standard free energy of adsorption, shown in Figure 64, is just about constant between these concentrations. This would tend to reflect a constant mode of adsorption. Since the residual solution contents decreased, the coal surface became more hydrophobic and therefore the hydrocarbon chains of the adsorbed molecules must be pointed into the liquid. However, the ionic end of the molecule is positive as is the coal solid surface, and not negative as in the anionic cases, which seems to be an incompatable situation. An explanation has already been stated in the description of the general adsorption standard free energy curve. The dodecyl pyridinium ion may be adsorbed in the outer Helmholtz plane separated from the coal surface by an adsorbed layer of hydroxyl ions and hydration water. This is also reasonable because dodecyl pyridinium chloride

is derived from a quarternary ammonium compound and such derivatives according to Hummel [66] "tenaciously retain water" as evidenced by his infra-red absorption experiments.

This assumption is also supported by the electrokinetic studies of Cambell and Sun [22] who found that the adsorption of a cationic surfactant, dodecylamine acetate, on coal completely reversed the polarity of the zeta potential while adsorption of the anionic surfactants effected little change. Similar electrokinetic behavior has also been reported by Saleeb and Kitchener [59] in the adsorption of Aerosol-OT and cetyltrimethyl ammonium bromide on carbon blacks. The charge on molecules adsorbed in the outer Helmholtz plane would more likely have a direct effect on influencing the measured potential at the plane of shear, i.e., the zeta potential, than molecules adsorbed at the inner plane. Let us restate the electrokinetic findings. When coal, which initially has a negative zeta potential and therefore a positive surface, adsorbs a cationic surfactant, presumably in the Outer Helmholtz plane, the zeta potential changes greatly even enough to change polarity. In adsorbing an anionic surfactant little change in the zeta potential is observed. One would expect therefore that a solid which initially had a positive zeta potential and hence a negative surface would adsorb an anionic surfactant in the Outer Helmholtz plane effecting a great change in the zeta potential even as far as changing polarity. This is exactly what Fuerstanau [23] has observed for alumina which does have a positive zeta potential of + 60 mv in neutral aqueous solutions.

With the ionic head of the dodecyl pyridinium ion fixed in the outer Helmholtz plane, an additional adsorption orientation is possible, that

with the hydrocarbon chains adjacent to the less water avid areas of the coal surface and not out into the solution, as illustrated in Figure 70, since they would like to get as far out of the water as possible. And, in addition, the hydrocarbon chains can also associate with the aliphatic portion of the coal. The net orientation, however, must be as first supposed. If we then assume that at 2.0×10^{-6} mole fraction the number of molecules adsorbed begins to be dense enough to show a net hydrocarbon shield and cover the hydrophilic groups then we can calculate another effective specific surface area for the coal. With the molecules able to adsorb in two orientations in the first layer, no minimum in the retained solution contents would be expected to occur. No great increase in the adsorption free energy due to hydrocarbon chain association would occur as before since now the hydrocarbon chains can associate with the solid surface, and with some oriented up and some oriented down the number of associations possible per molecule is decreased. For example, half the total number in the upper plane and half in the lower plane. Therefore, there is insufficient association on the liquid side of the outer Helmholtz plane to force formation of a hemi-micelle.

The standard free energy curve reflects this model, i.e., a constant value indicative of coulombic attraction which then monotonically decreases as the concentration increases.

The specific surface area is then calculated to be 2.0×10^{-6} mole fraction, i.e., 2.75×10^{-7} moles or 1.7×10^{17} molecules of dodecyl pyridium chloride adsorbed per gram of coal. The value obtained for the area of the molecule was $34 \mathring{A}^2$. These values give an area for the coal of 563 cm^2/gm, also in agreement but somewhat larger than those of the anionic sur-

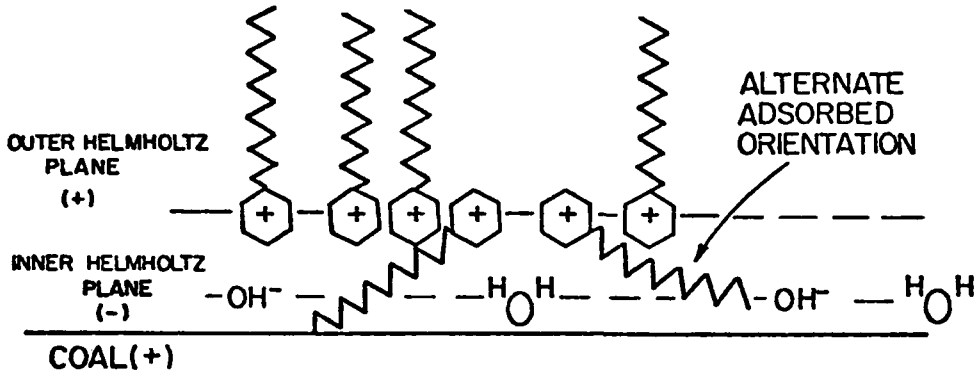

FIGURE 70. ADSORBED LAYER OF DODECYL PYRIDINIUM IONS SHOWING AN ALTERNATE ORIENTATION FOR THE MOLECULES.

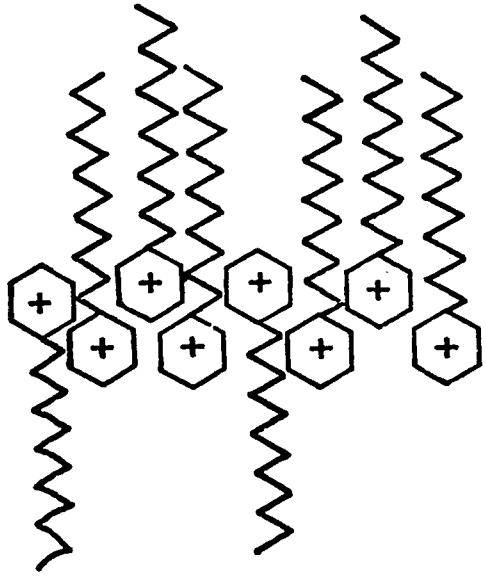

FIGURE 71. CLOSELY PACKED ADSORBED LAYER OF DODECYL PYRIDINIUM IONS.

factants. Since the residual solution contents never increased again past 7×10^{-6} mole fraction the net number of hydrocarbon chains facing the solution must have remained constant. Using the area of 500 cm^2/gm for the coal surface and values from the adsorption isotherm, we can back calculate the size of the molecule adsorbed at 7×10^{-6} mole fraction. This calculation gives an area per molecule of only about $9\mathring{A}^2$. Oddly enough this is approximately the area of the methyl group at the end of a hydrocarbon chain. Solidified, hydrocarbon chains have been determined [63] to be $3.5\mathring{A}$ apart. This diameter gives a circular area of $9.6\mathring{A}^2$ which appears to indicate that the molecules of the adsorbed surfactant have compacted themselves so as to resemble the packing of solid hydrocarbons, something like this is shown in Figure 71. Beyond this concentration more molecules are adsorbed but the net orientation must be such that the number of hydrophobic sites remained constant. A net pair-wise adsorption as described above would be reasonable.

Let us now consider the last surfactant investigated, ie., nonionic Triton X-114. The isobaric plots of Figure 38 show that the retained solution content began to decrease as the concentration of surfactant in the solution exceeded about 3.0×10^{-7} mole fraction. The vacuum dewatering data of Figure 43 are in agreement with this and furthermore show something of a small minimum at 9.5×10^{-7} mole fraction. The adsorption isotherm shows that the amount of surfactant adsorbed continues to increase through these concentrations. The standard free energy of adsorption curve shows a constant value up to about 5.0×10^{-7} mole fraction after which it declines. A constant free energy again implies a constant mode of adsorption, Langmuir type adsorption as before.

The Triton X-114 molecule is not ionic, but it does have polar groups. It is not only highly polar due to the large number of ethylene oxide units but also because of the hydrophilic hydroxyl group contained at one end: all of which leads to the hydrophilic portion of the molecule having a negative polarity. Since the molecules of Triton X-114 do adsorb, causing the coal surface to become more hydrophobic Therefore, the molecules must have arranged themselves such that the hydrocarbon chains were extended away from the coal surface and, as implied, the polyoxyethylene chain must have adsorbed onto the coal surface. The constant free energy of adsorption is then the free energy of the polar interaction. At low concentrations, the Triton X-114 molecules probably stretch out allowing the entire length of the polyoxyethylene chain to adsorb onto the coal surface. Schick [67, 68] has investigated molecules of this type adsorbed at the aqueous solution-air interface, and finds that the polyoxyethylene chains must be coiled in the water phase at the interface to explain their apparent adsorbed area. If stretched straight the Triton X-114 molecule should have an end cross sectional area similar to the dodecyl pyridinium ion because of the similar aromatic centers which would be $34\mathring{A}^2$. The area obtained for the Triton X-114 molecule from the Gibbs equation and the interfacial tension data of Figure 48 was $56\mathring{A}^2$. Schick found similar discrepencies and, hence, the coil theory. Furthermore, the molecular model of Figure 14 was found to be quite flexible. This implies that the molecule can contort itself to give an area appropriate to the prevailing circumstances, i.e., it can present a variable adsorbed surface area per molecule. This makes a determination of a specific surface area of the coal an arbitrary matter. However, we can make some sound estimates as to the adsorption

process. If the ethylene oxide chains are adsorbing, then no improvement in hydrophobicity of the coal surface would be expected to occur until the molecules began to impinge upon one another. The length per ethylene oxide unit in a polyoxyethylene chain has been reported as 2Å [63]. The average length of the polyoxyethylene chain in Triton X-114 is 7.5 units giving a length of 15Å. Using this as an effective diameter we can determine the effective circular area occupied by the chain. This approach is similar to Onsager's covolume concept for highly asymmetric molecules [69]. The area obtained is $177Å^2$. Let us assume that this is the area occupied by the adsorbed molecules of Triton X-114 at the point of crowding, i.e. when the molecule could be in an "L" configuration as shown in Figure 72. If we choose 4.0×10^{-7} mole fraction as the concentration at which this happens, then from the adsorption isotherm about 5.0×10^{-8} moles or 3.0×10^{16} molecules are adsorbed per gram of coal. Multiplying this by $177Å^2$ we arrive at a value of 533 cm^2/gm for the specific surface area of the coal. Again in excellent agreement with the values determined with the other surfactants.

We can also consider the slight minimum in the retained solution contents at 9.5×10^{-7} mole fraction since there is also an indication of a change in the standard free energy curve at this concentration. Assuming that this may be an attempt at hemi-micelle formation, we can determine an area of the adsorbed molecules using the value of 500 cm^2/gm for the specific surface area of the coal and see if the value is reasonable. At 9.5×10^{-7} mole fraction of Triton X-114, 1.0×10^{-7} moles or 6.0×10^{26} molecules are adsorbed per gram of coal. This is approximately two times the number observed previously. Dividing 500 cm^2/gm by this value we

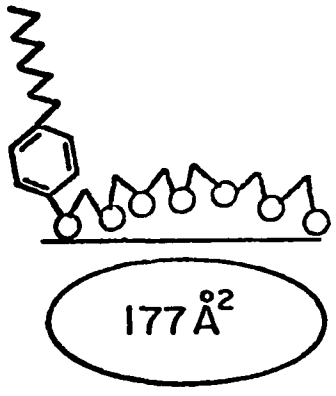

FIGURE 72. POSSIBLE "L" CONFIGURATION OF THE ADSORBED TRITON X-114 MOLECULE AT THE POINT OF CROWDING.

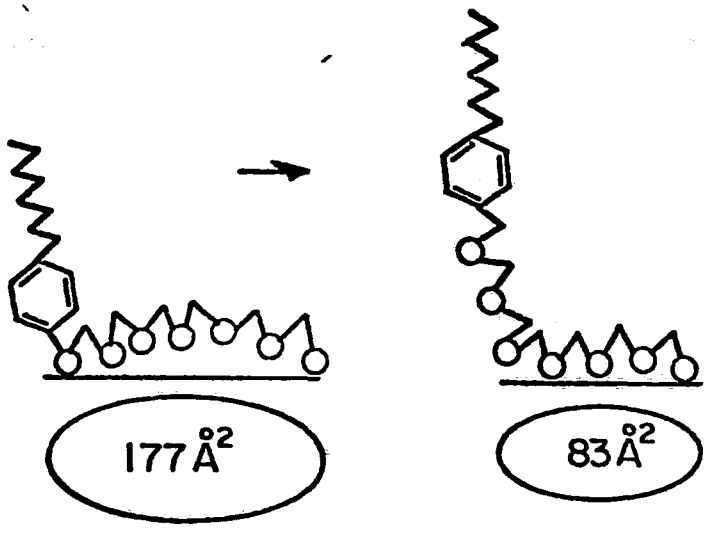

FIGURE 73. CHANGE IN THE ADSORBED AREA PER TRITON X-114 MOLECULE TO ACCOMODATE MORE ADSORBED MOLECULES.

obtain an area per molecule of $83\mathring{A}^2$ which is approximately half the area of that determined before. Doubling the number of molecules adsorbed decreased the area occupied by each by half. The molecules seem to have stood up more as is illustrated in Figure 73. The area obtained is reasonable since the smallest area possible would be about $34\mathring{A}^2$ and the area at the liquid-air interface was only $56\mathring{A}^2$.

At this point, let us summarize. A specific qualitative model for the adsorption behavior of the surfactants onto the coal surface was formulated, and using this model, values for the specific surface area of the coal occupied by the adsorbed surfactant molecules were determined. The values obtained, which are summarized in Table X, were found to be consistant in the case of all five surfactants involved. Therefore, the proposed model, which was adopted from an explanation of surfactant adsorption on a rather homogeneous and well defined crystal, viz., alumina seems appropriate for the adsorption behavior of surfactants on complex, heterogeneous coal.

The model is successful in producing at least a consistent set of results. Let us now consider these results. What we have found consistency in is a specific surface area of the coal. The topographical heterogeneity of coal has already been introduced in section III. COAL. This must be critically taken into account when determination of a specific surface area is considered. Methods by which specific surface areas are determined rely on some observable property dependent upon the extent of the surface, which is theoretically relatable to the actual surface area. Surface areas determined by different methods should, in general, be expected to be different. The main difference between methods

TABLE X

SPECIFIC SURFACE AREA OF THE COAL

DETERMINED ON THE BASIS OF THE SURFACTANT ADSORPTION MODEL

SURFACTANT	AREA PER ADSORBED MOLECULE $\mathring{A}^2$	SPECIFIC SURFACE AREA OF THE COAL (cm^2/ g)
Aerosol A - 196	68	512
Aerosol - OT	64	482
	70	527
Sodium Dodecyl Sulfate	59	533
Dodecyl Pyridinium Chloride	34	563
	9	500
Triton X-114	177	533
	83	500

and their results is in the extent to which the surface irregularities can be considered [70].

One estimate of the specific surface area of the coal is a calculation of the geometric surface area, assuming the coal particles are spherical. Assuming the particles to have an average diameter of 324 μm, ie., the log average value used above in the treatment of capillary theory, and that the density of the coal was 1.3 g/cm, the specific surface area obtained is 142 cm^2/g. This value would be indicative of the lowest value expected, since no surface irregularities were considered. Even assuming that all the coal particles were of the smallest diameter known to be present, i.e., 250 μm, only brings the value to 185 cm^2/gm.

We have already determined another value for the specific surface area of the coal based on a method which would tend to reflect a more accurate description of the situation. This was the value generated from the data of the dewatering experiments. Although the bed was assumed to be approximated by a bundle of cylindrical capillary tubes, the volume used in calculating the area includes the volume occupied in any accessible surface indentation or irregularity. The value obtained was 284 cm^2/gm, which was determined for a partially saturated bed. If empirically corrected for complete liquid saturation in a "flow" situation it was 342 cm^2/gm. Even the "flow" value would be expected to be low since theoretically this area is assumed to be the area seen by the contacting liquid as it flows through the pore system established by the packed particles. Stagnant and blind passages are not included, nor the area between touching particles; nor would the area reflect the situation for particles of complex shape in this simple treatment.

Another method of surface area determination is by gas adsorption. As stated previously, typical values of the specific surface areas of coal determined by gas adsorption are in the range of 100 - 200 m^2/gm, four orders of magnitude higher than the values above! Nitrogen [71] is a typical gas used in this determination and its molecular area is only about $16\mathring{A}^2$. In this case, any space on the order of $16\mathring{A}^2$ will be included in the determination. This includes much of the internal pore area of each coal particle.

The area obtained by the surfactant adsorption of the present work was found to be about 500 cm^2/g, which more nearly reflects the geometric and capillary areas than that found by gas adsorption. The only reasonable conclusion that this allows is that the surfactant molecules must be too large to "see" most of the area of the coal contained in the internal pores of its gel structure and that they adsorb only on the accessible irregularities of the "external" surface of the particles.

Further support for this conclusion comes from the work of Saleeb and Kitchener [59] who investigated the adsorption of Aerosol-OT and cetyl trimethyl ammonium bromide on carbon blacks. Such carbon blacks have no internal pores to speak of and are usually used as reference surfaces in gas adsorption studies. The particle diameters used were less than a micron. The surface areas, therefore, determined form nitrogen gas (area = $16\mathring{A}^2$) adsorption are the external surface areas of all the particles, and should be equally accessible to the larger surfactant molecules. From a knowledge of the nitrogen specific surface area (about 10 m^2/gm) and the number of moles adsorbed at the CMC, beyond which no more adsorption was found, they determined the area of the adsorbed molecules. They found excellent

agreement with the areas of molecular models of the surfactants oriented vertically. Their value for Aerosol-OT of $70\mathring{A}^2$ is already listed in Table IX.

Further support can be obtained by noting that the free energies of hemi-micellation should be similar to the standard free energies of micellation of surfactants in the bulk liquid. The standard free energies of micellation of a few surfactants: sodium dodecyl sulfate, sodium decyl sulfate, dodecyl trimethyl ammonium bromide, and dodecyl pyridinium bromide, for example, have been reported as -5.3 kcal/mole [73], -4.5 kcal/mole [73], -7.8 kcal/mole [64], and -5.03 kcal/mole [74] respectively in agreement with the magnitudes of hemi-micellation determined in the present work using a value of 500 cm^2/gm for the effective specific surface area of the coal.

The standard free energies of hemi-micellation should even tend towards more negative values than those of bulk liquid micellation, due to the presence of the highly oriented adsorbed first layer, which would tend to reduce the entropy of the formation of hemi-micelles. This was found to be the case in general. An example is the standard free energy at the point of hemi-micellation calculated for sodium dodecyl sulfate, shown in Figure 65. The value was about -6.1 kcal/mole, approximately 1 kcal/mole more negative than the value for bulk micellation of -5.3 kcal/mole cited above.

The fact that better agreement with the theory is expected for energy values more negative than those of bulk micellation further supports the magnitude of the specific surface area derived from that theory. According to Equation (6) , the Stern-Grahame adsorption equation, a

trend towards more negative energies favors a smaller specific surface area, not larger by orders of magnitude.

Additional evidence supporting the order of magnitude obtained for the specific surface area of the coal comes from an examination of the standard free energies of adsorption calculated for each surfactant adsorption isotherm. To calculate the standard free energy of adsorption curves plotted in Figures 62 - 66 for each surfactant, a value for the specific surface area accessible to the molecules had to be assumed. Therefore, the actual magnitude of the energies obtained was determined by this value. These values, however, are only sensitive to the order of magnitude of the surface area chosen, because of the logarithmic relationship between the two variables as contained in Equation (6). The value used, chosen by hindsight, was 500 cm^2/g.

The magnitudes of the standard free energies of adsorption calculated from this value ranged about -5 to -6 kcal/mole, which is in the region of physical adsorption, in agreement with the supposition of the adsorption model presented. The region of chemisorption is assumed to be considerably higher, e.g., in excess of -10 kcal/mole and often larger than -20 kcal/mole [72].

The curves of Figures 62-66 also show that the magnitude of the standard free energy of adsorption for each surfactant does not vary greatly through the concentration range investigated, as would be expected for a situation in which, through this range, the adsorption process was only changing modes of physical adsorption, the energy of each being small and approximately the same.

The standard free energy of adsorption of sodium dodecyl sulfonate on alumina reported by Fuerstenau [23], ranged from -3.6 to -5.0 kcal/mole,

with the higher value at the point of hemi-micellation, in excellent agreement.

Therefore, the proposed adsorption model is supported not only by consistent results but by the actual value of these results calculated on the basis of the model.

Let us now consider why the final retained solution contents of the coal bed show such a large increase for additions of Aerosol A-196, Aerosol-OT, and sodium dodecyl sulfate, the anionic surfactants, at the point of hemi-micelle formation, a case which, in fact, makes the coal surface even more hydrophilic than it appeared originally.

The adsorption model, as presented, although sufficiently satisfactory to explain the observed adsorption phenomena, however, is too simple to be all encompassing. For example, the coal surface during the development was regarded as being homogeneous in net positive charge, yet as explained earlier, coal is a heterogeneous material. The measured zeta potential is actually an average of all of the local potentials at the plane of shear. In local areas some patches may be positive and some negative but arranged as to give a net negative zeta potential to whole coal.

Let us now envision the adsorption of the surfactants on a surface more like that of real coal. Let us assume, as illustrated in Figures 74 - 77 that a typical section of the whole coal surface is made of ten adsorption sites. Let six of these sites represent the aromatic ring structure, two represent a mineral, and two represent aliphatic hydrocarbon areas, as shown in Figure 74. The potential of the aromatic sites is positive, the mineral negative, and the aliphatic areas neutral.

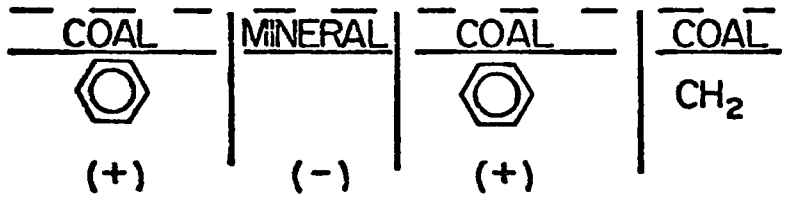

FIGURE 74. PORTION OF A HYPOTHETICAL REAL COAL SURFACE WITH TEN POSSIBLE ADSORPTION SITES.

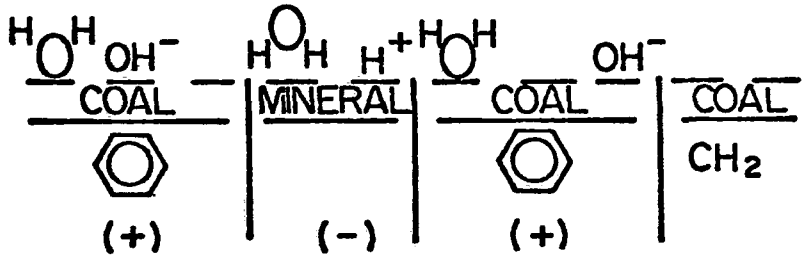

FIGURE 75. PORTION OF A HYPOTHETICAL REAL COAL SURFACE WITH ADSORBED WATER MOLECULES.

Figure 75 shows a possible situation when this coal surface is in contact with water alone. The aromatic portions have attracted the OH^- ions from water and/or the negative poles of the undissociated water molecules. The hydronium ions and the other pole of the water molecules on the other hand have been attracted to the mineral areas. The aliphatic sites, cyclic or otherwise, are hydrophobic and do not attract the water. In this example, therefore, 6/10 sites are hydrophilic and 4/10 are hydrophobic, which appears to describe the coal used in these experiments.

In Figure 76 the coal surface is shown with an adsorbed monolayer of anionic surfactant. The aromatic sites have adsorbed as we have already assumed. The mineral sites, with their opposite charge, have forced the ions to be adsorbed in the Outer Helmholtz Plane in much the same way as was speculated for the adsorption of a cationic surfactant on the positive areas of the coal, and are possibly oriented as shown. The aliphatic sites have adsorbed the hydrocarbon chains of the surfactant molecules since this area is governed by the Van der Waals attraction between hydrocarbon chains and the hydrophobic effect. In this situation only 4/10 of the surface sites are hydrophilic to the water phase and 6/10 hydrophobic. Therefore, the average surface has become slightly more hydrophobic than before.

Figure 77 shows the case when adsorption occurs in the second layer, i.e., the point of hemi-micellation as described above. The portions of the surface of Figure 76 where hydrocarbon chains were extended to the water phase have adsorbed the hydrocarbon chains of the surfactants. Areas with head groups outwards cannot attract hydrocarbon chains and,

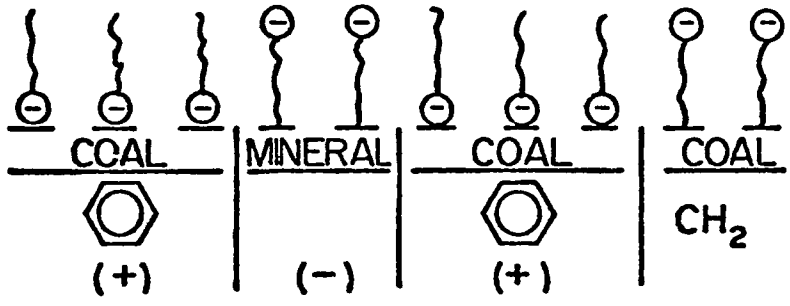

FIGURE 76. PORTION OF A HYPOTHETICAL REAL COAL SURFACE WITH AN ADSORBED LAYER OF ANIONIC SURFACTANT MOLECULES.

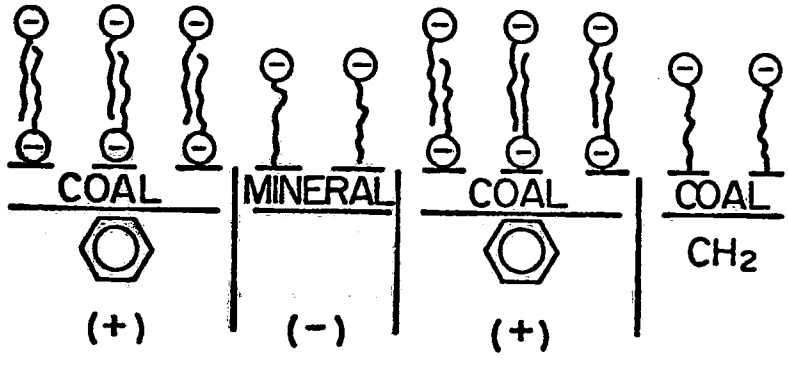

FIGURE 77. PORTION OF A HYPOTHETICAL REAL COAL SURFACE WITH THE ADSORBED ANIONIC SURFACTANT MOLECULES IN THE HEMI-MICELLE STATE.

in addition, must repel the like charges so that no second layer can be formed. Therefore, in this case 10/10 of the sites have become hydrophilic and none are left hydrophobic. All the sites which were made hydrophobic by the adsorption of the surfactants at the lower concentrations are changed at the point of hemi-micellation Therefore, as this example illustrates, it is possible to make the coal surface much more hydrophilic than it can be made hydrophobic by the addition of these surfactants.

Up to this point we have attempted to correlate the complex dewatering behavior induced by the addition of the surfactants with an overall adsorption model. The model, which incorporates changes in the mode of physisorption, seems appropriate enough to explain the changes in retained solution content of the coal beds, as a function of the concentration of the surfactant present. We have established that all the surfactants investigated, improved the residual solution content at some point. We have also found that should hemi-micellation on the coal surface occur, the coal becomes drastically more hydrophilic. With this in mind let us compare the maximum degree to which each surfactant reduced the liquid retention of the coal beds. Two ways of comparing the surfactants with respect to this are: (1) by the maximum percentage decrease in retained liquid content effected by addition of the surfactant over the pure water case, and (2) by the lowest retained liquid content value obtained with each surfactant. To compare the surfactants this way on as equal a basis as possible it was decided to use the 20 min. - 1 atm exposure data of the vacuum dewatering experiments of each surfactant presented in Figures 42 - 46. Table XI lists the values determined for each surfactant according to both methods. As evidenced in the table

TABLE XI

SURFACTANT EFFECTIVENESS

SURFACTANT	Max. % decrease over pure water (Δ%)	Lowest wt. % retained (wt. %)
Dodecyl Pyridinium Chloride	-47	3.2
Aerosol-OT	-45	2.2
Triton X-114	-42	2.8
Aerosol A-196	-35	4.2
Sodium Dodecyl Sulfate	-26	4.8

both methods rank the surfactants in the same order with the exception of cationic dodecyl pyridinium chloride.

Let us now examine this ordering more closely for the two similar surfactants Aerosol-OT and Aerosol A-196. From Table XI we can see that an effective monolayer of Aerosol-OT seems more hydrophobic than an adsorbed monolayer of Aerosol A-196. As pointed out in Section VI. MATERIALS (Surfactants), these molecules differ only in their hydrocarbon chain groups, which are the entities the adsorption model assumes to be in contact with the water phase at this point. Also as stated earlier, a convenient and concise way of comparing the relative hydrophobicities of the surfactants is by the HLB index and group numbers, a partial listing of which was given in Table I. Using Table I we can calculate the effective hydrophobic number appropriate for the two surfactants, assuming that the number for the $-CH_2-$ groups is additive irrespective of the chain being cyclic or branched. The number for Aerosol-OT was calculated for only the two ethylhexyl groups and for Aerosol A-196 for the two cyclohexyl groups. The numbers are, respectively -7.6 and -5.7. The number for Aerosol A-196 is 25% less than that of Aerosol-OT. This would imply that the monolayer of Aerosol A-196 was 25% less hydrophobic than that of Aerosol-OT. From Table XI, the maximum percentage decrease in retained liquid content for Aerosol A-196 is 22% less than that of Aerosol-OT, in remarkable agreement; this, however, may be fortuitous.

Due to the dissimilarity between the other surfactants a detailed comparison such as above was not considered as valid and was not attempted. Furthermore, use of the HLB index and group numbers may not be exactly appropriate in determining the relative hydrophobicity of adsorbed mono-

layers, since the group numbers are for parts of a molecule which are in a free state; and, it is not obvious how adsorption of a group alters its hydrophobicity. Nevertheless, additional agreement with the relative order of the surfactants as listed in Table XI, was found using the HLB as a guide. One example, using the total HLB index for each surfactant is also in agreement. This is the case of Triton X-114 and sodium dodecyl sulfate which have HLB index numbers of 12.4 and 40 respectively. The high number, implying more hydrophilic, for sodium dodecyl sulfate comes from the hydrophilic group number for the SO_4 group of the molecule which according to Table I is the most hydrophilic group listed. This may be the reason why sodium dodecyl sulfate was the poorest dewatering agent shown in both columns of Table XI.

The fact that dodecyl pyridinium chloride had the maximum percentage decrease and only a fair value for the lowest retained amount of solution may be indicative of the way in which it was assumed to be adsorbed, i.e., in the outer Helmholtz plane, on top of an adsorbed water layer. The correct orientation of the molecule would allow for the improvement of dewatering, but the underlying water layer would prevent the lowest value of retained water from being achieved.

Therefore support for the proposed surfactant adsorption model also comes from a more detailed examination of the molecular structure in relation to the hydrophobic nature of each adsorbed molecule.

X. CONCLUSION

The addition of the surfactants investigated has been found to have a two-fold influence on the dewatering of coal. They were found to effect the pressure differentials required for dewatering in addition to the residual water contents of the coal beds attainable by this dewatering.

Both effects are the result of surfactant adsorption. Adsorption at the liquid-air interface, results in a decrease in the interfacial tension between the two phases. The effect this decrease had on the pressure differentials required for dewatering was found to be in agreement with that predicted by the capillary theory applied to the system.

Adsorption at the solid-liquid interface was correlated with the complex behavior of the residual water contents as a function of surfactant addition. A comprehensive model for the adsorption of the surfactants onto the coal was presented, based on the Stern-Grahame theory of adsorption at an electrical double layer. The model allowed for the mode of physisorption to change as the amount of surfactant adsorbed increased, and also for a phenomenon known as hemi-micellation. Using the model, consistent and reasonable results were found for the specific surface area of the coal and for the standard free energies of adsorption. The model was also found to be appropriate when the heterogeneous nature of the coal was considered. Furthermore, the hydrophobicity of the molecular groups of the molecules, expected from the model to be controlling the hydrophobicity of the interface, was also found to be in agreement with that predicted by other means.

Therefore, a complete knowledge of the adsorption behavior of the

surfactants in the coal-water system is the key in determing the criteria for optimum utilization in a dewatering situation.

Finally, an ideal surfactant for aiding the dewatering of coal should possess the following characteristics:

1. The molecules should adsorb on the coal oriented with the hydrocarbon tails extended to the water phase.

2. The hydrocarbon tail should be as hydrophobic as possible, and still retain a degree of water solubility of the whole molecule. (An increase in the number of hydrocarbon tails per molecule may be necessary).

3. The head group should be the least hydrophilic group possible, and still retain the solubility of the whole molecule.

4. The adsorbed molecule should have a large effective area so that fewer molecules are required to affect the interfaces.

5. The surfactant should decrease the interfacial tension at the liquid-air interface as much as possible at the lowest concentration.

6. The molecules should not be prone to hemi-micellation or if they are, it should occur at a sufficiently high concentration, to be avoided.

It should be recognized that these conclusions may be strongly dependent on the rank of the coal under investigation as well as the nature of the mineral matter therein. Therefore it is recommended that the data and conclusions generated herein be examined next as a function of these variables.

APPENDIX A

Surfactant Adsorption Kinetics

The lowering of the liquid-air interfacial tension of aqueous surfactant solutions has been attributed to the adsorption of the solute molecules or ions at the interface. A finite time is required for the surface system to develop and establish equilibrium with the two bulk phases. In the case of aqueous surfactant solutions the time required to establish equilibrium can vary from less than a second to a few days [75], depending primarily upon the specific surfactant molecule and its concentration in the solution. This effect is often referred to as surface aging.

There exists some controversy in ascribing the rate process responsible for this effect. One postulate [76] is that the ions arriving at the interface first, establish an electrical double layer, which sets up a potential barrier to inhibit the introduction of additional ions. Other theories are concerned with a pre-existing surface phase in which molecular penetration and reorientation is considered [77].

Regardless of the appropriate theory, the existence of an aging effect in the interfacial tension of surfactant solutions should be recognized and taken into account whenever an application of surfactants is considered.

The precautions taken in the present work to alleviate any problems with this, have already been stated. Furthermore, it was assumed that adsorption of the surfactant molecules at the solid-liquid interface was also time dependent, and at least of the same order of magnitude as that found at the liquid-air interface. Therefore the time which was allowed for the surfactants to adsorb onto the coal was much, much greater than the longest time found for a solution surface to come to equilibrium. The time allowed was usually on the order of an hour.

APPENDIX B

TABLES OF DATA FOR THE ADSORPTION ISOTHERMS

TABLE B 1

DATA FOR THE ADSORPTION ISOTHERM OF AEROSOL A-196

SURFACTANT CONCENTRATION x (mole fraction)	MOLES OF SOLUTION n	WEIGHT OF COAL SAMPLE w (g)	CONCENTRATION CHANGE OF SOLUTION ON ADSORPTION ΔX	AMOUNT ADSORBED PER GRAM OF COAL n_1^s (moles/g)
9.37×10^{-7}	1.95	20.0098	3.22×10^{-7}	3.13×10^{-8}
1.94×10^{-6}	1.95	20.0098	1.26×10^{-6}	1.22×10^{-7}
3.86×10^{-6}	1.96	20.0098	2.76×10^{-6}	2.71×10^{-7}
9.49×10^{-6}	2.00	20.0098	5.77×10^{-6}	5.76×10^{-7}
1.85×10^{-5}	2.05	20.0098	1.04×10^{-5}	1.07×10^{-6}
4.88×10^{-5}	1.94	20.0200	3.71×10^{-5}	3.60×10^{-6}
8.55×10^{-5}	2.22	20.0200	5.29×10^{-5}	6.58×10^{-6}
1.14×10^{-4}	2.49	20.0200	6.33×10^{-5}	7.87×10^{-6}
1.37×10^{-4}	2.77	20.0200	6.86×10^{-5}	9.49×10^{-6}
1.71×10^{-4}	3.32	20.0200	6.44×10^{-5}	1.07×10^{-5}
1.85×10^{-4}	3.59	20.0200	6.94×10^{-5}	1.25×10^{-5}
1.96×10^{-4}	3.87	20.0200	6.14×10^{-5}	1.19×10^{-5}
1.14×10^{-3}	3.51	19.9662	1.30×10^{-4}*	2.29×10^{-5}

* determined gravimetrically

TABLE B 2

DATA FOR THE ADSORPTION ISOTHERM OF TRITON X-114

SURFACTANT CONCENTRATION x (mole fraction)	MOLES OF SOLUTION n	WEIGHT OF COAL SAMPLE w (g)	CONCENTRATION CHANGE OF SOLUTION ON ADSORPTION ΔX	AMOUNT ADSORBED PER GRAM OF COAL n_1^s (moles/g)
1.89×10^{-8}	2.78	20.1948	1.64×10^{-8}	2.26×10^{-9}
3.39×10^{-8}	2.78	20.1948	3.07×10^{-8}	4.22×10^{-9}
9.44×10^{-8}	2.78	20.1948	8.28×10^{-8}	1.14×10^{-8}
1.88×10^{-7}	2.79	20.1948	1.69×10^{-7}	2.33×10^{-8}
2.82×10^{-7}	2.79	20.1948	2.54×10^{-7}	3.51×10^{-8}
3.73×10^{-7}	2.80	20.1258	3.31×10^{-7}	4.61×10^{-8}
4.67×10^{-7}	2.81	20.1258	4.10×10^{-7}	5.73×10^{-8}
9.27×10^{-7}	2.83	20.1258	7.40×10^{-7}	1.04×10^{-7}
1.38×10^{-6}	2.29	20.1258	1.11×10^{-6}	1.26×10^{-7}
1.71×10^{-6}	2.31	20.1258	1.37×10^{-6}	1.57×10^{-7}
2.25×10^{-6}	2.33	20.2047	1.68×10^{-6}	1.94×10^{-7}
3.30×10^{-6}	2.39	20.2047	2.22×10^{-6}	2.63×10^{-7}
5.27×10^{-6}	2.50	20.2047	3.57×10^{-6}	4.42×10^{-7}

TABLE B 3

DATA FOR THE ADSORPTION ISOTHERM OF DODECYL PYRIDINIUM CHLORIDE

SURFACTANT CONCENTRATION x (mole fraction)	MOLES OF SOLUTION n	WEIGHT OF COAL SAMPLE w (g)	CONCENTRATION CHANGE OF SOLUTION ON ADSORPTION ΔX	AMOUNT ADSORBED PER GRAM OF COAL n_1^s (moles/g)
1.41×10^{-6}	2.82	20.3999	1.42×10^{-6}	1.96×10^{-7}
3.46×10^{-6}	2.89	20.3999	3.32×10^{-6}	4.71×10^{-7}
9.19×10^{-6}	2.79	20.4030	8.63×10^{-6}	1.18×10^{-6}
1.53×10^{-5}	2.81	20.4030	1.29×10^{-5}	1.77×10^{-6}
3.02×10^{-5}	2.83	20.4030	2.23×10^{-5}	3.09×10^{-6}
3.91×10^{-5}	2.85	20.4030	2.86×10^{-5}	3.99×10^{-6}
5.93×10^{-5}	2.89	20.4030	4.02×10^{-5}	5.69×10^{-6}
9.64×10^{-5}	1.77	20.4018	5.59×10^{-5}	4.85×10^{-6}
1.40×10^{-4}	1.83	20.4018	8.94×10^{-5}	8.02×10^{-6}
2.21×10^{-4}	1.94	20.4018	2.12×10^{-4}	2.02×10^{-5}

TABLE B 4

DATA FOR THE ADSORPTION ISOTHERM OF SODIUM DODECYL SULFATE

SURFACTANT CONCENTRATION x (mole fraction)	MOLES OF SOLUTION n	WEIGHT OF COAL SAMPLE w (g)	CONCENTRATION CHANGE OF SOLUTION ON ADSORPTION ΔX	AMOUNT ADSORBED PER GRAM OF COAL n_1^s (moles/g)
5.67×10^{-7}	2.78	20.0098	4.27×10^{-7}	5.93×10^{-8}
1.12×10^{-6}	2.79	20.0098	5.70×10^{-7}	7.95×10^{-8}
2.25×10^{-6}	2.80	20.0098	1.15×10^{-6}	1.61×10^{-7}
2.93×10^{-6}	2.80	20.0098	1.58×10^{-6}	2.21×10^{-7}
3.93×10^{-6}	2.81	20.0098	1.82×10^{-6}	2.55×10^{-7}
5.03×10^{-6}	2.83	20.0098	2.73×10^{-6}	3.86×10^{-7}
6.68×10^{-6}	2.84	20.0098	2.93×10^{-6}	4.16×10^{-7}
1.59×10^{-5}	1.36	20.0098	1.09×10^{-5}	7.41×10^{-7}
2.05×10^{-5}	1.39	20.0098	1.41×10^{-5}	9.79×10^{-7}
2.98×10^{-5}	1.44	20.0098	2.00×10^{-5}	1.44×10^{-6}
3.83×10^{-5}	1.50	20.0098	2.63×10^{-5}	1.97×10^{-6}
3.90×10^{-5}	1.42	20.0098	3.10×10^{-5}	2.20×10^{-6}
4.98×10^{-5}	1.44	20.0098	3.86×10^{-5}	2.78×10^{-6}
5.27×10^{-5}	1.50	20.0098	4.12×10^{-5}	3.09×10^{-6}
5.76×10^{-6}	1.50	20.0098	4.36×10^{-5}	3.27×10^{-6}
6.10×10^{-5}	1.55	20.0098	4.75×10^{-5}	3.68×10^{-6}

TABLE B 5

DATA FOR THE ADSORPTION ISOTHERM OF AEROSOL-OT

SURFACTANT CONCENTRATION x (mole fraction)	MOLES OF SOLUTION n	WEIGHT OF COAL SAMPLE w (g)	CONCENTRATION CHANGE OF SOLUTION ON ADSORPTION ΔX	AMOUNT ADSORBED PER GRAM OF COAL n_1^s (moles/g)
1.09×10^{-7}	2.78	20.3994	1.09×10^{-7}	1.49×10^{-8}
1.09×10^{-7}	2.78	20.3992	1.09×10^{-7}	1.49×10^{-8}
2.18×10^{-7}	2.79	20.3994	1.38×10^{-7}	1.89×10^{-8}
2.18×10^{-7}	2.79	20.3992	1.63×10^{-7}	2.23×10^{-8}
2.85×10^{-5}	2.76	20.0662	1.54×10^{-6}*	2.12×10^{-7}

*determined gravimetrically

REFERENCES

1. Lowery, H.H., ed., Chemistry of Coal Utilization, John Wiley & Sons, Inc., New York, 1963, pp. 204, 307.

2. Adamson, A.W., Physical Chemistry of Surfaces, Third Edition, John Wiley & Sons, Inc., New York, 1976, p. 51.

3. Gray, V.R., J. Inst. Fuel, 31, 96 (1958); also cf. Discussion, Ibid., 32, 72 (1959).

4. Taggart, A.F., Handbook of Mineral Dressing, John Wiley & Sons, Inc., New York, 1945.

5. Deurbrouck, A.W., U.S. Bureau of Mines Report of Investigation No. 7633 (1972).

6. Miller, K.V., U.S. Bureau of Mines Report of Investigation No. 7822 (1973).

7. reference (2) p. 464.

8. Wakeman, R.J., Filtration Post-Treatment Processes, Elsevier Scientific Publishing Co., Amsterdam, 1975.

9. Kozeny, J.S.B., Akad, Wiss, Wein, Math-Naturw., Klasse 136 (Abt. IIa), 271 (1927); Wasserkr. u. Wasserwirtz, 22, 67, 86 (1927).

10. Carman, P.C., Trans. Inst. Chem. Engrs., 15, 150 (1937).

11. Brownell, L.E., and Katz, D.L., Chem. Engng. Progr., 43, 601 (1947); and ibid., 43, 703 (1947).

12. Dombrowski, H.S., and Brownell, L.E., Industr. Engng. Chem., 46, 1207 (1954).

13. Silverblatt, C.E., and Dahlstrom, D.A., Industr. Engng. Chem., 46, 1201 (1954).

14. Dolina, L.F., and Kaminskii, V.S., Coke and Chemistry (U.S.S.R.) (translation of Koks i Khimiya), No. 10, 16 (1971).

15. Nicol, S.K., Aus. I.M. & M. Proceedings, No. 260, 37 (1976).

16. reference (2) p. 339, 345.

17. Bailey, R., and Gray, V.R., J. Appl. Chem., 8, 197 (1958).

18. Bailey, M.E., J. Chem. Education, 51, 446 (1974).

19. reference (1) Chapter I.

20. reference (2) Chapter V.

21. reference (2) Chapter IV.

22. Campbell, J.A.L., and Sun, S.C., "An Electrokinetic Study of Bituminous Coal Froth Flotation and Flocculation," Special Research Report SR - 74, Penn. State Univ. May 23, 1969.

23. Fuerstenau, D. W., and Raghavan, in Flotation, Fuerstenau, M.C. ed., AIMME, New York, 1976, p. 21.

24. Baker, A.F., and Miller, K.J., U.S. Bureau of Mines Report of Investigation No. 7518 (1971).

25. Thomas, Jr., J., and Damberger, H.H., "Internal Surface Area, Moisture Content, and Porosity of Illinois Coals: Variations with Coal Rank", Illinois State Geological Survey Circular 493 (1976).

26. Tanford, C., The Hydrophobic Effect: Formation of Micelles and Biological Membranes, John Wiley & Sons, Inc., New York, 1973.

27. Griffin, W.C., J. Soc. Cosmetic Chem., 1, 311 (1949); ibid., 5, 249 (1954).

28. Davies, J.T., Proc. 2nd Int. Congr. Surface Activity, London, Vol. I, p. 426.

29. reference (2) p. 506.

30. Stern, O., "The Theory of the Electrolyte Double Layer", Electrochem., 30 (1924).

31. Grahame, D.C., Chem. Rev., 41, 441 (1947).

32. Wakamatsu, T., and Fuerstenau, D.W., Advan. Chem. Series 79, 161 (1968).

33. Garner, W.E., McKie, D., and Knight, B.D.J.G., J. Phys. Chem., 31, 641 (1927).

34. Fowkes, F.M., J. Phys. Chem., 57, 98 (1953).

35. Analysis done by Otisca Industries, Ltd., LaFayette, New York.

36. Chi, Y.M., Master's Thesis in progress, Syracuse Univ., 1978.

37. reference (2) p. 21.

38. Instruction Manual, Fisher Surface Tensiomat Model 21, Catalog No. 14-814, Instrument Division, Fisher Scientific Co.

39. Handbook of Chemistry and Physics, 57th Edition, CRC Press, 1976-1977.

40. reference (39) p. F-11.

41. reference (39) p. F-10.

42. Murkerjee, P., and Mysels, K.J., Critical Micelle Concentrations of Aqueous Surfactant Systems, NSRDS - NBS 36, 1971, (Nat. Stand. Ref. Data Ser., Nat. Bur. Stand., U.S.).

43. Vijayendran, B.R., J. Colloid Interface Sci., 60, 418 (1977).

44. Miles, G.D., J. Phys. Chem., 49, 71 (1945).

45. Brady, A.P., J. Phys. and Colloid Chem., 53, 56 (1949).

46. Nilsson, G., J. Phys. Chem., 61, 1135 (1957).

47. Rehfeld, S.J., J. Colloid Interface Sci., 31, 46 (1969).

48. Rohm and Haas Surfactants and Dispersants, "Handbook of Physical Properties", Rohm and Haas Co., Philadelphia, Pa., C5-16, July 1976.

49. Cushman, A., Brady, A.P., and McBain, J.W., J. Colloid Sci., 3, 425 (1948).

50. Weiner, N.D., and Zografi, G., J. Pharm, Sci., 54, 436 (1965).

51. Elworthy, P.H., and Mysels, K.J., J. Colloid Sci., 21, 331 (1966).

52. Miura, M., and Matsumoto, T., J. Sci. Hiroshima Univ., Ser. A-II, 21, 51 (1957).

53. Williams, E.F., Woodberry, N., and Dixon, J.K., J. Colloid Sci., 12, 452 (1957).

54. Aerosol Surface Active Agents, American Cyanamid Company, Process Chemicals Department, Wayne, N.J., PRC 102 (2-1227 cM 5/72).

55. reference (2) p. 4.

56. Haines, W.B., J. Agric. Sci., 17, 264 (1927); ibid., 20, 97 (1930).

57. Dick, S.G., Fuerstenau, D.W., and Healy, T.W., J. Colloid Interface Sci., 37, 595 (1971).

58. reference (2) p. 68.

59. Saleeb, F.Z., and Kitchener, J.A., J. Chem. Soc. (Lond.) 911 (1965).

60. Salley, D.J., Weith, A.J., Argyle, A.A., and Dixon, J.K., Proc. Roy. Soc., 20, 519 (1950).

61. Tajima, K., Muramatsu, M., and Sasaki, T., Bull. Chem. Soc. Japan, 43, 1991 (1970).

62. Ginn, M.E., in Cationic Surfactants Jungermann, E., ed., Marcel Dekker, Inc., New York, 1970, p. 364.

63. Rosch, M., in Nonionic Surfactants, Schick, M.J., ed., Marcel Dekker, Inc., New York, 1967, p. 753.

64. Anacker, E.W., in Cationic Surfactants, Jungermann, Ed., ed., Marcel Dekker, Inc., New York, p. 217.

65. reference (26) p. 78.

66. Hummel, D., Identification and Analysis of Surface-Active Agents, Interscience, New York, 1962, p. 109.

67. Schick, M.J., J. Colloid Sci., 17, 801 (1962).

68. Schick, M.J., J. Am. Oil Chemists' Soc., 40, 680 (1963).

69. Onsager, L., Ann. N.Y. Acad. Sci., 51, 627 (1949).

70. reference (2) p. 524.

71. reference (2) p. 569.

72. reference (2) p. 552.

73. Elworthy, P.H., Florence, A.T., and MacFarlane, Solubilization by surface-active agents, Chapman and Hall Ltd., London, 1968, p. 52.

74. reference (64) p. 222.

75. Schwartz, A.M., and Perry, J.W., Surface Active Agents, Interscience Publishers, Inc., New York, 1949, p. 286.

76. Doss, Kolloid-Z., 86, 205 (1939); ibid., 87, 272 (1939).

77. Ross, J. Am. Chem. Soc., 67, 990 (1945); J. Phys. Chem., 49, 377 (1945); Dognon and Gougerot, J. Chim. Phys. 40, 127 (1943); Addison, Nature, 156, 600 (1945).

TECHNICAL REPORT DATA
(Please read Instructions on the reverse before completing)

1. REPORT NO. FE-9001-1(EPA-600/7-79-008)	2.	3. RECIPIENT'S ACCESSION NO.
4. TITLE AND SUBTITLE Surface Phenomena in the Dewatering of Coal		5. REPORT DATE January 1979
		6. PERFORMING ORGANIZATION CODE
7. AUTHOR(S) D. V. Keller, Jr., G. J. Stelma, and Y. M. Chi		8. PERFORMING ORGANIZATION REPORT NO. DoE FE-9001-1
9. PERFORMING ORGANIZATION NAME AND ADDRESS Syracuse University Department of Chemical Engineering and Materials Science Syracuse, New York 13210		10. PROGRAM ELEMENT NO. EHE623A
		11. CONTRACT/GRANT NO. EPA Interagency Agreement DXE685AK
12. SPONSORING AGENCY NAME AND ADDRESS EPA, Office of Research and Development Industrial Environmental Research Laboratory Research Triangle Park, NC 27711		13. TYPE OF REPORT AND PERIOD COVERED Final; 6/75 - 11/78
		14. SPONSORING AGENCY CODE EPA/600/13

15. SUPPLEMENTARY NOTES Project officers: D. A. Kirchgessner (IERL-RTP); and R. E. Hucko (DoE), Div. of Solid Fuel Mining and Preparation, Pittsburgh PA 15213.

16. ABSTRACT The report gives results of a study of the influence of certain surfactants on the dewatering of fine coal. The surfactants were found to have a two-fold effect: they were found to affect the pressure differentials required for dewatering, in addition to the residual water contents of the coal beds attainable by this dewatering. Both effects were attributed to surfactant adsorption. Adsorption at the liquid/air interface resulted in a decrease in the interfacial tension between the two phases. The effect this decrease had on the pressure differentials required for dewatering agreed with that predicted by the capillary theory applied to the system. Adsorption at the solid/liquid interface was correlated with the complex behavior of the residual water contents as a function of surfactant addition.

☆ U.S. GOVERNMENT PRINTING OFFICE: 1979—640-092/ 733

17. KEY WORDS AND DOCUMENT ANALYSIS

a. DESCRIPTORS	b. IDENTIFIERS/OPEN ENDED TERMS	c. COSATI Field/Group
Pollution	Pollution Control	13B
Coal	Stationary Sources	08G,21D
Dewatering		13H,07A
Surfactants		11K

18. DISTRIBUTION STATEMENT Unlimited	19. SECURITY CLASS *(This Report)* Unclassified	21. NO. OF PAGES 186
	20. SECURITY CLASS *(This page)* Unclassified	22. PRICE $9.00

EPA Form 2220-1 (9-73)